Report 94047
March 25, 1991

NAS5-30088

SBIR- 09.20-7640
release date- 6/18/91

IN-18-CR
140699

p. 101

LOW COST ATTITUDE CONTROL SYSTEM
SCANWHEEL DEVELOPMENT
FINAL REPORT

Prepared for

National Aeronautics and Space Administration
Goddard Space Flight Center
Greenbelt, MD 20771

Prepared by:

ITHACO, Inc.
735 W. Clinton St.
P.O. Box 6437
Ithaca, NY 14851-6437

SBIR RIGHTS NOTICE (APRIL 1985)

This SBIR data is furnished with SBIR rights under NASA Contract No. NAS5-30088. For a period of 2 years after acceptance of all items to be delivered under this contract the Government agrees to use this data for Government purposes only, and it shall not be disclosed outside the Government (including disclosure for procurement purposes) during such period without permission of the Contractor, except that, subject to the foregoing use and disclosure prohibitions, such data may be disclosed for use by support contractors. After the aforesaid 2-year period the Government has a royalty-free license to use, and to authorize others to use on its behalf, this data for Government purposes, but is relieved of all disclosure prohibitions and assumes no liability for unauthorized use of this data by third parties. This Notice shall be affixed to any reproductions of this data, in whole or in part.

TECHNICAL REPORT STANDARD TITLE PAGE

1. Report No.	2. Government Accession. No.	3. Recipient's Catalog No.
4. Title and Subtitle Low Cost Attitude Control System (formerly Full-Sky Scanner) SCANWHEEL Development Final Report		5. Report Date 6. Performing Organization Code
7. Author(s) William Bialke / Vaughn Selby		8. Performing Organization Report No. 94047
9. Performing Organization Name and Address ITHACO, Inc. 735 W. Clinton St. P.O Box 6437 Ithaca, NY 14851-6437		10. Work Unit No. 11. Contract or Grant No. NAS5-30088
12. Sponsoring Agency Name and Address Mr. Seymour Kant NASA/Goddard Space Flight Center Greenbelt, MD 20771		13. Type of Report and Period Covered Final Report 14. Sponsoring Agency Code

15. Supplementary Notes

16. Abstract

In order to satisfy a growing demand for low cost attitude control systems for small spacecraft, development of low cost scanning horizon sensor coupled to a low cost/low power consumption Reaction Wheel Assembly was initiated. This report addresses the details of the versatile design resulting from this effort. Tradeoff analyses for each of the major components are included, as well as test data from an engineering prototype of the hardware.

17. Key Words (Selected by Author(s))	18. Distribution Statement		
Attitude Control System Reaction Wheel Momentum Wheel Earth Sensor			
19. Security Classif. (of this report)	20. Security Classif. (of this page)	21. No. of Pages	22. Price

TABLE OF CONTENTS

TABLE OF CONTENTS (Cont'd)

1.0 PREFACE

1.1 Objective

This report documents and summarizes the development work performed under Small Business Innovation Research Contract NAS5-30088.

1.2 Scope of Work

In order to make a low cost attitude control system viable for small, inexpensive satellites, development of a low cost scanning horizon sensor combined with a low cost/low power consumption reaction wheel was completed. The development effort performed included all of the detail design, fabrication, and testing of an engineering model SCANWHEEL.

1.3 Conclusions

The development effort did not encounter any insurmountable obstacles which would preclude the low-cost manufacture of a low-power consumption SCANWHEEL. Simplistic and reliable techniques were employed to result in a rugged, yet efficient, design. Processes are in place to manufacture the SCANWHEEL in large or small quantities, and with options for various levels of traceability and documentation.

2.0 PHASE I SUMMARY

The purpose of the Phase I portion of the SBIR was to determine the feasibility of a Full-Sky Sensor (FSS) to detect the Earth, Sun and Moon from a spinning spacecraft. This sensor, with ground processing, would be capable of accurately locating the centroid of these bodies from low orbits to the L1 libration point. Coverage was to be 4π steradians with provisions for recognizing or blanking spacecraft appendages.

The Phase I study proved the feasibility of a FSS, utilizing a brushless DC motor to spin a scanning mirror rotating orthogonally to the spin axis of the spacecraft. By adjusting the speed of the scanner, the scan pattern could be moved across the sky. Resolution between scan paths is strictly a function of the relative speeds between the motor and the spacecraft. A pyroelectric detector was investigated and found to have advantages over a bolometer.

The final report of the Phase I effort is contained in ITHACO Report 93226.

3.0 PHASE II GOALS

The original goals of the Phase II effort were to develop the FSS, and fabricate and test a breadboard model of the hardware to meet the requirements of the ISTP missions. After pursuing that end, it became obvious that the ISTP prime contractors were not interested in utilizing the Full Sky Scanner due to the high nonrecurring cost associated with qualifying the new design. As a consequence of this disinterest, and the lack of any other potential Phase III applications, Goddard Space Flight Center discussed the possibility of changing the emphasis of those parts of the contract that were common and applicable to the Low Cost Attitude Control System which was also under development by ITHACO under Contract NAS5-30307.

In order to make the most judicious use of the remaining funds, and satisfy a growing need for low cost attitude control systems for small spacecraft with minimal power resources, the Phase II objectives were redirected to complete the Horizon Scanner portion of the Low Cost Attitude Control System.

A major obstacle in the production of a low cost attitude control system was the availability of a low cost reaction wheel. Magnetic torquers and control electronics could be built inexpensively, but no source had yet existed for low cost reaction wheels. In addition, typical reaction wheels on the market consume too much power for the stringent power budgets of small spacecraft. A second obstacle in the production of a low cost attitude control system was the expense and power consumption of a horizon sensor. Development of a combined reaction wheel and horizon scanner provides solutions to the cost and power consumption concerns of conventional hardware for a low cost attitude control system. A combined reaction wheel and horizon scanner, or SCANWHEEL, requires only one set of bearings and one motor, which reduces the power consumption, weight, and cost over two separate pieces of hardware, while improving the system reliability.

One potential spacecraft application for a low cost/low power consumption attitude control system is the NASA Standard GAS CAN Satellite. This 150 pound satellite currently known as XSAT (Exceptional Satellite) was designed to be ejected from a Get Away Special (GAS) Cannister on the Space Shuttle. An attitude control system is intended to be added to XSAT on a mission peculiar basis in order to accommodate the requirements of each specific payload. In order to take advantage of this potential low cost satellite bus, a primary goal for the Phase II SBIR was to ensure that the SCANWHEEL design was compatible with XSAT.

The remaining funding for this SBIR was only sufficient to support the development of the horizon scanning portion of the SCANWHEEL. The related SBIR contract (NAS-30307) for a low cost reaction wheel developed the momentum and motor portion of the SCANWHEEL. A goal in this SBIR, then, was to design a scanning horizon sensor capable of being coupled to a reaction wheel to form a SCANWHEEL. The development performed per contract NAS-30307 is documented in Final Report 94044.

A photograph of the reaction wheel developed under contract NAS-30307 and the hardware developed in the Phase II effort of this SBIR is shown in Figure 3-1.

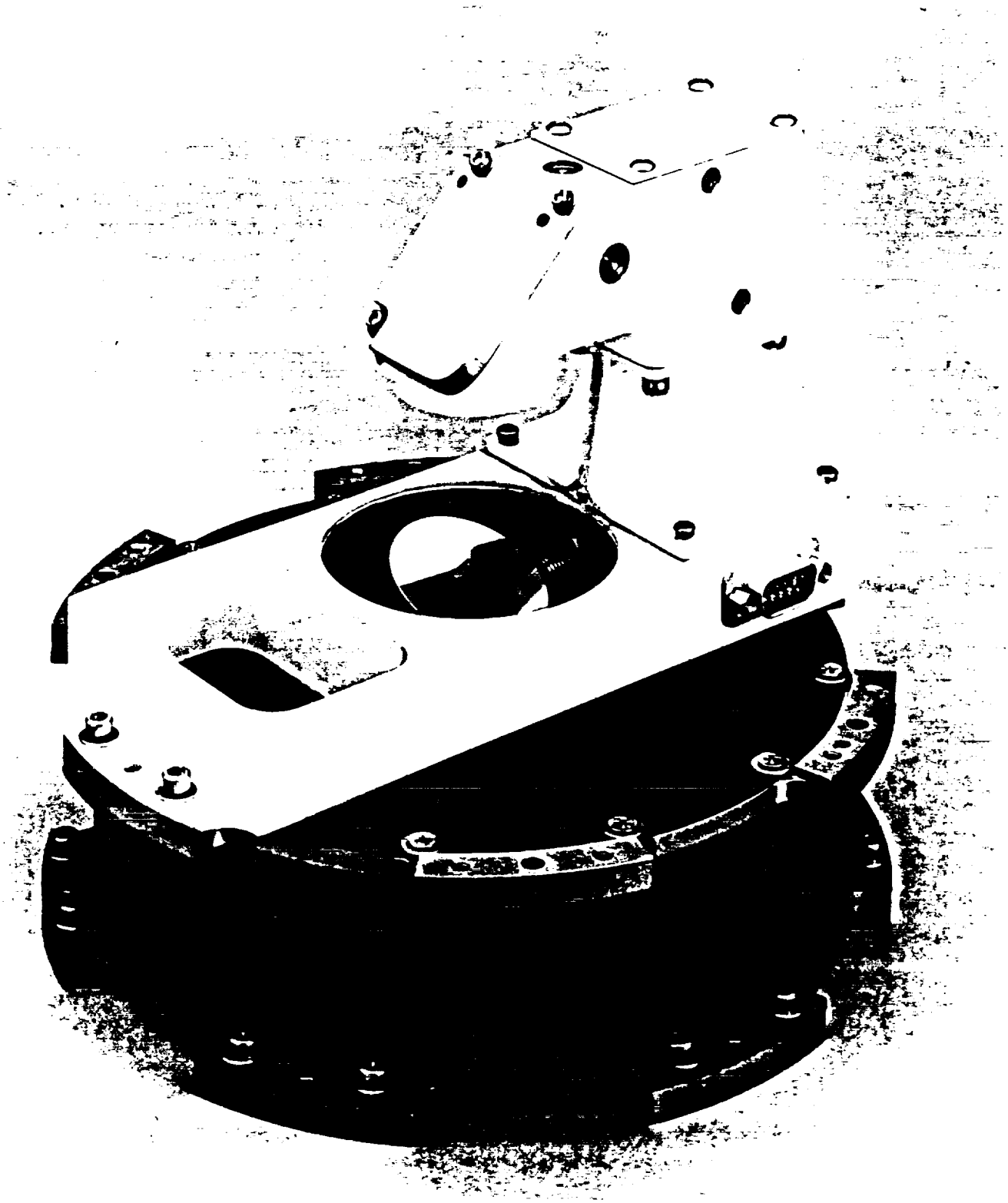

Figure 3-1: The combined hardware from the related SBIR contracts consists of a reaction wheel with an integral earth scanner, or SCANWHEEL

4.0 HARDWARE DESIGN APPROACH

A set of ground rules was established early in the design phase of the SCANWHEEL, in order to ensure that the design tradeoff decisions made during the hardware development were compatible with the ultimate program goals. The basic approach to achieve low cost was to maintain simplicity by taking advantage of standard components and common materials. At the same time, a rigid ground rule was established to maintain the ability to upgrade any feature in the design to Class S spacecraft hardware. Modularity in the design was also stressed as a ground rule, to take advantage of quantity buys of components and batch processing of subassemblies, and to minimize manufacturing costs. In order to accommodate a variety of users with the same hardware, versatility in the design was a prominent goal. This was to be accomplished by allowing for the addition of various options to the hardware without impact to the basic components. Being able to satisfy the specific requirements of a variety of users is directly in line with the pursuit of low cost hardware.

A ranking of the critical tradeoff parameters was established to be used in the tradeoff analyses during the design process. These basic parameters are power consumption, cost, reliability, weight, and accuracy.

The highest ranked tradeoff parameter was deemed to be power consumption. Small spacecraft typically have a minimum amount of surface area for solar cells, thus power is at a premium. As an example, the XSAT satellite has a total power generation capability of 7.8 Watts. The power consumption of the basic bus is 2.5 Watts average, so the power consumption of the attitude control system must be restricted to less than 3 watts total to leave just over 2 Watts for the experiment. The low power consumption was therefore imperative to enable the SCANWHEEL to be practical, given this type of power budget.

The second ranked tradeoff parameter was cost. It was reasoned low cost production of hardware was essential to allow an attitude control system to be within the reach of the budgets of small satellites. If the costs were too high, the small satellite experimenters would inevitably sacrifice the attitude control system. In addition, the market already has sources for expensive, separate earth sensors and reaction wheels, with little room for unproven competition. The only way to break into this market was with unique, low cost hardware.

The third ranked tradeoff parameter was reliability. The long term reliability and lifetime are less important in the low cost/high value spacecraft for which the hardware was targeted. While maintaining the ground rule of upgradeability, the approach was to design the hardware for a one year mission as a minimum, with a goal of three years. Typical spaceflight hardware is designed with 5 to 10 year missions in mind. The design approach to fulfill the one year mission was to keep each component as simple as possible, while leaving room for the 'bells and whistles' in case the hardware is commissioned to be used on a longer term mission.

4.0 HARDWARE DESIGN APPROACH (CONT'D)

The lowest ranked tradeoff parameter was weight. In small satellites such as XSAT, weight is not as critical as power, cost, and reliability. In some cases, hardware designs are taken to great extremes in order to minimize weight. The heroic efforts taken during this process can significantly increase the costs by increasing the complexity and decreasing the dimensional tolerances of the mechanical parts, and can lower the reliability by reducing clearances and safety margins. However, good engineering practices of mechanical design were to be used to result in the lowest practical weight. In order to minimize material costs, the use of exotic material was discouraged. Beryllium, magnesium, titanium and composites are frequently used in spaceflight hardware to minimize structural weight, but in keeping with low cost and simplicity, these materials were not to be used in the design.

Accuracy was a fairly nebulous tradeoff parameter, since it was deemed that low cost spacecraft may not require an extremely accurate sensor. A baseline accuracy of ±0.5° was established in the early phases of the program. However, the groundrule of upgradeability conflicted with this coarse specification, since a typical electo-optical system requires redesign from the ground up to improve accuracy. As a result, it was determined that the accuracy of the system would not be compromised during the development, in order to satisfy the highest number of potential users. A target accuracy of ±0.1° was established, since it covers a broad range of attitude determination requirements, and is comfortably achievable with a earth scanning sensor.

4.1 Design Specifications

The design specifications for the SCANWHEEL were established and documented in ITHACO Report 93691. A summary of the relevant specifications is presented in Table 4-1. The size was established as that expected for a small satellite on the order of XSAT. The 6 volt bus was chosen for the same reason, as that is the bus voltage of the XSAT bus. The typical bus voltage for spacecraft is 28 volts, but smaller spacecraft have fewer solar cells to string together in series, so the bus voltage is usually lower. A goal of the design was to make it useable with either a 28 volt bus or a 6 volt bus.

Table 4-1
SCANWHEEL Baseline Design Specifications

Parameter	Minimum Requirement	Goal
REACTION WHEEL SUBASSEMBLY		
Nominal Operating Speed	1000 rpm	±3000 rpm
Operating Life	1 year	3 years
Storage Life	5 years	5 years
Torque Capability	>0.02 N-m (2.8 oz-in)	increasable
Torque Ripple	none	<0.002 N-m (<10%)
Angular Momentum @ 1000 rpm	0.67 N-m-s (0.5 ft-lbf-sec)	increasable
Power Consumption @ 1000 rpm	<1.0 W	<0.5 W
Weight	<2.5 Kg (5.5 lbm)	
Temperature Range	0°C to 50°C	-34°C to 71°C
Bus Voltage	6 V	6 V, 15 V or 28 V
SCANWHEEL		
Scan Cone Angle	45±1°	45° to 85° variable
Scan Beam Width	1.5° (0°±0.75°)	
Blanking	90° allowed	
Optical Passband	14-16 μ	14.3μ-15.6μ
Optical Efficiency	65% minimum	
Sun Rejection	no damage	
Aperture	XSAT FOR maximum	Ø1.25" minimum
Position Sensor	once per revolution index pulse	
Accuracy	±0.5°	±0.1°

5.0 HARDWARE DESIGN TRADEOFFS

The following sections address the specific tradeoff analyses performed in the design and selection of the major components of the SCANWHEEL. A layout of the final design configuration is shown in Figure 5-1.

The SCANWHEEL concept is not a new one. ITHACO has delivered numerous SCANWHEELs for a variety of spacecraft missions with a licensed mechanical design from Bendix Guidance Systems (Allied Signal Aerospace). A cross section of the original ITHACO SCANWHEEL is shown in Figure 5-2. This design features a hollow shaft motor, a flywheel with an integral rotating prism/lens, an immersed bolometer for infrared detection, magnetic pickups for speed and scan phasing information, and an AC induction motor contained within a hermetically sealed magnesium housing. This design is not compatible with small, low cost, low power spacecraft for a variety of reasons. The hollow shaft motor required to feed the bolometer leads through the on-axis optical path requires large diameter bearings which have a correspondingly large amount of drag torque friction. This high drag torque coupled with the low efficiency of the AC induction motor results in unacceptably high steady state power consumption for a small spacecraft. In addition, the complex bearing arrangement and exotic materials used in the construction result in fabrication costs which are out of the range of small spacecraft financial budgets.

5.1 Motor

The motor was defined by the goals for the program to be a self contained reaction wheel developed on SBIR contract NAS5-30307. The reaction wheel development performed per contract NAS-30307 is documented in Final Report 94044. The reaction wheel development was performed in parallel with the SCANWHEEL development, in order to result in mutually compatible designs. As shown in the section view in Figure 5-3, the motor consists of a flywheel driven by an ironless armature brushless DC motor. The ball bearing suspension system was designed to accomodate the addition of a rotating scan mirror to the shaft. Figure 5-4 shows the suspension arrangement. A double nut scheme is used to secure the bearing inner races to the stainless steel shaft. The first nut secures the bearing inner race to the shaft, and the second nut provides positive locking for the first nut. Epoxy staking is used to positively lock the second nut, in an area safely removed from the critical surfaces of the bearings. By removing the second nut on the scanner end of the motor, a threaded interface is provided to attach a scan mirror. This opens an additional path for lubricant evaporation towards space vacuum. In order to minimize the molecular flow of lubricant out of the bearing volume, an additional labyrinth seal is incorporated between the bearing cartridge and the mirror shaft.

5.2 Optical System

The design of the optical system was subcontracted to Space Sciences Corporation, located in Bronxville, New York. A large portion of the material included in the following optical design tradeoff discussion is taken from a final report prepared by the Space Sciences team.

The SCANWHEEL optical system required the following functions:

1. A 45° (half angle) Scan Mechanism
2. A Focusing Mechanism
3. A Spectral Filter
4. An Infrared Detector

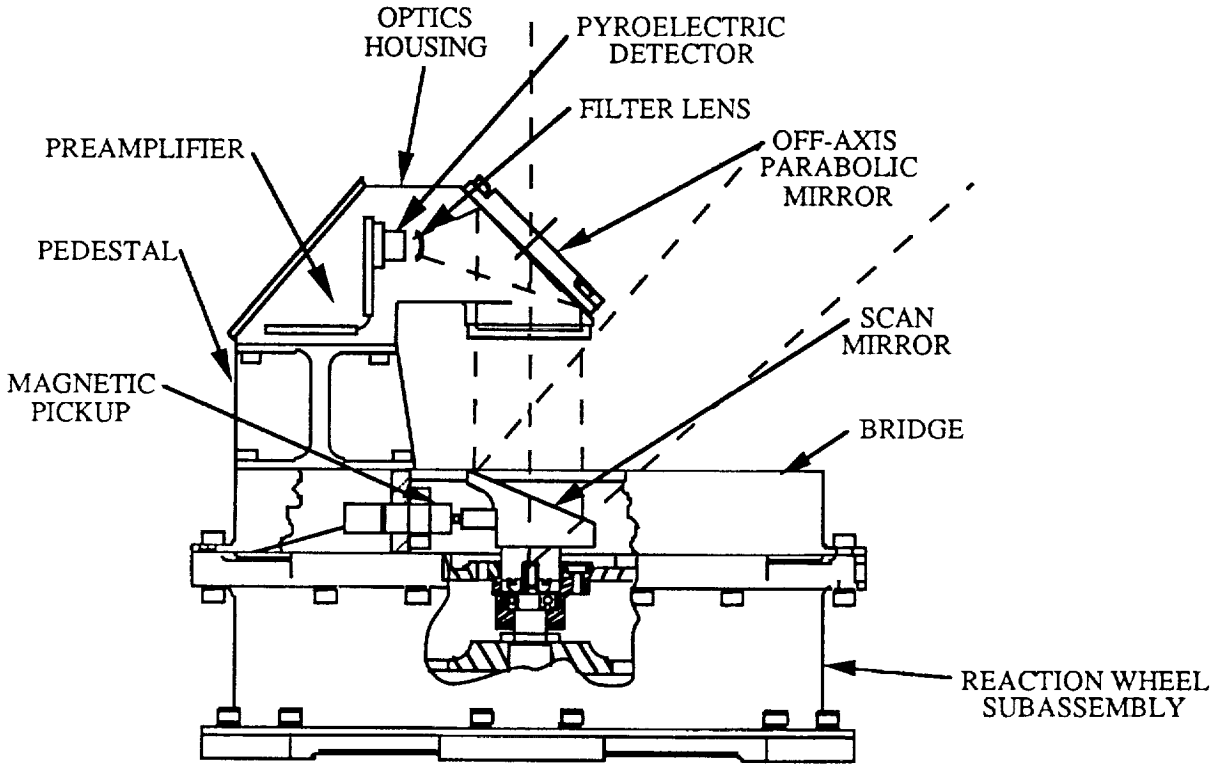

Figure 5-1: The final configuration of the SCANWHEEL uses a modular approach to capitalize on the reaction wheel development of a related SBIR.

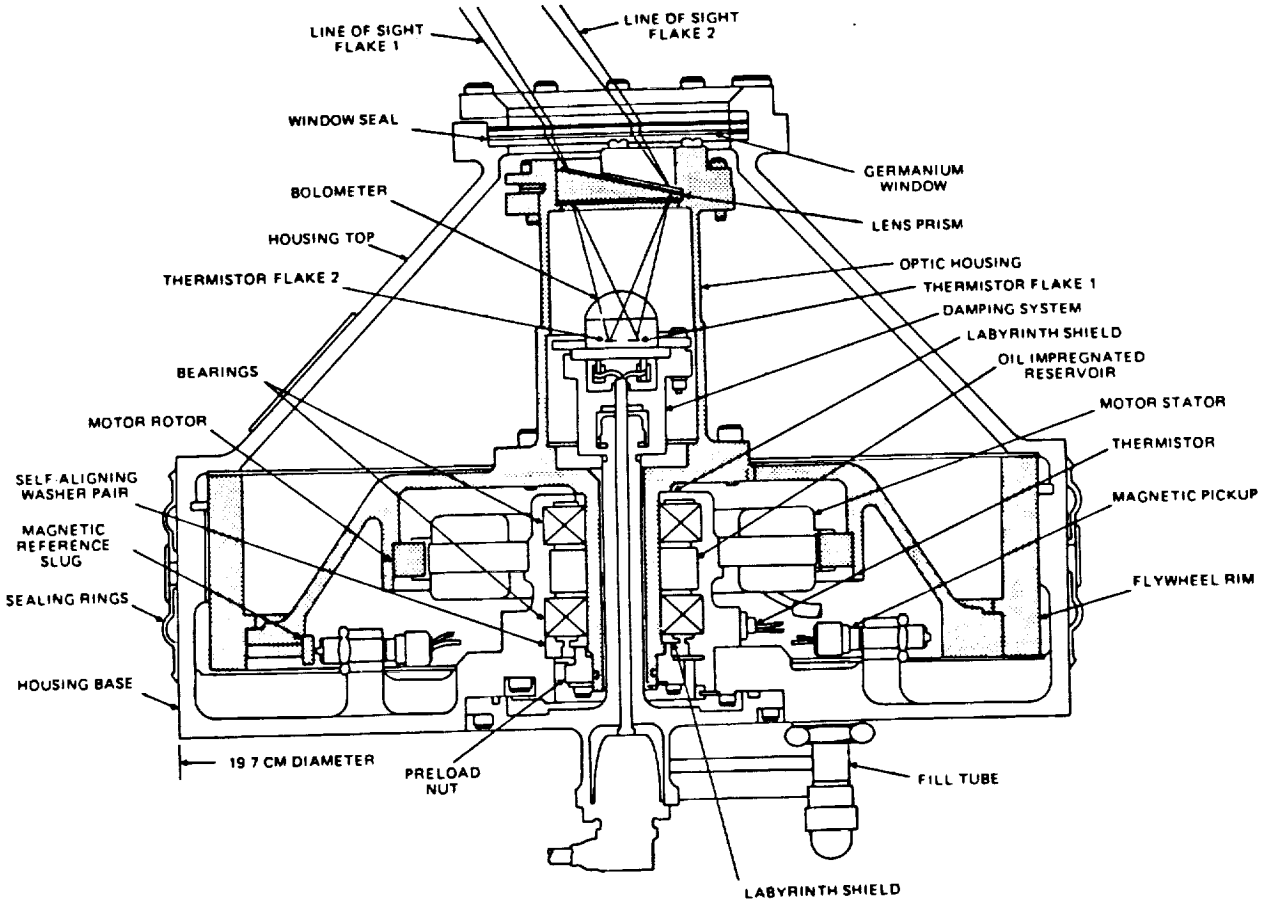

Figure 5-2: The original ITHACO Type B SCANWHEEL was manufactured by Bendix Corp. Shading indicates rotating components consisting of flywheel and prism assembly.

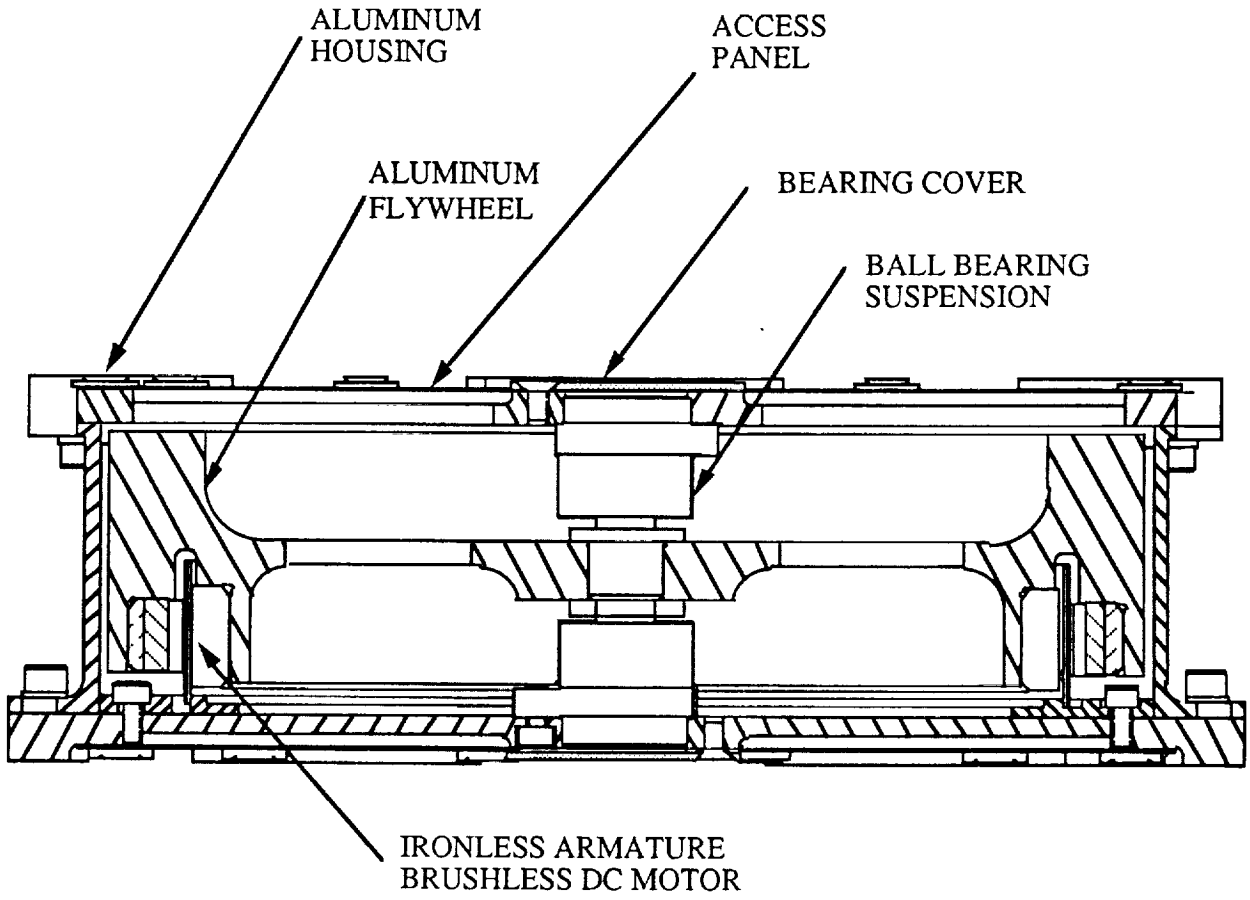

Figure 5-3: The reaction wheel subassembly features a high inertia ironless armature brushless DC motor for optimum weight and power.

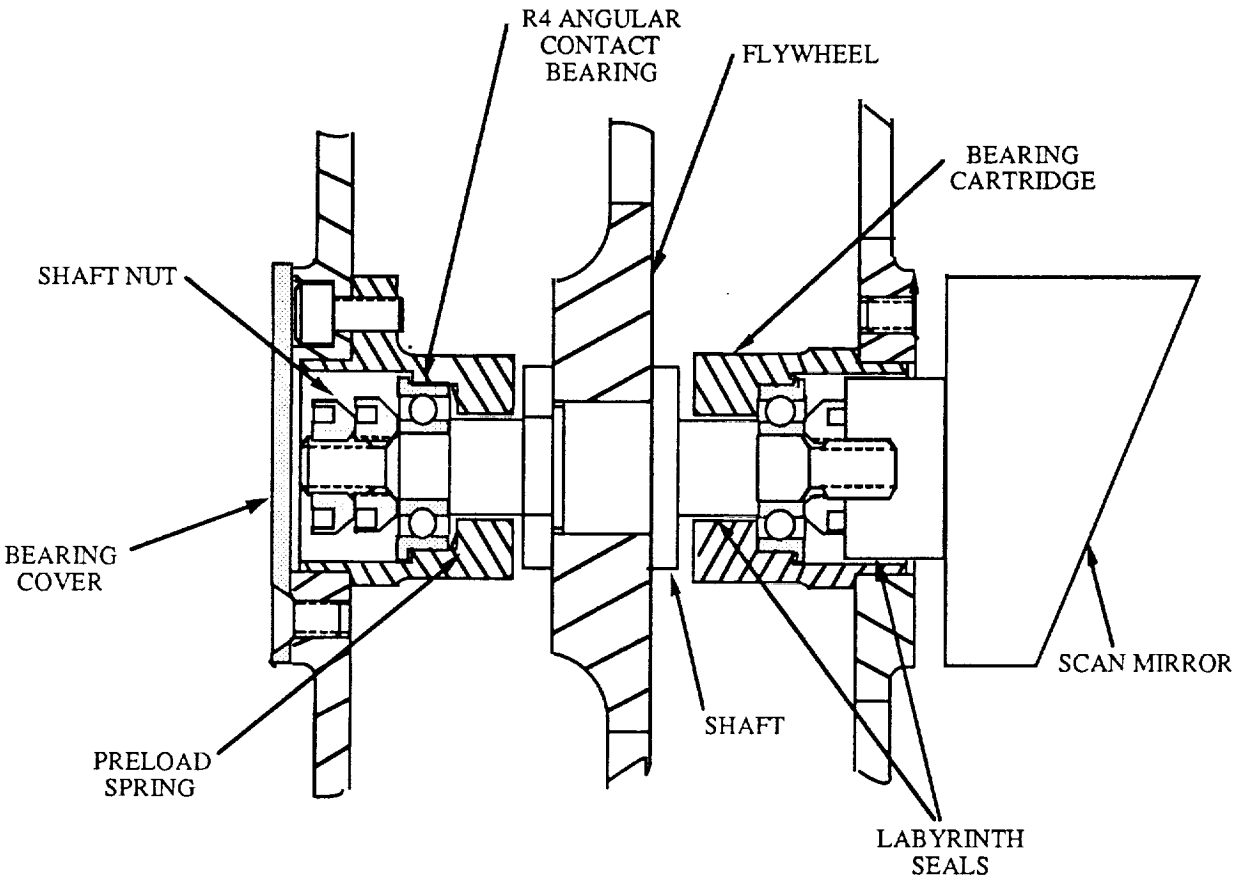

Figure 5-4: The reaction wheel ball bearing suspension system was designed to allow addition of a scan mirror with no modifications.

5.2 Optical System (Cont'd)

The optical system of ITHACO's previously manufactured SCANWHEEL is shown in Figure 5-5, which is basically the same system of ITHACO's Conical Earth Sensor. A rotating Germanium prism and lens scans through a Germanium spectral filter window to stimulate an immersed bolometer. This optical design has been flown on a large number of spacecraft. In spite of this extensive heritage, it is not compatible with a system optimized for low power consumption due to the hollow shaft motor required to access the infrared detector. A hollow shaft motor requires large diameter bearings, which impact the bearing drag torque and increase the steady power consumption.

5.2.1 Scan Mechanism

An off-axis optical scan geometry is necessary in the absence of the access provided by a hollow shaft motor, so the scan mechanism of choice is a planar, first surface mirror. Refractive scan elements do not readily lend themselves to the off-axis system topology, and thus were not considered further. The high optical efficiency of the reflective elements contributes to their favorable selection. Figure 5-6 shows two candidate layouts which were considered in the optical scan geometry tradeoff. A full 360° scan perimeter is possible in the off axis configuration shown in Figure 5-6(a), where an off axis parabolic mirror is suspended from the center of an infrared window. This configuration is very cumbersome, for it requires a large, complex and extremely expensive infrared window. The transmission losses through the window and the large amount of weight and volume required for the support of the window make this option undesirable. The configuration shown in Figure 5-6(b) shows the configuration selected for the design, which consists of an off-axis parabolic mirror is suspended by a pedestal in one section of the scan path. This requires blanking a 90° sector of the scan perimeter. However, most spacecraft require a blanked region to avoid optical interference with solar panels or antenna booms, so this is not a serious consequence. In addition, the configuration in Figure 5-6(b) allows modification to the scan cone angle by merely changing the scan mirror. Figure 5-7 shows how this configuration can be used with alternate mirrors to vary the scan cone angle from 45° to 85° for higher altitude applications.

Design constraints imposed by the XSAT spacecraft bus limited the scan path geometry. A sketch of the XSAT bus is shown in Figure 5-8. In order to minimize the power generation capability sacrificed in order to afford the SCANWHEEL a clear field of view, the scan path was limited to the area of four solar cells. The XSAT spacecraft fits within an 18" diameter cannister as a Get-Away Special (GAS) payload. This means that the top of the sensor cannot protrude beyond the outline of the satellite, which limits the aperture to the basic geometry shown in Figure 5-9.

In order to maximize the signal of a detector using focused radiation, a large aperture is desirable. The available aperture is directly related to the available scan cone clearance. The aperture available within the constraints of the XSAT bus was maximized by locating the blanked region of the scan path in the zenith pointing direction, as shown in Figure 5-10. This gives full earth coverage in the nominal orientation and during a 180° maneuver, and provides a single earth edge for 90° maneuvers in either direction. With this configuration, an aperture of 1.25" was possible. This is a factor of 1.7 over the aperture area in previous optical designs used at ITHACO. This additional energy could be used to either improve the signal to noise ratio of the detector, or to reduce the field of view for higher accuracy. It was decided to use the energy to optimize the field of view. The field of view which corresponds to the width of an earth edge viewed from 1500 Km (assuming 40 Km of detectable atmosphere) is 1.5°. It is desirable to have the field of view less than this horizon angle for altitudes up to 1500 Km. The smaller field of view also results in less extreme radiance errors.

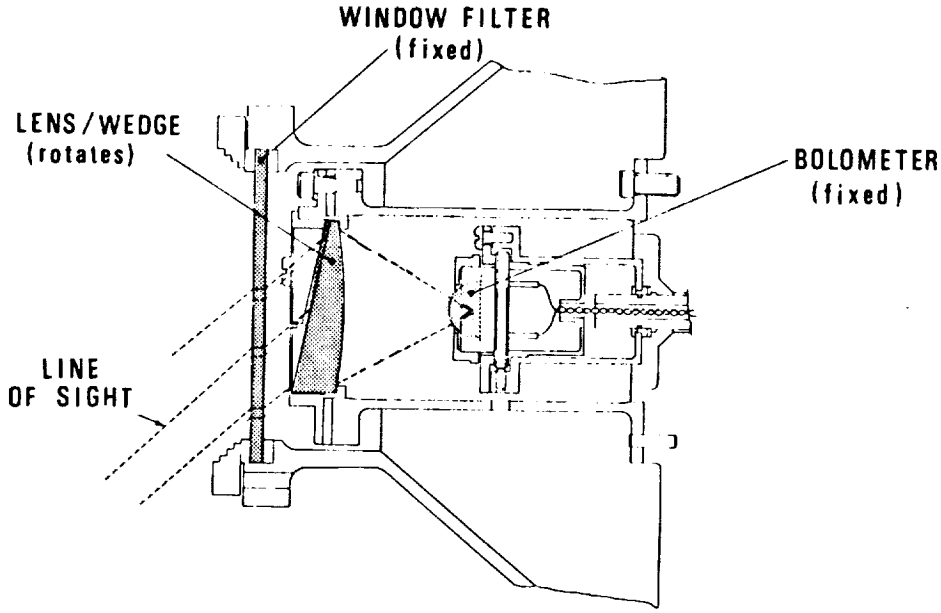

Figure 5-5: The original ITHACO SCANWHEEL utilized refractive optics and a hollow shaft motor

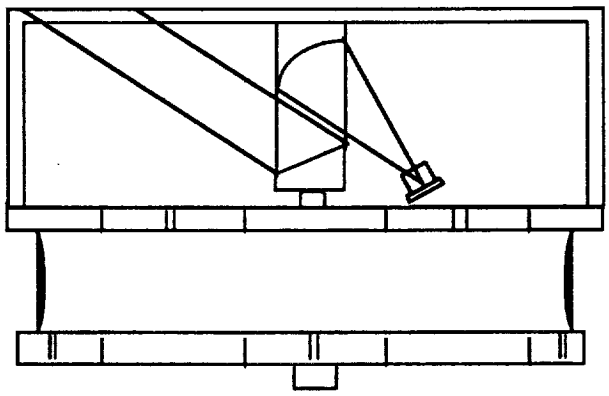

Figure 5-6(a): This off-axis optical configuration affords a 360° unobstructed scan path, but requires an awkward, expensive window to support the secondary mirror.

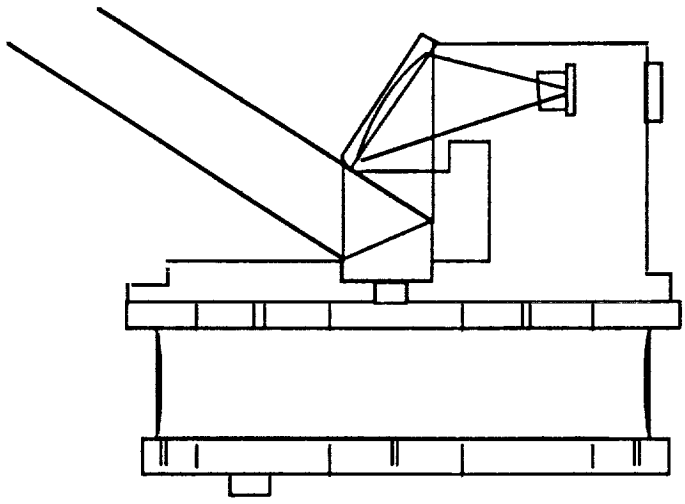

Figure 5-6(b): The blanked portion of the scan inherent in this configuration is frequently required to prevent the sensor from seeing solar panel arrays or antennas on a spacecraft.

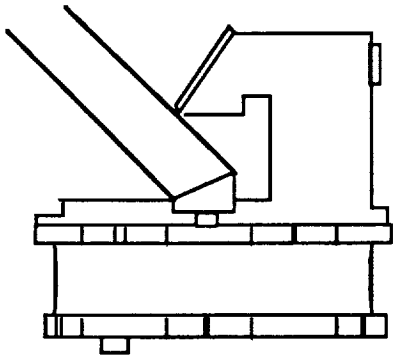

22.5° mirror - 45° scan cone

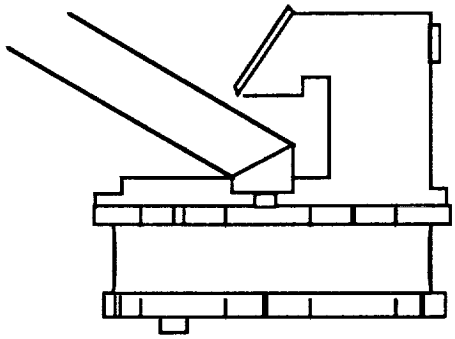

30° mirror - 60° scan cone

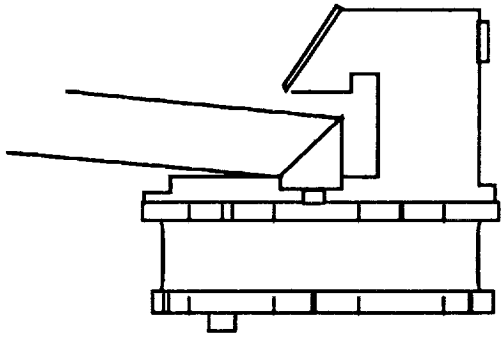

42.5° mirror - 85° scan cone

Figure 5-7: The scan cone half-apex angle can be modified by substituting alternate scan mirrors

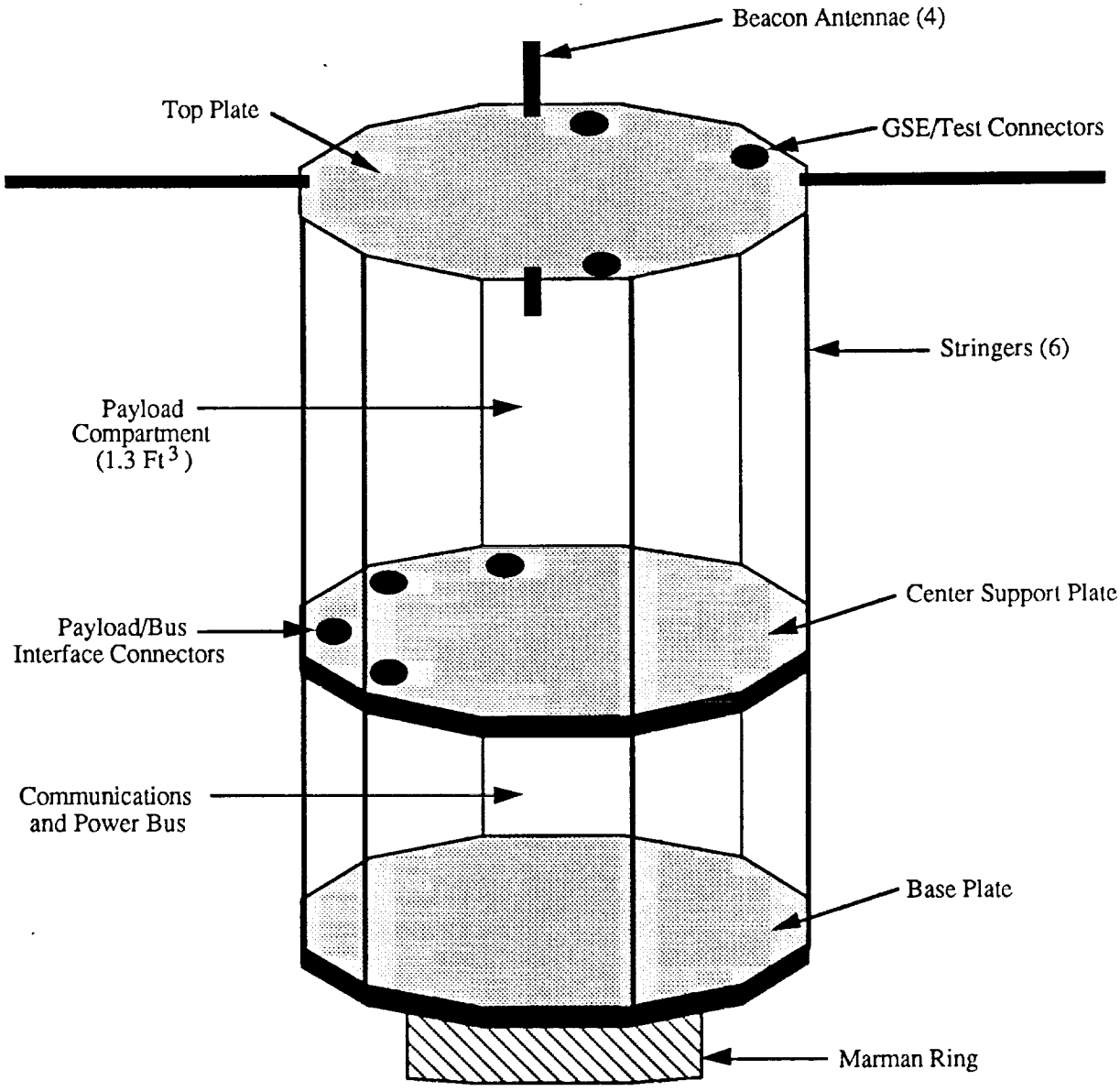

Figure 5-8: X-SAT Structure

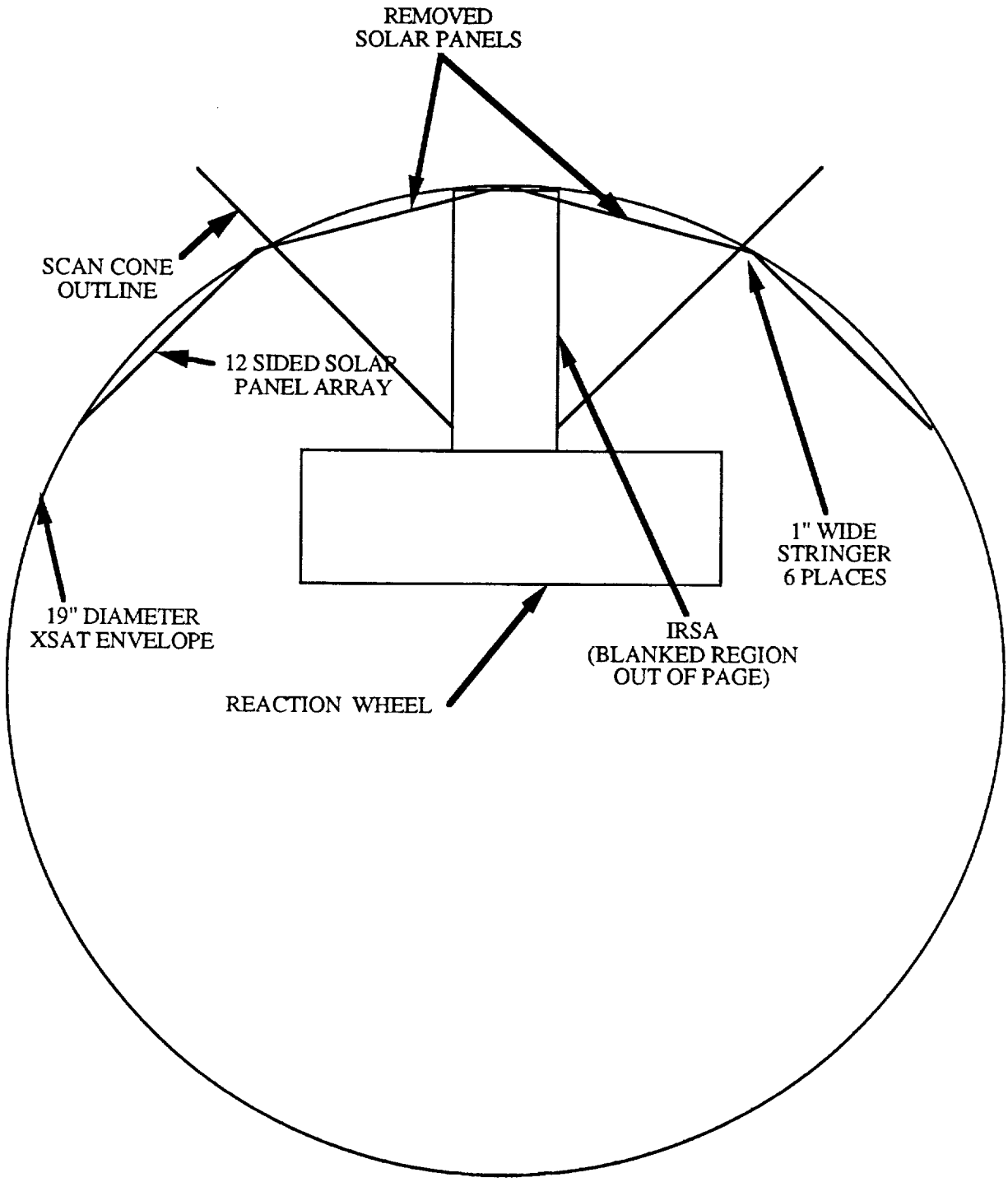

Figure 5-9: The GAS cannister inside diameter limited the available field of view of the SCANWHEEL optical system

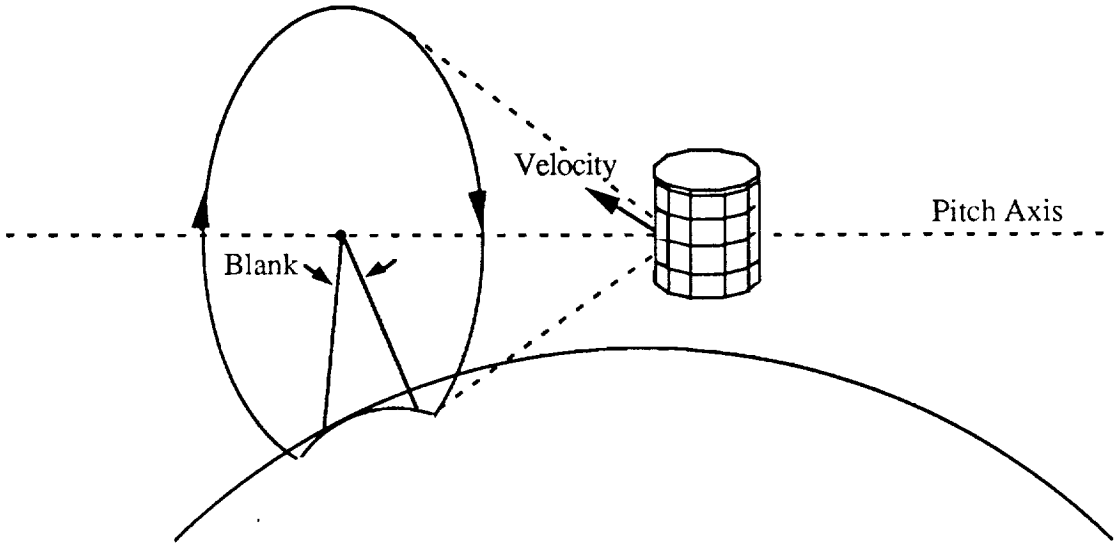

Figure 5-10: The aperture of the SCANWHEEL was maximized by placing the blanked region in the center of the earth for the X-SAT application.

5.2.2 Focusing Mechanism

The first approach which was considered added power to the scan mirror, as shown in Figure 5-11. This would result in a minimum component count system and would eliminate any optical folds. Unfortunately, for an off-axis reflective system, the aperture stop must be placed just prior to the objective mirror to reduce aberrations. Hence the resultant mechanical structure would be quite awkward, if not impossible, to construct.

The focusing function can be combined with a secondary first surface mirror. In assessing the viability of this option, the available techniques for focusing the imagery onto the detector element should be reviewed.

There are two canonical approaches to implementing horizon sensor detector optics. The first system utilizes a field lens and a reimaging technique. The second approach employs an immersion lens. In general, the object of the optical system is to limit the field of view, collect as much energy as possible for a given minimum detector size, and spread the incident energy uniformly over the detector surface. In theory it is optimum to condense the energy to the smallest possible image size.

A limit exists as to how small the image may be condensed. For a circular field of view and circular image disk this relation is $A\alpha/nD<1$ where, for our system, A is the diameter of the entrance pupil, α is the half angle of the field of view, n is the refractive index of the medium in which the detector is immersed, and D is the diameter of the detector.

A Field Lens Systems, as shown in Figure 5-12, is characterized by an optical element located at or near the objective lens' image plane. the field lens essentially reimages the exit pupil of the objective system onto the surface of the detector. In this way the field of view of the detector is substantially increased.

The Immersion Lens System, as shown in Figure 5-13, employs a hemispherical or hyperhemispherical lens with the detector at the center of curvature of, and in optical contact with, the plano surface of the lens. In this arrangement the immersion lens does not introduce any spherical aberration and the image is reduced by the index of the lens. In the hyperhemispherical aplanatic case (where the magnification of the lens is the numerical reciprocal of the index of refraction) the apparent image size may be as great as n^2, however the $A\alpha/nd<1$ must still be satisfied.

A third approach, shown in Figure 5-14, uses near direct imaging via the objective lens coupled with a low power meniscus spectral filter. This is the simplest and most cost effective system with the caveat of the detector area being sufficiently large to accept the incoming image. For systems utilizing a bolometer, this approach is not possible since active areas associated with horizon sensor bolometers are typically 0.15 mm (circular diameter). Pyroelectric detectors, in contrast, possess an almost two order of magnitude improvement in active area, with typical active circular diameters on the order of 1 mm.

Since a pyroelectric detector was chosen for the design (as described in Section 5.2.4 of this report), the third approach was chosen, utilizing a first surface planar scan mirror coupled with an off-axis, aspheric, parabolic fold mirror. Figure 5-15 is an optical schematic of the resulting system. As shown, the aperture stop is located just prior to the parabolic fold mirror in collimated space. The off-axis parabolic fold mirror bends the beam 90° and focuses the energy through a germanium meniscus spectral filter and onto a pyroelectric detector.

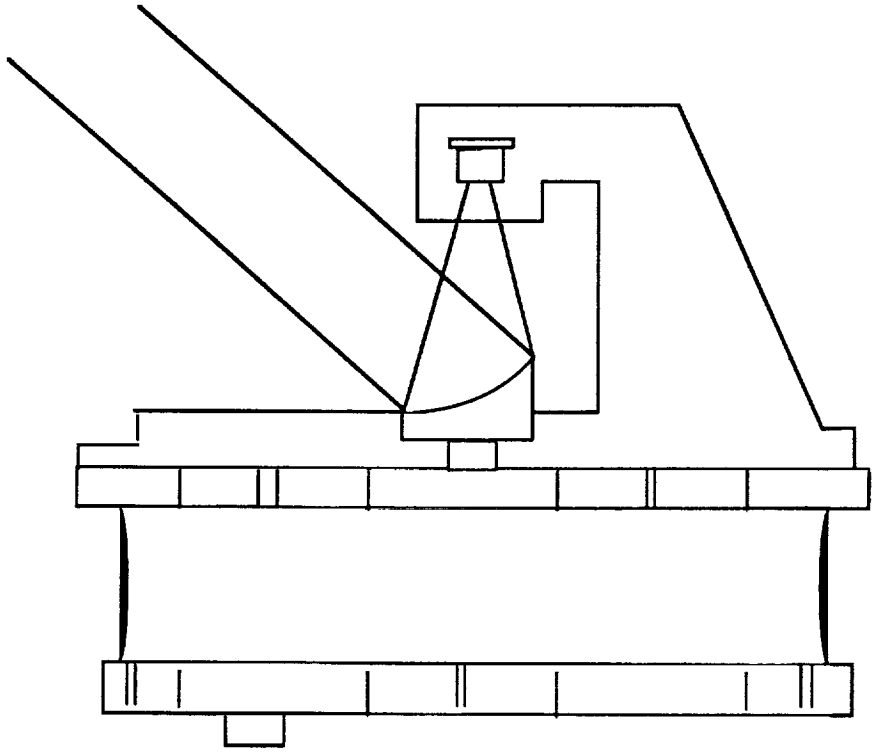

Figure 5-11: A focusing scan mirror would result in a minimum optical component count, but optical and mechanical limitations preculde its implementation.

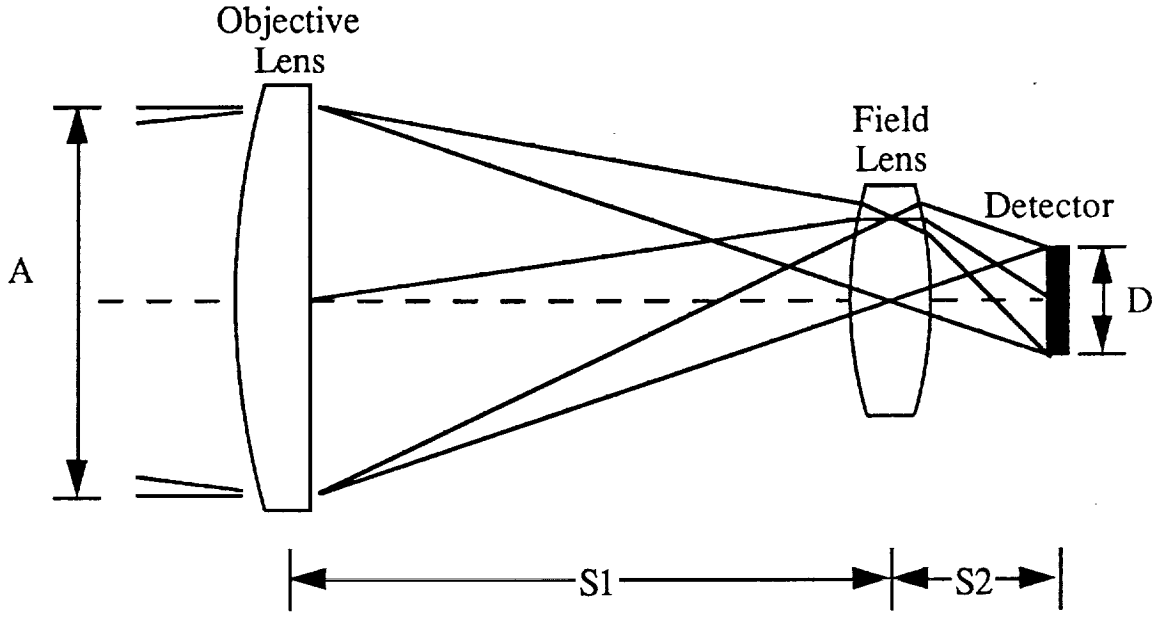

Figure 5-12: Field Lens System

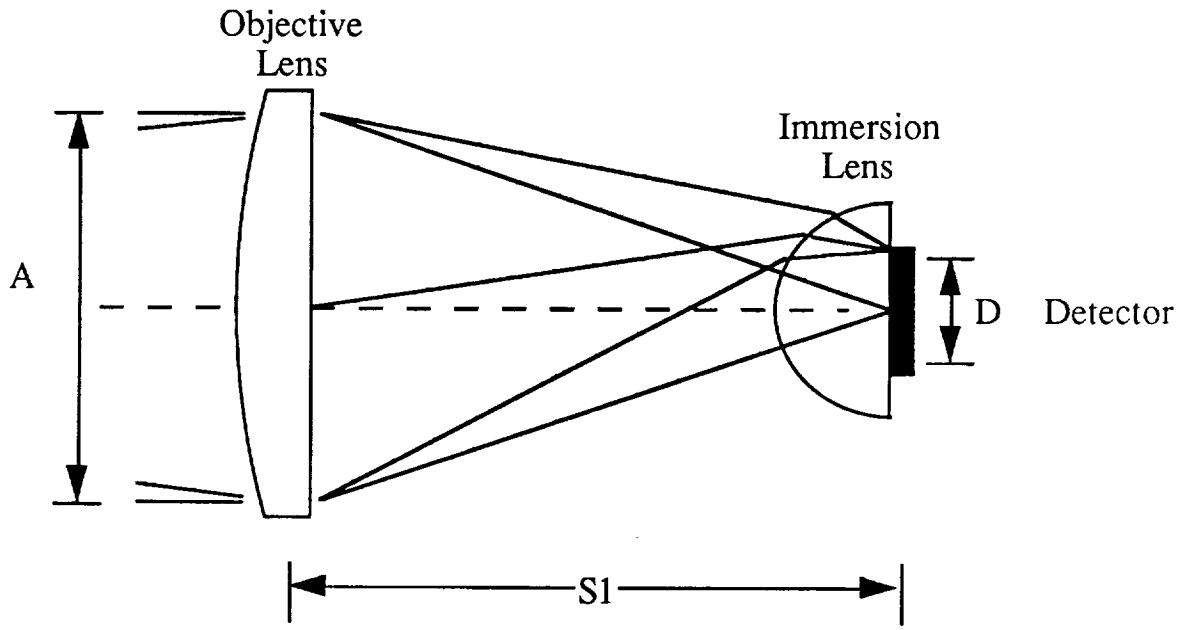

Figure 5-13: Immersion Lens System

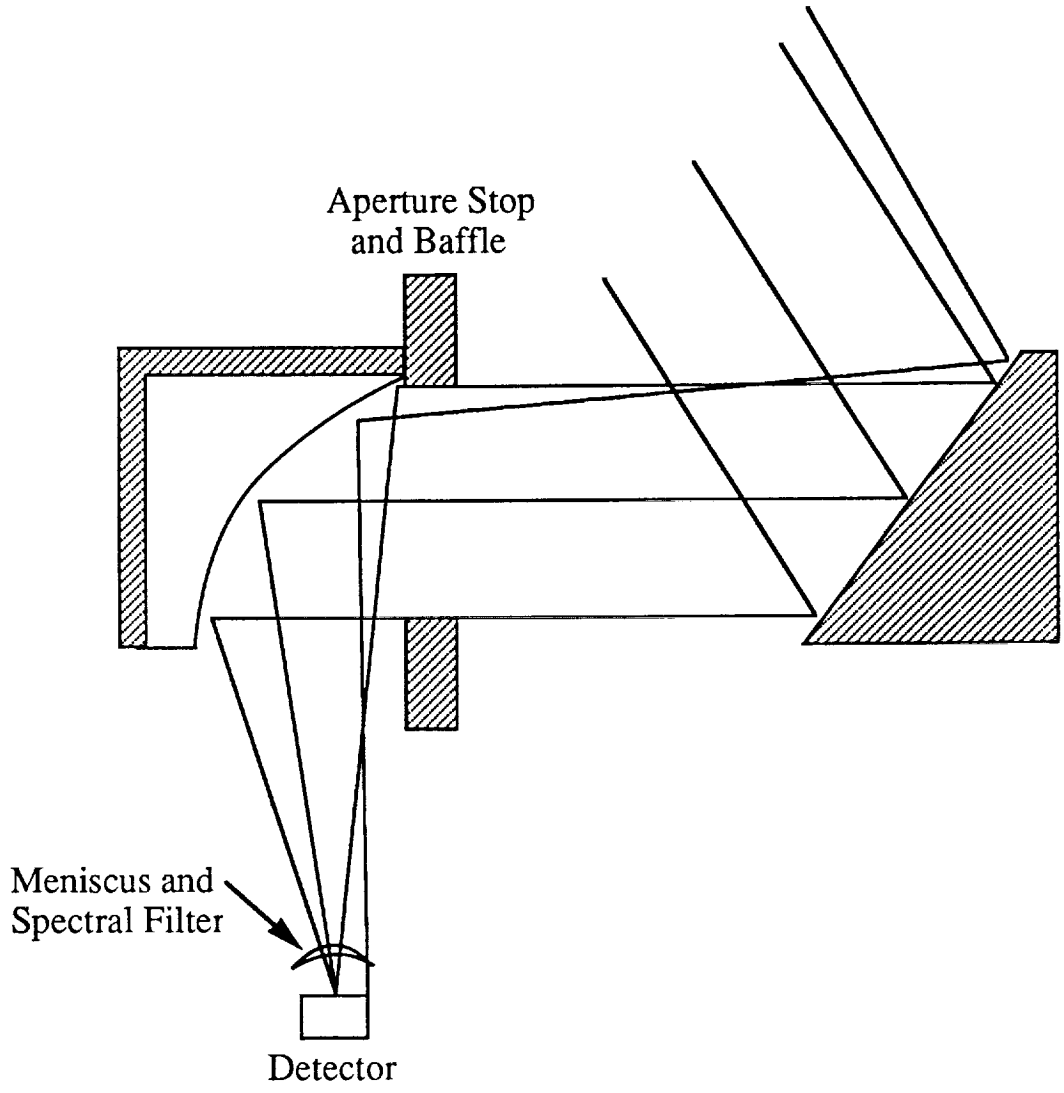

Figure 5-14: Meniscus Lens System

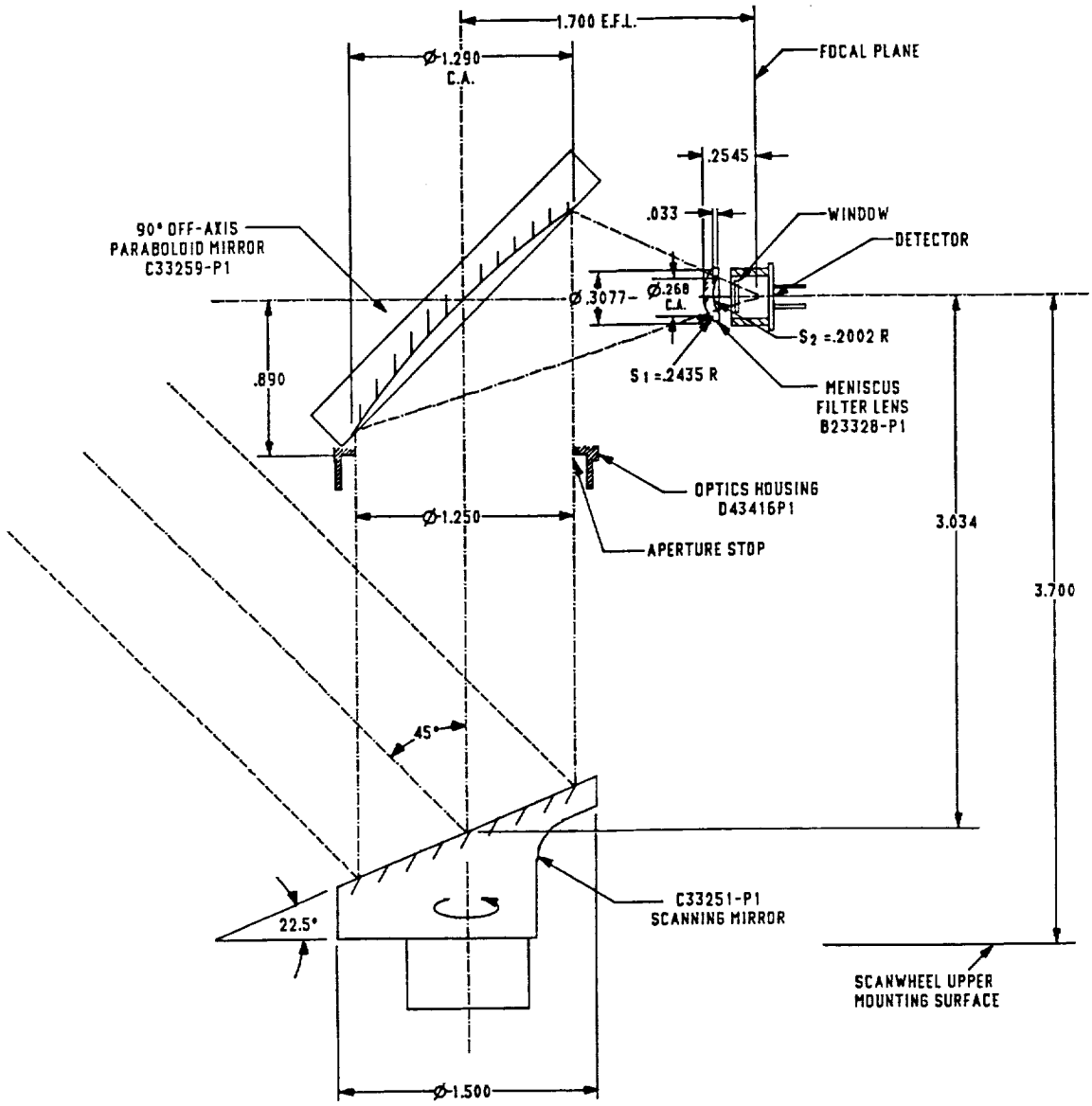

Figure 5-15: SCANWHEEL Optical Schematic

5.2.3 Optical Elements

The actual optical elements consist of a first surface planar scan mirror, a first surface off-axis parabolic objective/fold mirror, a meniscus filter lens, and a planar window for sealing the detector.

5.2.3.1 Mirrors

The scan mirror contains an integral soft-iron slug to stimulate a once per revolution index pulse from a magnetic pickup. In order to accomodate this, while minimizing the residual imbalance in the scan assembly attached to the rotating flywheel, the geometry had to be carefully selected. The result was a truncated aluminum cylinder, with a recess to compensate for the imbalance due to the soft iron slug. The geometry makes the scanning mirror inherently balanced to a small percentage of the overall imbalance specification, which allows addition and removal of the mirror without rebalancing the rotor. In order to maximize the refectance in the infrared wavelengths and minimize corrosive effects of atomic oxygen, the diamond machined mirror surface is gold plated. The off-axis parabolic mirror is also a diamond machined component, with a gold plated finish.

5.2.3.2 Filter Lens

A germanium meniscus filter lens is placed in front of the detector, primarily to provide a substrate for the optical passband filter coating. As graphically illustrated in Figure 5-16, the ideal filter must block above 15.7 microns and below 14.3 microns. An excellent discussion of spectral filter passbands is given in NASA Technical Memorandum 86181 entitled Infrared Horizon Sensor Modeling for Attitude Determination and Control: Analysis and Mission Experience. As shown in Figure 5-16, the intensity of the spectral emittance in this region is quite stable, ranging from 200°K to 250°K over latitude, season, and cold cloud effects. Thus with this passband, the radiance received by the IRSA will be nearly independant of atmospheric effects below the tropopause or the temperature on the earth's surface, providing an extremely stable reference and minimizing radiance errors.

The filter lens is located after the objective lens, which means that the angles of incidence on a planar filter window located in front of the detector would not be uniform. The curvature of the meniscus lens used was selected in order to minimize the angles of incidence on the coated surface.

The vendor selected for fabrication and coating of the filter lenses was Optical Coating Laboratory, Inc. (OCLI). A sample transmission curve for the first lot of filter lenses purchased is shown in Figure 5-17.

5.2.3.3 Sealing Window

A 1 mm thick planar sealing window is used to seal the detector housing. Zinc Selenide with a high transmission, anti-reflection coating is used to minimize losses through the window.

5.2.3.4 Optics Housing

The interior of the optics housing is baffled and anti-reflection treated in order to prevent stray optical paths from influencing the detector. Anti-reflective surfaces are achieved by blasting the desired surfaces with aluminum oxide grit, and subsequently black anodizing these roughened surfaces. The entrance pupil, or aperture stop is machined directly into the optics housing.

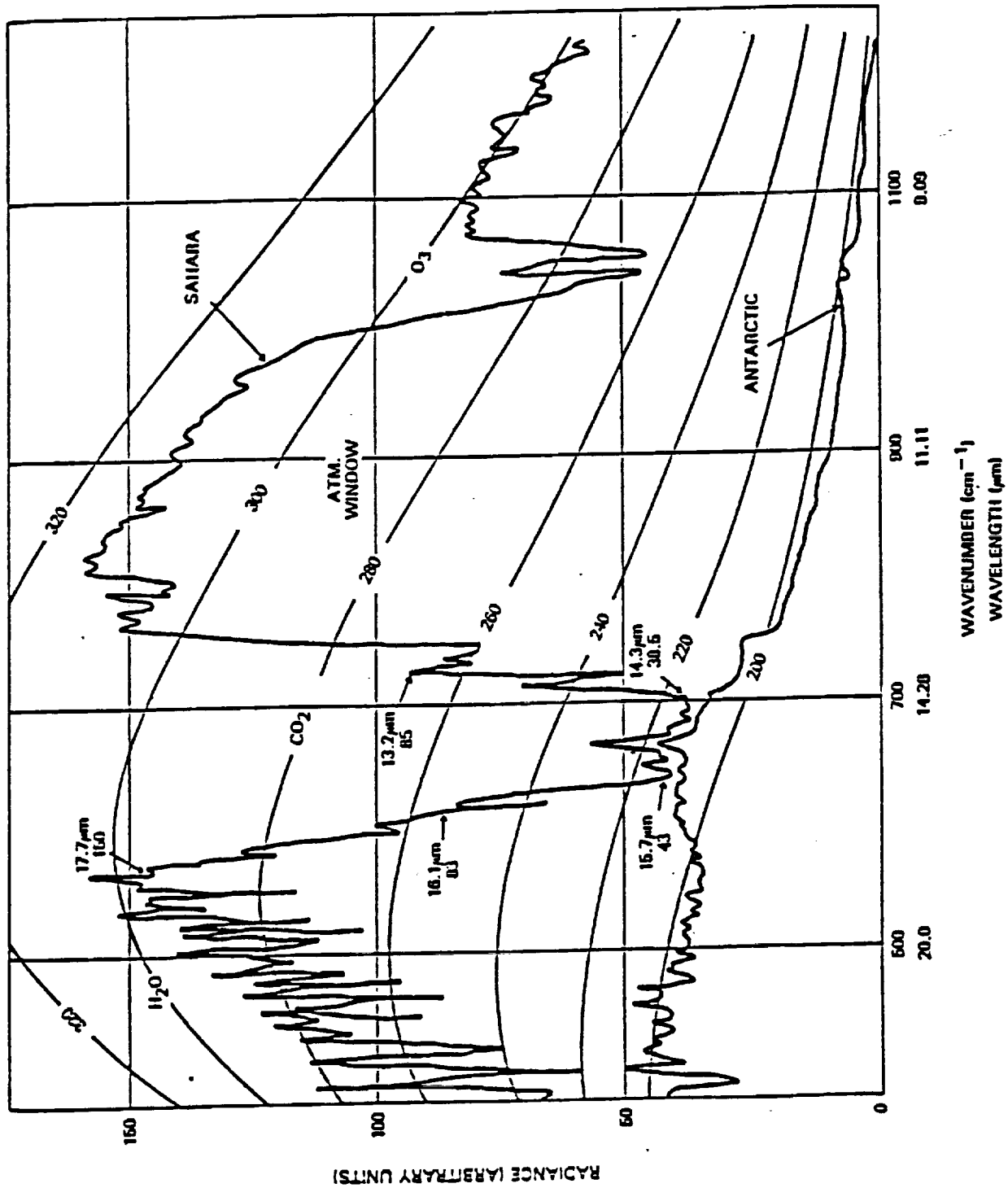

Figure 5-16: Earth IR spectrum as viewed from space for two extremes, the Sahara and the Antarctic

OPTICAL COATING LABORATORY, INC.
2789 Northpoint Parkway
Santa Rosa, California 95407-7397
Telephone 707/545-6440
Telex II 510-744-2083

SPECTRAL PERFORMANCE

DATA IDENTIFICATION
OCLI W'O 14-54224-400
Lot 1
Run No. 542-007/010
Serial No.

SAMPLE IDENTIFICATION
Filter Type
Substrate Germanium
1.0" ϕ
Thickness .040"
☐ Actual Part ☒ Witness

INSTRUMENT OPERATING PARAMETERS
☐ Beckman DK-2 ☐ Cary 2390
☐ Cary 14 ☐ Nicolet
☐ Cary 17 ☐ PE 180
☐ Cary 90 ☒ PE 983 S-68
☐ Cary 210 ☐ PE 1800
☐ Cary 2300 ☐ Shimadzu
Resolution 3.0
Scan Speed Mode: 4
Response Nc & Filter: 1
Aperture
Expansion 0-100%
☒ Percent Transmission
☐ Percent Reflection

TEST CONDITIONS
Temp. Amb. Angle 0°
Cryostat ☐
Analyst RF/MK Date 4/19/90
OCI 87
☐ Micrometers
☐ Nanometers
☒ Wavenumber

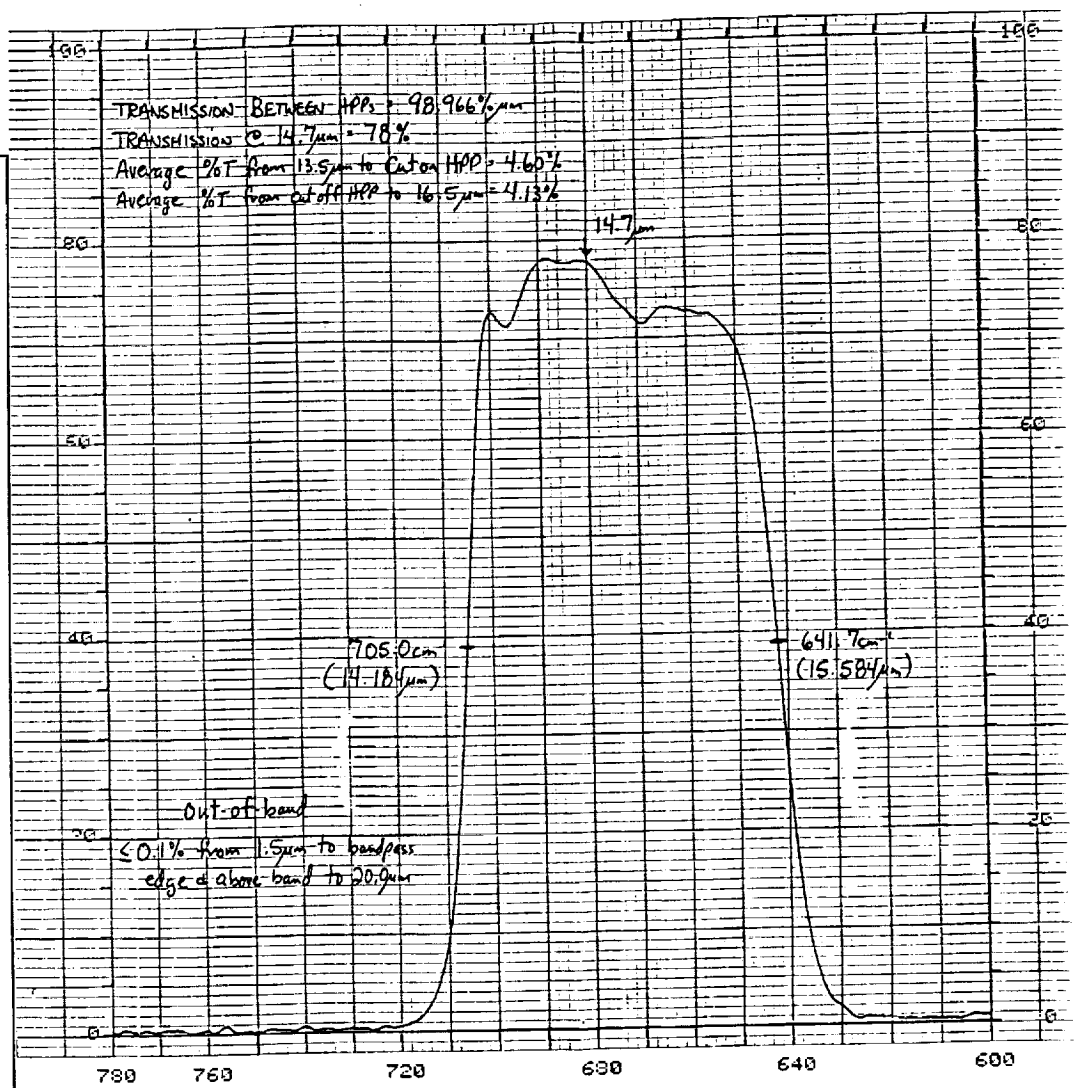

Figure 5-17: The tight optical passband on the maniscus filter lens was established with remarkable accuracy by the coating vendor

5.2.4 Infrared Detector

After surveying the current body of infrared detectors which are:

- capable of sufficient detectivity in the 14 to 16 micron CO_2 absorption bank
- perform under expected environmental conditions without cryogenic cooling
- and possess flight heritage

the field was narrowed to pyroelectric detectors and thermistor bolometers, both of which are members of the thermal detector family.

Quantum detectors, which exhibit: excellent sensitivity, short time constants, uniform response, and operate relatively narrowband, unfortunately also require cryogenic cooling to operate at our far infrared 14 to 16 micron wavelength region. This inherent fundamental limitation originates from the relatively low energy of the LWIR photons ($h\nu$ - where h is Plank's constant and ν equals frequency), along with the need to have a commensurately low band gap energy threshold. Expendable cryogens would severely, and unnecessarily, limit the IRSA's on-orbit life while other forms of cooling, such as a modified Stirling Cycle refrigerator, are costly, power consumptive, and possess poor long-term reliability. Hence, quantum detectors were not considered for the SCANWHEEL.

Of the available types of thermal detectors, (thermopiles, Golay Cells, thermistor bolometers, and pyroelectrics), only thermistor bolometers and pyroelectric detectors are appropriate for the requirements. Thermopile detectors exhibit excessively long-time constants. Golay Cells, which are quite sensitive, are much too fragile to be embedded within a low cost flight instrument.

Thermistor bolometers are widely employed in flight-qualified horizon sensors and have demonstrated extremely reliable operation over their 30-year flight history. Bolometers are essentially temperature sensitive resistors which utilize a high voltage, low noise, bias supply to accurately sense small resistance changes. Time constants are typically shorter than 5 milliseconds. Bolometers are "DC" type detectors. As such, they require internal ambient temperature compensation to eliminate environmental temperature fluctuations from the measurement signal.

Pyroelectric detectors consist of a thin slab of ferroelectric material sandwiched between two electrodes. It should be noted that pyroelectric detectors respond to the rate of change of temperature, which limits their application to scanning instruments. Pyroelectric detectors offer enhanced performance when compared with their bolometer counterparts. Drawbacks to pyroelectric detectors include microphonics, which arise from piezoelectric pickup, along with environmental limitations on certain types of materials.

5.2.4.1 Thermistor Bolometers

The thermistor bolometer belongs to the family of thermal detectors which includes devices operating on the bolometric, thermovoltaic, thermopheumatic, and pyroelectric effects. The first bolometer was developed by Langley in 1880. This bolometer consisted of a thin blackened platinum foil which was employed in solar observations.

The bolometric effect is a change in the electrical resistance of a responsive element due to temperature changes induced by the absorption of incident radiation. In the simplest sense, a bolometer consists of a resistor with negligible thermal capacity and a large temperature coefficient. Incident radiation increases the temperature of the resistor and produces a measurable change in the resistance of this detector. In practice, the resistance is measured by applying an accurate bias to the detector and measuring the output voltage.

Thermistor bolometers were a by product of the United States World War II technology effort, where they were employed for heat-seeking missions and infrared spectroscopy. Bolometers may be employed in a bridge circuit configuration for DC operation or in the more canonical bolometer detector circuit shown in Figure 5-18, "Bolometer Construction & Electronic Schematic". Since the SCANWHEEL scans at a relatively high rate (2000 RPM), this discussion will be restricted to AC-coupled configurations which offer better overall performance and design simplicity for this application.

As shown, the detector is comprised of an active and compensating flake, each with a resistance of approximately 250 K ohms. Modern bolometers are constructed from a sintered mixture of semiconducting oxides which exhibit higher resistance temperature coefficients than their metal competitors. Temperature coefficients are a function of band gap, impurity states, and dominant conduction mechanisms. The type of material considered for the SCANWHEEL was a SERVO Corporation proprietary mixture of nickel, magnese, and cobalt quite similar to Bell Labs Number 2 Material.

The active flake would be a 0.15 x 0.15 mm detector with a sensitive area of 0.1 x 0.1 mm. The active flake will be optically centered beneath an N-type germanium hyperhemispherical immersion lens (radius 0.15 in.) included to increase the apparent size of the detector to an acceptable level. The lens will be used in lieu of a meniscus spectral filter cited earlier. The lens does not introduce any spherical aberration or coma nor does it have a salient affect on the previous assumptions employed in this analysis.

The baseline thermistor bolometer is similar to the flight-qualified detector utilized in the ITHACO Conical Earth Sensor. The salient performance parameters of this detector are summarized below:

Responsivity	300 Volts/Watt
Time Constant	<5.0 milliseconds (32 Hz)
Noise (at 25°C, 1 sigma)	220 nanovolts $Hz^{-1/2}$ RMS at 2 Hz 70 nanovolts $Hz^{-1/2}$ RMS at 10 Hz 50 nanovolts $Hz^{-1/2}$ RMS at 100 Hz 35 nanovolts $Hz^{-1/2}$ RMS at 500 Hz 30 nanovolts $Hz^{-1/2}$ RMS at 2000 Hz

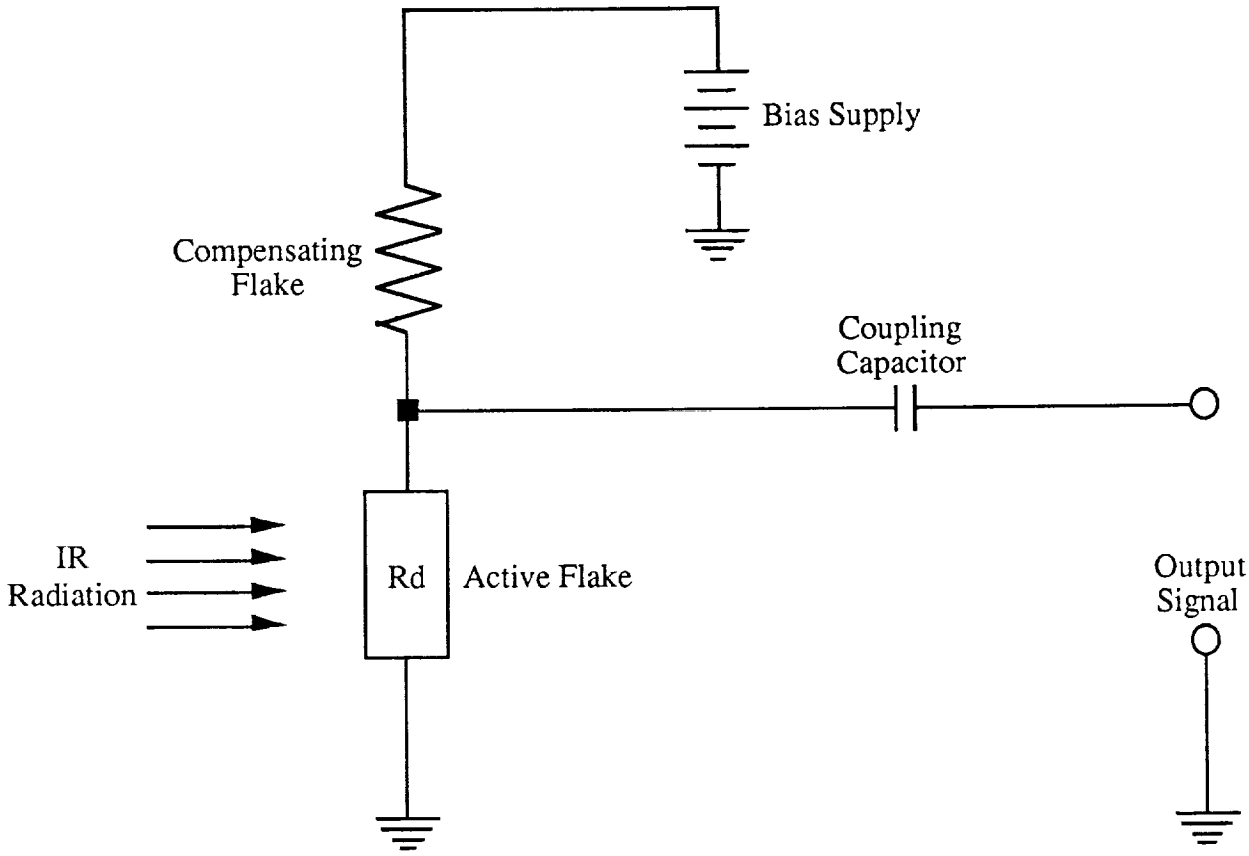

Figure 5-18: Bolomter Construction and Electrical Schematic

5.2.4.1.1 Bolometer Performance

Assuming that the SCANWHEEL system has been optimized for operation at a maximum rate of 2000 RPM and a 45° scan cone, the system bandwidth is 2.2 KHz. Incidentally, the system bandwidth for larger half angles and slower scan rates would be quite similar. Bandwidths may be chosen based on minimizing radiance errors, noise equivalent angle, or a vector combination of the two.

Minimizing radiance errors typically entails holding maximum signal fidelity throughout the signal processing system, while minimizing noise equivalent angle required maintaining the maximum slope to noise ratio. Noise will be the dominant concern, based on the choice of spectral filter.

Integrating the bolometer noise spectrum with a fully compensated analog processing channel, (6 dB pole at 32 Hz), the integrated noise reflected to the detector input is 33.9 (10^{-6}) Volts RMS. The signal received by the detector viewing a worst case 200 °K earth is 0.523 (10^{-6}) Watts, thus the detector output signal is 0.523 (10^{-6}) Watts x 300 Volts/Watt = 156.7 (10^{-6}) Volts. For a 250°K earth the output signal improves to 407.9 (10^{-6}) Volts. Under near worst case conditions the signal is only 4.6 times greater than the 1 sigma noise.

Referring to Figure 5-19, which illustrates our normalized crossing ramp in conjunction with its 1st and 2nd derivatives, a rate of threshold crossing for the 1st derivative is 0.135 microwatts/degree x 300 volts/watt. This yields 40.5 microvolts/degree. With a 1 sigma noise of 33.9 microvolts, the resultant noise equivalent angle is 0.837 degrees per edge. Each edge may be averaged 16.667 times per second, hence our result is a 0.205 degree, 1 sigma - 1 second time constant, noise equivalent angle.

Phase knowledge is derived by the numerical average of the four edge crossings. This results in a phase noise gain of 0.5, hence our phase noise equivalent angle is 0.103 degrees (1 sigma). Chord utilizes the difference between the trailing edge and leading edge crossing points. Our noise gain is unity, resulting in a chord noise equivalent angle of 0.205 degrees (1 sigma).

All values cited here are in terms of instrument coordinates. Actual on-orbit values must include other instrument error terms, both correlated and uncorrelated, added as their frequency dependent vector sum, and reflected through the appropriate spacecraft mounting geometry, spacecraft attitude and altitude, and attitude determination algorithm.

Since the dominant high frequency noise is Johnson Noise, our high temperature specification extremum of 71°C will affect both our signal and slope-to-noise performance by approximately the ratio of the square roots of the temperatures, or an effective noise gain factor of 1.69 when comparing performance at 25°C and 71°C.

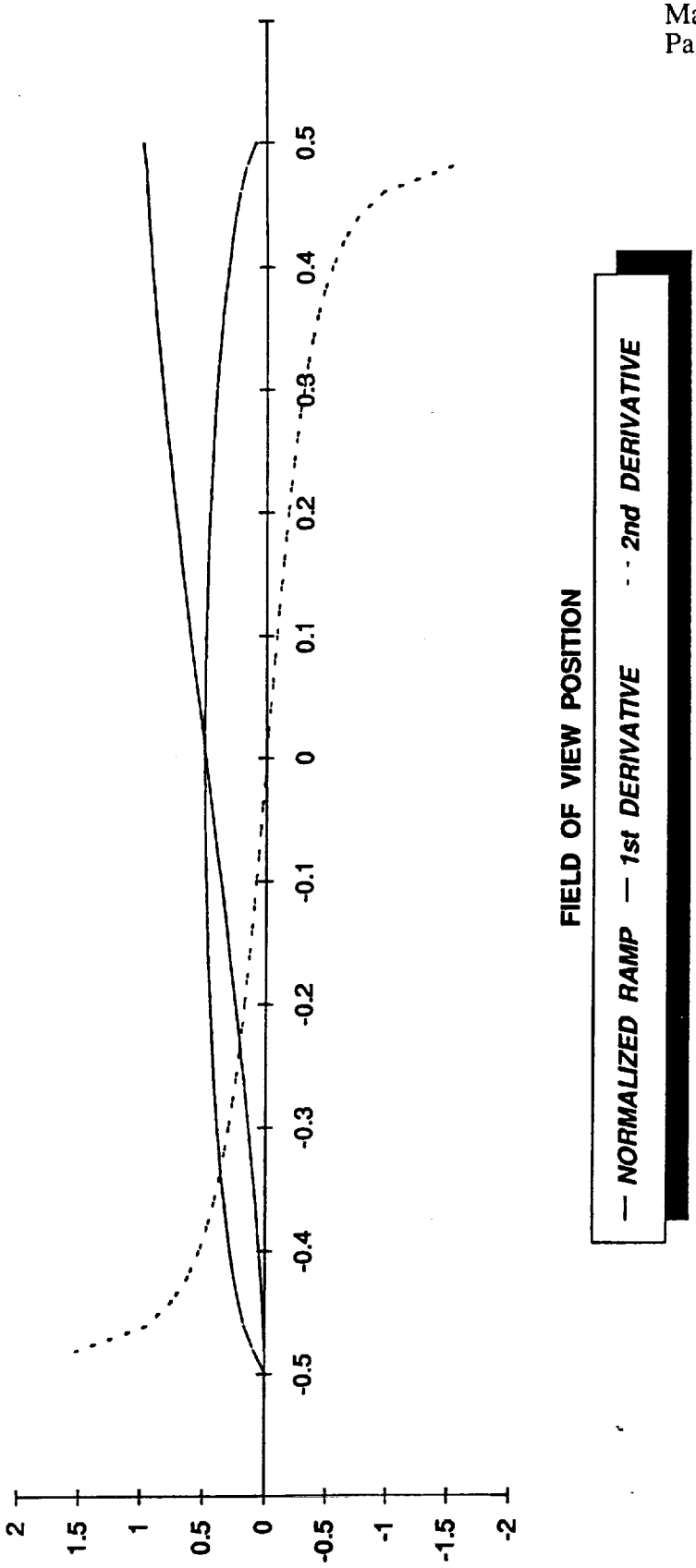

Figure 5-19: Normalized earth crossing ramp with 1st and 2nd derivatives

5.2.4.2 Pyroelectric Detectors

As a result of the studies of crystallographic structures, both ferroelectricity and pyroelectricity have been discovered. In particular, although many of the non-centrosymmetric crystals exhibit a strong spontaneous electric polarization effect, no electric field is normally observed at the external surfaces since the material is typically a conductor. In this case the mobile charge carriers assume a distribution which neutralizes the internal dipole moment.

Good pyroelectric materials, which then are necessarily good insulators, have relatively stable extrinsic charge distribution and even low frequency changes in the detector flake will produce changes in both the lattice spacing and dipole moment. Since the stray surface charges will not rapidly respond to these changes, an external electric field is produced which may be measured. Figure 5-20 illustrates the architecture of the pyroelectric detector and its equivalent electrical schematic.

The temperature coefficient of the external dipole moment is known as the pyroelectric coefficient. For the purposes of this analysis we will express the pyroelectric coefficient (dP_s/dT) in terms of Coulombs $cm^{-2}°K^{-1}$.

A number of excellent pyroelectric materials are available. Unfortunately, all ferroelectrics loose their polarization if a limit known as the Curie temperature is exceeded. The two pyroelectric materials which are known to possess significant flight heritage are Lithium Tantalate ($LiTaO_3$) and Deuterated Triglycine Sulfate (DTGS). $LiTaO_3$ has a Curie temperature which has a moderate dependency upon crystal composition. For our material of choice, the Curie point is in excess of 460°C. DTGS, which possesses better responsivity than $LiTaO_3$, also demonstrates a much lower Curie point of 62.9°C. DTGS is both hygroscopic and relatively fragile, so it was eliminated from consideration and a 1 mm diameter $LiTaO_3$ flake was considered for the baseline pyroelectric detector design.

It is well known that the responsivity of a pyroelectric detector is inversely proportional to its area. Overall performance is also governed by the effective voltage divider created by the detector capacitance against the gate capacitance of the field effect transistor impedance amplifier. Hence, decreasing the detector area further does not result in a significant improvement and would also introduce a number of significant constraints on the optical system design.

The salient performance parameters of a sample pyroelectric detector are summarized below:

Responsivity	1400 Volts/Watt
Time Constant	≈5.0 milliseconds (30 Hz) (-6 dB gain slope at 30 Hz)
Noise (at 25°C)	210 nanovolts Hz-1/2 RMS at 0.03 to 30 Hz (-4 dB gain slope at 30 Hz)

At the thermal break point the signal drops at -6 dB while the noise decreases at only -4 dB. This results in an effective 2 dB per octave noise gainslope.

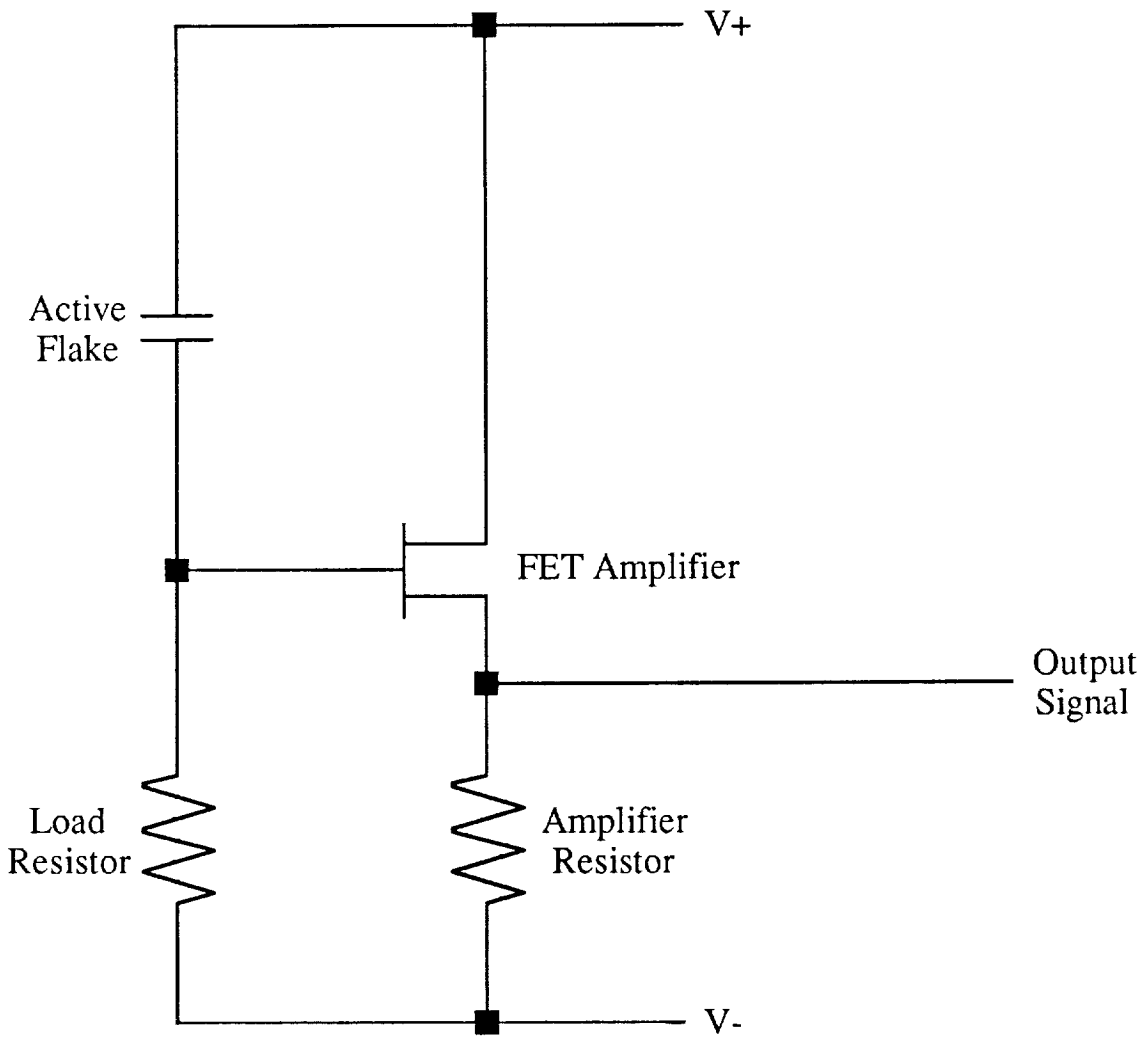

Figure 5-20: Pyroelectric detector construction and electric schematic

5.2.4.2.1 Pyroelectric Detector Performance

Using analysis techniques similar to those employed previously on our bolometer, the integrated noise for a fully compensate 2.2 KHz system bandwidth is 33.4 microvolts RMS. The signal received by the detector viewing a worst case 200°K earth is 0.523 (10^{-6}) watts, thus our detector output signal is 0.523 (10^{-6}) watts x 1400 volts/watt = 732.2 (10^{-6}) volts. In this instance the detector output signal is 21.9 times the 1 sigma noise value. For a 250°K earth our output signal, improves to 1.903 (10^{-3}) Volts.

Each threshold crossing has a slope of 0.135 microwatts/degree x 1400 volts/watt which yields 189.0 microvolts/degree. With a 1 sigma noise of 33.4 microvolts, the resultant 1 sigma noise equivalent angle is 0.1767 degrees per edge. As before, each edge may be averaged 16.667 times per second, hence our result is a 0.0433 degree, 1 sigma - 1 second time constant, noise equivalent angle.

Phase knowledge, employing a noise gain of 0.5, is 0.0216 degree (1 sigma). Chord, with a noise gain of unity, possesses a noise equivalent angle of 0.0433 degree (1 sigma).

5.2.4.2.2 Microphonics

Lithium tantalate, as with all pyroelectric materials, is fundamentally piezoelectric in nature. Piezoelectric pickup originates from the same inherent mechanism of dipole movement which is the basis for pyroelectricity. Some crystals, even those which are not pyroelectric, can develop a spontaneous dipole moment when mechanically strained; i.e., by suitable squeezing, their crystal structures they many be distorted to ones which can sustain a dipole moment. These crystals are defined as piezoelectric.

In order to minimize for the potential microphonics in a pyroelectric detector, a compensation flake was initally suggested in the detector to cancel out the detector response to mechanical accelerations. It was later established that a non-microphonic mount was a more suitable alternative to minimize the microphonic pickup.

5.2.4.3 Detector Selection

The performance factors for each detector are summarized in Table 5-1.

Table 5-1: Performance Trade-Off Matrix

Parameter	Thermistor Bolometer	Pyroelectric Detector
Noise Equivalent Angle (1 sigma, 1 sec)		
Phase	0.103°	0.0216°
Chord	0.205°	0.0433°
Microphonic Susceptibility	None	Yes
Environmental Range Limitations	1.6 NEA Degradation at 71°C	None
Flight Heritage	Yes	Yes
ROM Recurring Cost	6 to 8 K	<3 K
Sun Exposure	Unlimited	Unlimited
Bias Supply	Required	Not Required
Optical Design	Standard	Minimum Components

In lieu of the considerations delineated in Table 5-1, 1 mm diameter Lithium Tantalate Pyroelectric Detector was selected.

The primary considerations were:

- the bolometer performance is marginal
- bolometer cost are at least 2:1 greater
- reliability is enhanced through the elimination of a bias supply
- the optical subsystem component count is minimized

5.2.4.4 Detector Performance Testing

Early tests with a detector that had been purchased for the Full Sky Scanner confirmed that microphonics could be a problem. The detector detected and amplified mechanical vibrations from the running wheel which masked any infrared signals that were observed. In order to minimize this pickup, a dual flake detector design was evolved in which one flake was mounted in such a manner that it would be exposed to infrared radiation. A second detector in the same housing would be masked. Field effect transistors buffering each detector were included. The preamplifier that was developed used the FETs in the detector as source followers. Identical low noise amplifiers with a voltage gain of six supplied the detector signal and the compensation signal to the outside world.

5.2.4.4 Detector Performance Testing (Cont'd)

The first stages of the associated signal processing electronics was designed to allow careful matching of the two detector signals. Gain adjustment and frequency response adjustment were provided for each flake. The plan was to subtract out common mode signals (presumable microphonics) while leaving the infrared signal (present in only the active flake channel) for use in attitude determination.

A specification control drawing for the detector was prepared and supplied to Servo Corporation. They were consulted on the design of the detector and supplied considerable information regarding detector construction. At their suggestion, a new copolymer detector material was suggested. It was anticipated that the new material would yield far superior performance over conventional materials. It was expected that the material would yield a response better than 10900 V/W while at the same time having a thermal time constant of a few milliseconds. The combination would yield better signal to noise ratios than were ever obtained with bolometers.

Considerable time elapsed while Servo struggled with the detector construction. The first disappointment came when the new copolymer was found to not operate as expected. It was difficult to handle and some processes that were required did not yet exist. As a result, Servo eventually decided to make at least the initial detectors using lithium tantalate.

Meanwhile, a parallel path was pursued by visiting Infrared Associates to discuss pyroelectric detectors. They were the builders of the detector that had been experimented with earlier. They indicated that they believed that the copolymer was an inferior material and that lithium tantalate was the best room temperature material available. They also commented that the previously supplied detector was microphonic and that they could easily build a nonmicrophonic version. They would prefer to build a T0-5 case unit, but would build some engineering units on a fast turn around basis using the ruggedized case similar to the units which were being procured from Servo. They did not feel that microphonics would be a problem. One unit was built with a single flake and one with a compensation flake in parallel with the active flake. They delivered two single flake units (one loaner) and one dual flake unit. Their detectors arrived at the same time that the Servo detectors arrived.

The Servo units were tested and it was found that the compensation flake did not match the active flake nor could it be made to match. That is, the microphonic pickup did not appear as a common mode signal at all, but seemed to be dependent upon the particular flake parameters. The dual flake Infrared Associates unit also did not compensate microphonics, but made them worse. Both single flake Infrared Associates devices and one of the Servo, Inc. devices exhibited little or no microphonics from the active flake. Thus, it was concluded that nonmicrophonic devices could be obtained which would thus be simpler to use and would also yield a 3 dB signal to noise improvement over that obtained with any microphonic compensation scheme. Both vendor's devices were similar when used in the single flake mode.

As a result of the experiments with the detectors, a new specification was prepared. Several other vendors were also contacted. It was found that the T0-5 configuration is a very common standard among vendors. Thus, the custom package approach was abandoned and designed for T0-5 case detectors that are available in a nonmicrophonic configuration from Servo, Infrared Associates, Molectron, and other vendors.

5.2.5 Position Sensor

A position sensor is required to establish the phasing of the earth scan relative to the fixed portion of the sensor. This is commonly referred to as the Top Dead Center (TDC) or Bottom Dead Center (BDC) pulse, and typically determines the pitch orientation of the spacecraft. The hall sensors used to commutate the brushless DC motor in the reaction wheel provide a digital tachometer signal, but do not provide any once per revolution clocking indication to establish the phasing of the scan. In order to maintain the modularity of the reaction wheel, it was decided to incorporate this position sensor in the Infrared Sensor Assembly (IRSA) which is attached to the reaction wheel. The stimulus for the position signal, or index pulse, is located on the rotating scan mirror. This is desirable since it eliminates any clocking alignment required between the scan mirror and the index indicator, and it does not burden the reaction wheel with extra hardware required for a SCANWHEEL, but not for a stand alone reaction wheel. This type of index pulse is commonly generated by a magnetic pickup, an eddy current probe, or an optical switch.

Magnetic pickups are rugged, reliable, passive devices, used commonly in momentum wheel applications operating at a biased speed. The amplitude of the signal generated from these devices is proportional to speed, so the signal degrades as the speed is reduced. Since the SCANWHEEL must always operate at a biased speed, this operation is compatible with the SCANWHEEL design. The magnetic pickup consists of a permanent magnet with a series pole piece and a coil. As a soft-iron gear tooth is passed by the magnet, the change in the magnetic field produces a voltage in the coil, exactly as occurs in a conventional generator. Voltage and frequency are both directly proportional to actuator speed. This type of position sensor, is passive, so it consumes no power, and is extremely reliable due to its simplicity.

Signals derived from eddy current probes are insensitive to the speed of the flywheel, but require a complex, unreliable oscillator circuit to stimulate the eddy current effect. The accuracy of the eddy current systems is low and the power consumption is high relative to other devices.

Optical switches are also used as encoders in rotating mechanisms, and are commonly used for reaction wheel tachometers, especially where high resolution and high accuracy is desired. Light from an LED is directed towards a phototransistor and interrupted by a shutter or a alternately reflecting/absorbing surface. The simplicity of this design ranks it very high, but the high power consumption required to illuminate the LED is too high for an ultra-low power consumption design.

5.2.5.1 Position Sensor Selection

Due to its heritage, simplicity, reliability and ultra-low power consumption, the magnetic pickup was selected to derive the once per revolution index pulse. A soft iron slug was designed to be attached to the scan mirror, and a rugged magnetic pickup is threaded into a port in the lower part of the SCANWHEEL structure and secured with a jam nut.

5.2.6 Preamplifier

The FET in the detector is selected for low noise and low gate leakage current. The preamplifier uses the FET as a source follower driving a low noise operational amplifier stage with a gain of 11. The amplifier is configured to drive capacitive loads without oscillating. In order to allow the high gain, a second amplifier operates as an integrator and adjusts the FET gate voltage to maintain the source follower output at zero volts. As a result, the preamplifier output will remain near zero volts allowing additional gain in the input stages of the signal processor to be applied without additional AC coupling.

5.2.7 Signal Processor

One of the goals of the SCANWHEEL design was to make its performance comparable to that obtained with dedicated conical earth sensors. In order to avoid a compromise in accuracy, several steps were taken in the design of the signal processing that operates on the detector signal.

Previous SCANWHEEL systems used either a fixed radiance locator (Nimbus, HCMM, SAGE, etc.) or a normalized radiance locator (ERBES). Both the fixed radiance and the normalized radiance systems yielded 0.5 to 1.0 degree performance. A more accurate differentiating locator was subsequently developed for fixed speed scanners that promised to yield 0.1 degree performance. Flight data from the Landsat 4 and 5 programs showed that the locator did indeed perform to better than 0.1 degree accuracy except near the winter polar regions where accuracy degraded up to 0.3 degrees. It is believed that were the locator combined with a tighter optical passband, the performance could exceed 0.1 degree over any point of the earth, of course subject to altitude and oblateness corrections. The SCANWHEEL signal processor design shown in Figure 5-21 implements the differentiating locator.

The predicted signal-to-noise performance of the copolymer pyroelectric detector was used as a model for the design of the signal processing. The original effort concluded that an electronic bandwidth of 1000 Hz could be used before the signal to noise ratio would be too low for proper operation of the locator. Although wider bandwidth would be desirable for accuracy and ease of operation, the gain with the reduced optical passband and the differentiating locator is expected to yield excellent performance. Unfortunately, the detector performance with the lithium tantalate is not as good.

The primary difference between the anticipated detector and the ones which were purchased is their thermal time constant. The anticipated thermal time constant of 4 - 5 milliseconds implies that the electronic noise gain will be marginally higher than that used with thermistor bolometers (2 milliseconds). The available detectors cannot be manufactured with such a low time constant. The best obtained to date has a 65 millisecond time constant, resulting in a significant increase in the noise bandwidth of the electronics and a degradation in the signal-to-noise ratio that was anticipated.

Considerable effort, using ITHACO IR&D funds, has been expended examining and understanding the performance of the pyroelectric detector and searching for an optimum FET. New specifications and improved performance are anticipated for the next group of detectors. Based upon the anticipated performance, the signal processor was redesigned and the filter bandwidth reduced to 500 Hz. It is anticipated that this filter will allow proper operation of the system.

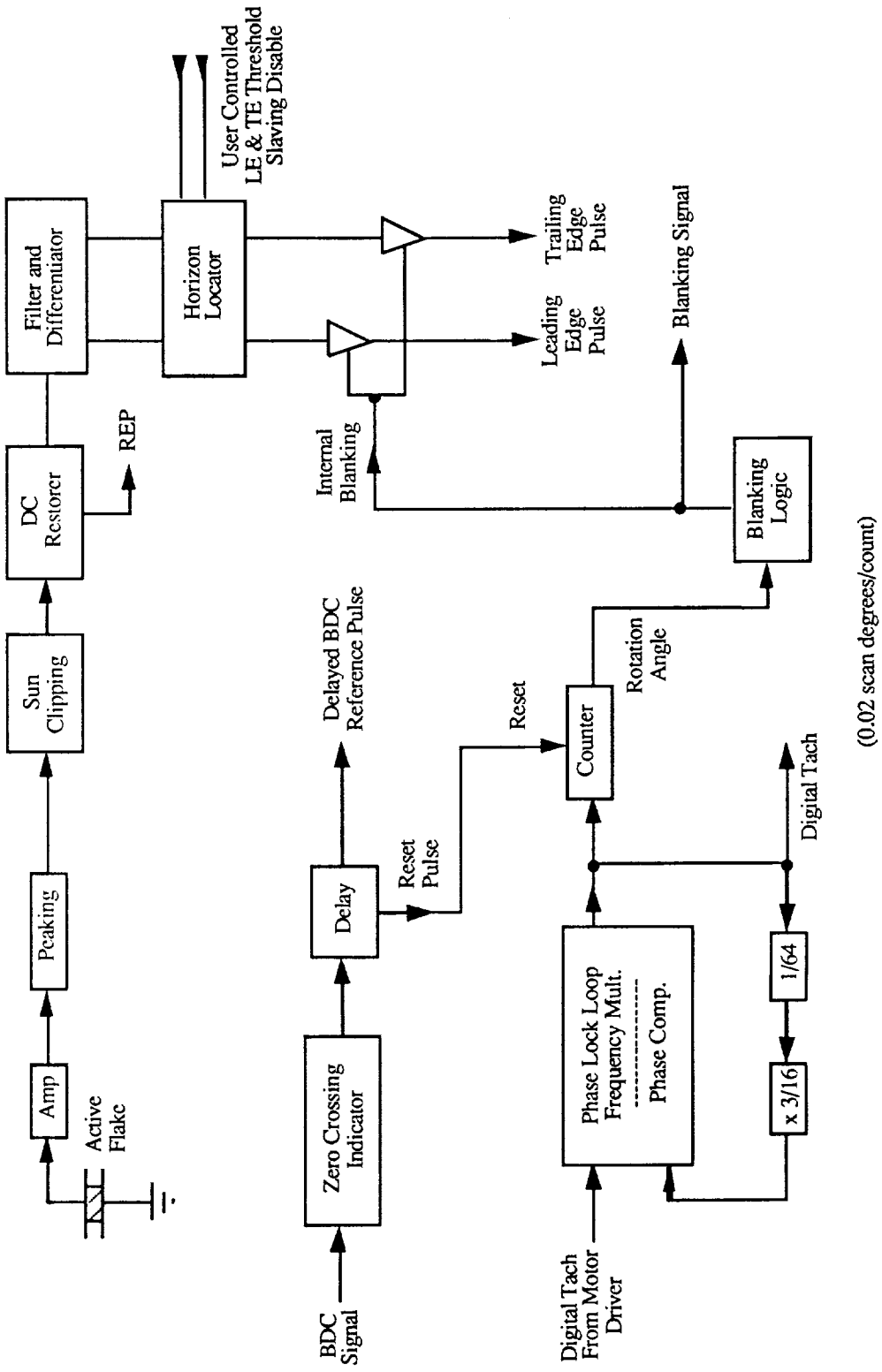

Figure 5-21: Signal Processor - Functional Block Diagram

5.2.7 Signal Processor (Cont'd)

The signal processor design follows classical signal processing steps that parallels previous systems. The preamplifier signal is first amplified and then treble boosted to compensate for the thermal lag of the detector. Once the treble boost (also referred to as peaking) is applied, the signal is DC restored and clipped to limit the power of a sun or moon signal. A classical analog signal processing problem, how to recover quickly from an overload, is solved by increasing the signal bandwidth and clipping.

DC restoration, at first glance, might not seem useful since the signal is differentiated again prior to applying the locator. There are two reasons for the DC restoration. First, the DC restoration allows more precise sun limiting. Second, the DC restorer will function even if the leading edge of the earth signal is hidden behind the blanked region of the scan. We must blank because the SCANWHEEL support structure obscures part of the viewing cone of the SCANWHEEL. The DC restorer signal is fed to later attitude processing electronics to assist in operation with the earth edge obscured.

Once the sun signal is clipped down, the signal bandwidth is reduced by a filter that can be tailored to a certain extent for the anticipated mission of the SCANWHEEL. The filter output is fed to a differentiator which provides a measure of the slope of the horizon crossing signal generated by scanning from the hot earth to cold space and back.

The edge signals are fed to a comparator which responds whenever the signal exceeds a level based upon an average of previous signals. The averaging scheme allows the threshold to adjust itself as the signals become weaker or stronger. By adjusting the threshold, optimum accuracy is obtained since amplitude variations due to varying earth temperatures or detector sensitivities are removed. The fast attack, slow decay system has been used on conical earth sensors with success. The comparator outputs are provided to attitude computation circuitry on other electronics.

A second portion of the signal processor monitors a once-around reference signal from the SCANWHEEL and also monitors signals from the motor commutation logic in the motor driver. A phase lock loop, locked to the commutation signals provides a high frequency pulse train (18432 pulses per turn) which is useful in attitude computation logic. Simply counting these pulses between leading edges and trailing edges of the earth will determine the length of the earth pulse without regard to the speed of the wheel.

The 18432 pulses per turn signal is also fed to a binary counter where it is counted down. A set of NAND and NOR gates allows selection of blanking in 5 degree steps at the time of assembly. In this manner, any portion of the scan can be selected to be predefined (blanked) so that the SCANWHEEL optics and any other portions of the spacecraft can intrude into the scan path of the sensor.

5.2.8 Structure

The requirements for the structural design are primarily dictated by the random vibration and thermal environments encountered by spacecraft hardware. The structure must be able to withstand the loads and stresses during launch, and not distort or degrade during exposure to ambient temperature changes and unidirectional exposure to direct sunlight.

The scheme devised for supporting the off-axis optics housing above the rotating scan mirror includes a bridge which spans two of the mounting tabs on the reaction wheel, as shown in Figure 5-1. A pedestal supports an optics housing which contains the detector, objective mirror, and the preamplifier. The position sensor and the connector are contained in the bridge portion of the assembly. The entire subassembly consisting of the detector, optics housing, objective mirror, detector, filter lens, pedestal, bridge, connector, position sensor, and preamplifer is referred to as the Infrared Sensor Assembly (IRSA). The mounting scheme for the IRSA expands the mounting options for the SCANWHEEL to the spacecraft. The SCANWHEEL can be mounted from the six mounting tabs on the bottom of the assembly, or the IRSA can be inserted into a cutout, and the four exposed tabs on the IRSA side of the SCANWHEEL can be used to interface with the spacecraft.

5.2.8.1 Structure Material

Aluminum was selected as the primary structural material due to its relative low cost, low weight, and high thermal conductivity. A variety of aluminum alloys are categorized as highly resistant to stress corrosion cracking in Table 1 of MSFC-SPEC-522A, which allows their use in structural applications on Space Shuttle payloads without a Material Usage Agreement. In order to eliminate all these potential waivers, it was decided to limit material selection to materials in Table 1 of MSFC-SPEC-522A, and dissimilar metal combinations were required to comply with MIL-STD-889.

The one drawback of the aluminum is its relatively high coefficient of thermal expansion (CTE). In an optical systems, materials with a low CTE are frequently used to minimize focal length changes which can defocus the system. The relatively long focal length and large detector area in the optical design result in small effects from focal length changes. This same effect is desirable to minimize the criticality of a precisely aligned detector. More critical than the CTE, then, was the ratio between the CTE and the thermal conductivity. This ratio will influence the tendency of the structure to thermally distort when it is placed in an ambient environment where it is heated on one side from direct sunlight exposure, and cooled on the other side due to radiation to cold space. Assessing the candidate materials of aluminum, magnesium, titanium, steel, copper and beryllium, aluminum is found to be superior to titanium, steel and magnesium, but slightly inferior to copper and beryllium. For structural and cost reasons, the aluminum was selected.

Aluminum alloy 6061-T6 was chosen for the SCANWHEEL structure for its low cost and its demonstrated dimensional stability.

5.2.8.2 Sealing

Many reaction wheel designs are hermetically sealed, for a variety of reasons. One reason is to maintain the same level of performance in ground testing as in orbit. This is achieved by either evacuating the interior to a hard vacuum and sealing for life, or temporarily evacuating and sealing the interior for all ground testing and venting the interior prior to launch so it will be exposed to space vacuum. An alternate method backfills the interior with one half atmosphere of inert gas and seals the housing for life, in order to minimize the evacuation stresses on the housing and maintain an operating pressure compatible with the vapor pressure of natural hydrocarbon oils. The backfilled approach also improves the heat transfer within the mechanism by utilizing forced convection from the rotor, at the cost of additional power consumption due to rotor windage.

The off-axis scanning mirror prohibits sealing of the unit without a large, complex and expensive infrared window. In order to eliminate the costs associated with both hermetically sealing the housing and incorporating this impractical window, it was decided to develop a vented design. The major penalty resulting from this decision is that the reaction wheel performance data taken in air will be skewed by the windage torque, requiring a bell jar or thermal vacuum test set-up to acquire actual performance data. However, the windage torque can be easily characterized and removed from the data by a computer data acquisition system. Vented designs have been successfully flown in many momentum wheel and scanner applications, so heritage is not a significant issue.

5.2.8.3 Alignment Scheme

The very nature of an attitude sensing instrument requires reliable alignment schemes in order to establish reference datums and ensure accuracy.

The most critical alignment required is to locate the off-axis parabolic mirror relative to the detector. In order to minimize costs associated with complicated assembly techniques and adjustment procedures, a set of bi-datum alignment pins was selected to allow interchangeability of the detail parts, and simplify assembly procedures. The bi-datum alignment scheme is a derivative of a classic pure kinematic mount, which restrains an object in only six degrees of freedom. As shown in Figure 5-22, the semi-kinematic mount used to mount the off-axis parabolic mirror uses three mounting pads for a primary datum, a precision dowel pin as a secondary datum, and a second precision dowel pin as a terciary datum. The mirror interfaces with these three datums with a flat surface to restrain it in three degrees of freedom, a precision hole to restrain it an additional two degrees of freedom, and a slotted precision hole to restrain it in the sixth degree of freedom. By only restraining the mirror by the minimum six degrees of freedom, distortions in the mirror and/or mounting surface are minimized. In addition, the repeatable assembly procedure allows interchangeability between various mirrors and optics housings.

The same bi-datum alignment scheme was used throughout the IRSA to ensure repeatable and accurate alignment of the bridge to the reaction wheel housing, the pedestal to the bridge, and the optics housing to the pedestal.

The alignment of the sensor on the spacecraft is also a consideration, requiring a repeatable alignment reference. A typical method of accommodating this is with a set of reference mirrors on the hardware. In the SCANWHEEL application, the calibration data taken during testing must be correlated to the reference mirrors. This is accomplished by taking the data relative to a hole/slot datum set on the mounting surface of the reaction wheel, and subsequently measuring the alignment relationship between the mirrors and the same mounting surface datum. The cumulated data can establish the relationship between the alignment mirrors and the calibration data.

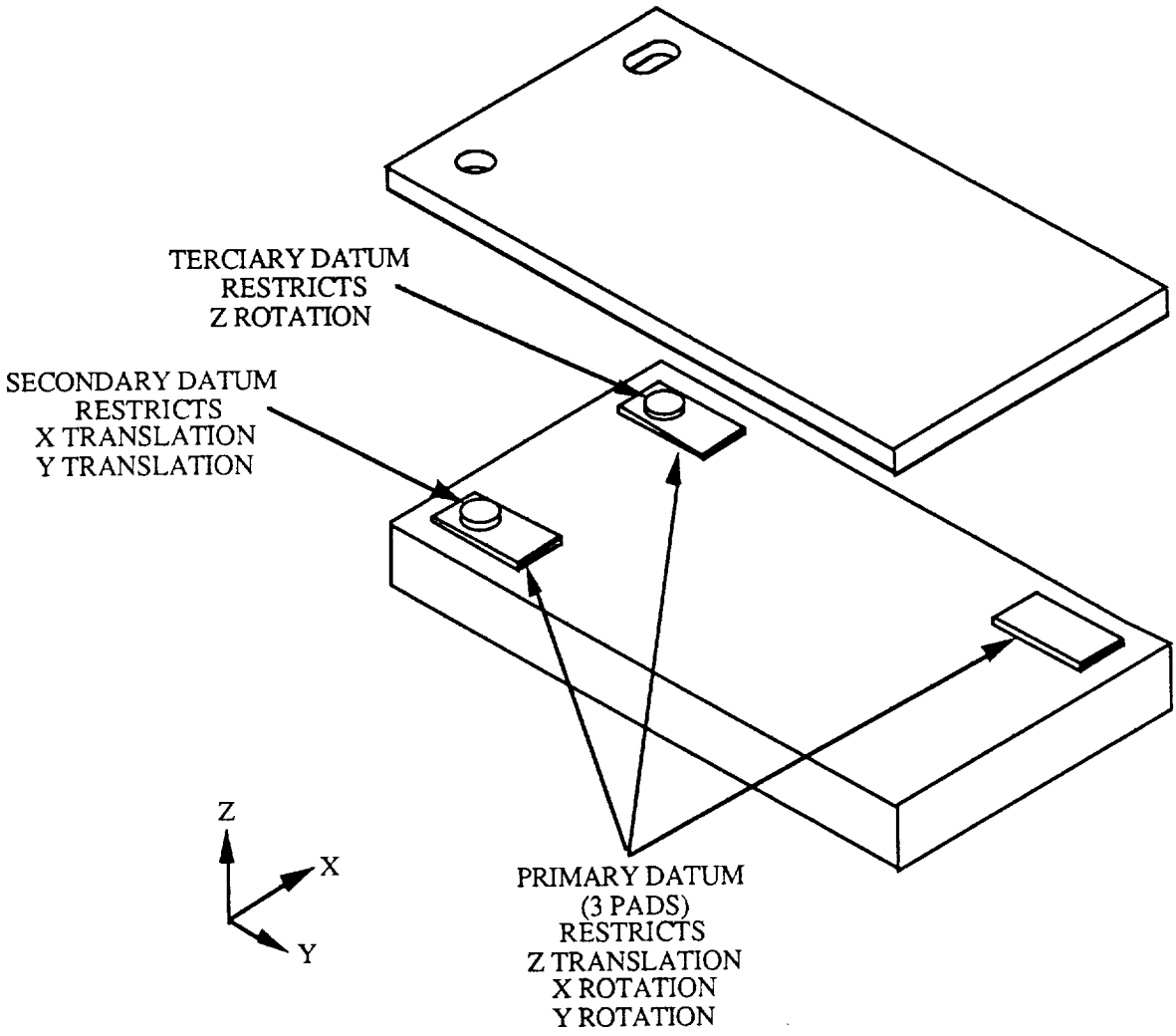

Figure 5-22: Mechanical alignment of precision components in the SCANWHEEL design use classical kinematic mounting schemes.

5.2.8.4 Thermal Design

Since the SCANWHEEL was design for minimum power consumption, the common thermal issue of heat rejection is not a serious consideration. Dissipation is minimal, and the all aluminum construction provides extremely low impedance thermal paths, resulting in worst case temperature rises during operation of less than 5°C. However, in order to provide the SCANWHEEL with the required field of view, it must be placed on the outside of the spacecraft. The primary thermal issue is exposure to cold space and direct sunlight.

The reaction wheel housing is painted with a high emmissivity Chemglaze Z306 black paint, in order to maximize the heat exchange rate with the surrounding equipment within the spacecraft. The IRSA may have a clear view factor out of the spacecraft, and is mildly sensitive to alignment distortion from unidirectional heating or cooling. The high thermal conductivity of the aluminum and the structural geometry result in very low temperature gradients from one side of the IRSA to the other, even during the worst case scenario of one side absorbing 100% of direct sunlight and the other side radiating to a black body at absolute zero.

5.2.8.5 Electronics Packaging

It is desirable for the pyroelectric detector preamplifer to be in close proximity to the detector. In order to accomodate this, and minimize the package outline of the IRSA, the preamplifer was packaged on a flexprint assembly, with rigid fiberglass epoxy portions for mounting the components. The detector leads are lap soldered directly to pads on the outside layer of the printed circuit board, with sufficient strain relief, and the assembly folds up into a compact package for integration directly into the rear portion of the optics housing.

The signal processor is packaged in a standard 6"x6"x1" ITHACO card frame. This can be mated to reaction wheel motor driver and provided with a cover and a mounting baseplate, or stacked together with a series of attitude control electronics assemblies.

6.0 FINAL DESIGN DESCRIPTION

The SCANWHEEL is a momentum/reaction wheel with an integral high accuracy Conical Earth Sensor. The SCANWHEEL provides both angular momentum and control torque while the Conical Earth Sensor obtains precise attitude information. By combining attitude determination and control functions into a single piece of hardware, only one set of bearings and one motor is required, which reduces weight, minimizes power consumption, and enhances the system reliability. A cross section identifying the major components of the SCANWHEEL assembly is shown in Figure 5-1.

6.1 Optical System

The SCANWHEEL optical system consists of a planar, first surface diamond machined scan mirror which is directly coupled to the reaction wheel flywheel, a diamond machined off-axis parabolic objective/fold mirror, a germanium meniscus filter lens, and a pyroelectric infrared detector. The scan mirror reflects light by 45° causing the field of view to sweep a 45° half apex angle cone in space. When the field of view alternately crosses cold Space and the hot Earth, the infrared signal produced by the Earth is detected, amplified, and sent to a separate electronics box for processing into pitch and roll attitude information.

6.2 Reaction Wheel Subassembly

The Reaction Wheel Subassembly, shown in Figure 5-3, consists of an aluminum flywheel with a thermal fitted stainless steel shaft suspended on ball bearings and driven by an ironless armature brushless DC motor. The housing structure is made up of two symmetrical aluminum plates which are separated by a cylindrical ring on the outside diameter and form a spider-web bridge to support the rotor. As is common with many flight proven reaction wheel assemblies, the housing is vented to space to minimize viscous drag torque from the flywheel due to windage.

6.2.1 Ball Bearing Suspension System

The flywheel is suspended by a pair of non-separable, angular contact, spring preloaded ball bearings. The inner races of the bearings are clamped onto a stainless steel shaft by spanner nuts, and the outer races are slip fit into stainless steel cartridges. A wavy washer preload spring provides a light preload to remove the axial and radial play in the bearings, and accommodate the axial thermal expansion of the shaft and housing. The two bearing cartridges are identical, and are aligned with a similar slip fit with the aluminum housing. Assembly machining of the bore through the housing ensures precision alignment of the bearings, and also provides excellent momentum vector alignment. A sketch of the suspension system layout is shown in Figure 5-4.

The bearings are a standard R4 configuration purchased to ABEC 7 tolerances. The arrangement shown was chosen for its stability and low drag torque, since a complete suspension can be accomplished with two bearings by preloading the bearings with a preload spring. An alternate method of preloading with duplex pairs requires twice the bearing count, which doubles both the power and cost of the bearing units. The angular contact bearings employ one piece phenolic ball separators, which do not significantly contribute to wear, and can be impregnated with a small supply of lubricant.

6.2.2 Lubrication System

Since the Reaction Wheel Assembly is vented to space, a low vapor pressure oil is used to minimize lubricant depletion due to outgassing. The Pennzane X2000 is a synthetic hydrocarbon with an extremely low vapor pressure, which has demonstrated excellent boundary lubrication capability when used with Lead Napthanate as an extreme pressure additive.

The bearings selected for ITHACO's Reaction Wheel use conventional 52100 steel races, and steel balls coated with titanium carbide (TiC) applied by chemical vapor deposition. The insolubility of the TiC ball coating with the steel races eliminates the microwelding during sub-EHD operation. In addition, the TiC coating provides an 'emergency lubrication' scheme, providing extended lifetime throughout the entire operating speed range even after the lubricant supply is completely exhausted. An optional high capacity bearing using 440C stainless steel balls and races is available for applications which have severe random vibration requirements.

Several features are incorporated into the design of the lubrication system in order to minimize the loss of lubricant from the bearings. Close clearance labyrinth seals are used between the rotating shaft and the bearing cartridges to restrict the flow of molecules toward the vacuum, and the surfaces inside the bearing cartridges are coated with a thin film of the bearing oil to provide a sacrificial oil atmosphere inside the bearing cartridge volume. This film not only serves to provide the oil atmosphere, thereby reducing the net evaporation rate from the bearings, but it will also inhibit the surfaces from becoming a condenser that would rob molecules from the atmosphere surrounding the bearings. In addition, the one piece phenolic retainers are vacuum impregnated with bearing oil in order to serve as a small oil reservoir within the bearing volume. Another source of lubricant depletion from bearings is surface migration. In order to prevent this, a barrier film coating is placed at strategic locations near the bearings. No barrier film is used directly on the bearings, in order to avoid contamination of the bearing surfaces, which would cause non-wetting of that area resulting in a local area of high wear.

6.2.3 Motor

The reaction wheel is driven by a discretely commutated, ironless armature, brushless DC motor. Maximum inertia to weight ratio is realized with the large diameter motor components and the unique feature of the ironless armature motor which strategically places all of the mass of the iron and magnets on the rotor. Hall sensors integrated directly on the armature sense the alternating flux field from the permanent magnets to provide commutation information for the motor driver, as well as a high resolution tachometer signal for speed and direction of rotation information. The motor driver is conveniently packaged in a 6" x 6" x 1" card frame, for integrating into a modular attitude control system, or as a separate enclosed electronics box.

6.3 Position Sensor

A once per revolution index pulse is provided by a magnetic pickup which senses a soft iron slug attached to the scan mirror. This information establishes the phasing of the earth scan relative to the fixed portion of the SCANWHEEL. This is commonly referred to as the Top Dead Center (TDC) or Bottom Dead Center (BDC) pulse, and typically determines the pitch orientation of the spacecraft.

6.4 Signal Processor

A signal processor conditions, amplifies, and limits the raw detector output which can then be subsequently processed into phase and chord information by an I/O card, and also prepares the once per revolution rotor position reference signal. The signal processor is conveniently packaged in a 6"x6"x1" card frame, which, together with the motor driver of similar configuration, can be integrated into a modular attitude control system, or provided as a separate enclosed electronics box.

7.0 BREADBOARD UNIT MANUFACTURE

An engineering breadboard model of the reaction wheel was fabricated in order to validate the design decisions and assess the manufacturability of the hardware. No serious problems were encountered during the fabrication of the hardware.

7.1 Breadboard Unit Configuration

The present configuration of the breadboard hardware is a complete assembled IRSA with a bridge, pedestal, optics housing and magnetic pickup. A preamplifier on a flex print circuit board is contained within the optics housing with interconnection through a 15 pin sub-miniature D connector. The magnetic pickup is interfaced through a 9 pin sub-miniature D connector on the side of the bridge. The IRSA and a scan mirror can be mated directly to the reaction wheel built to support Contract NAS5-30307 to form a complete engineering breadboard model SCANWHEEL. The signal processor is constructed on vector board.

8.0 BREADBOARD UNIT TEST DATA

The objective the testing performed on the breadboard hardware was to verify the optical design and assess the performance of candidate pyroelectric detectors.

8.1 Optical Design Verification

In order to verify the performance of the optical system, a test was set up to measure the field-of-view (FOV) of the engineering breadboard model. The SCANWHEEL Assembly was mounted on an optical bench which includes a collimated light source and a two axis gimbal for manipulation of the test specimen. A propane mantle is used as an energy source for the collimator, which is interrupted by a chopper wheel to produce an AC signal. A computer controls the movements of the two-axis gimbal set, and reads the output from the SCANWHEEL signal conditioner fed through a lock-in amplifer. The data are converted into a FOV plot of signal percentage versus angle. Figure 8-1 shows a FOV plot using a Servo detector. The 50% signal contour shows that the FOV of the optical system is approximately 1.5°x1.7°, versus a design of 1.5°. This is considered to be right on target, which verifies both the optical design and the optics fabrication.

8.2 Detector Performance Evaluation

In order to evaluate the performance of candidate pyroelectric detectors, the breadboard SCANWHEEL was set up on an earth simulator test station, which utilizes a hot plate and a room temperature crescent shape to simulate the earth/space (hot/cold) transition. An adapter plate is used to mount the SCANWHEEL on a two axis gimbal for adjustment of the attitude of the hardware relative to the co-ordinates of the simulated earth.

Testing of an off-the-shelf detector from Infrared Associates early in the program revealed that microphonic pickup could be a serious consideration in the performance of the pyroelectric detector. The detectors procured from Servo and a subsequent detector procured from Infrared Associates were fabricated with two flakes, one active and one masked for microphonic cancellation. Tests indicated that this compensation scheme was not effective. Matching between the detector responses was so poor that there was no advantage to the cancellation scheme, in fact the noise was increased by a factor of the square root of two. Noise tests were then performed using only the single active flake on the detectors, with the results shown in Table 8-1. Proprietary microphonic mounting techniques on the Infrared Associates detectors resulted in units with considerably less microphonic susceptibility.

Additional details on the detector performance testing is included in Section 5.2.4.4.

The test results indicated that a single flake with non-microphonic mounting techniques would satisfy the detector requirements.

A photograph of the differentiated output waveform within the signal processor showing leading edge and trailing edge pulses from a simulated earth is shown in Figure 8-2.

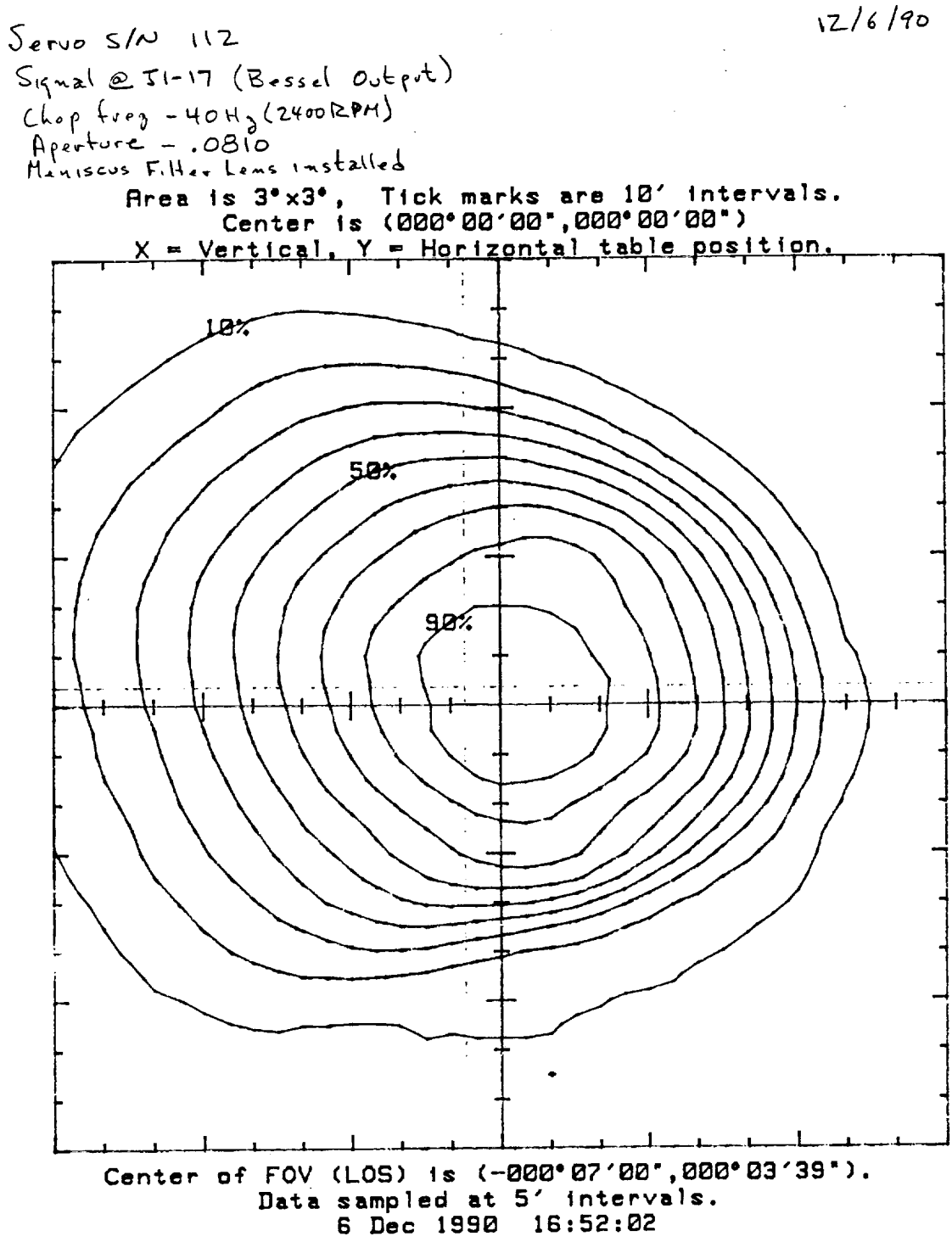

Figure 8-1: A field of view measurement confirms the accuracy of the optics design and fabrication

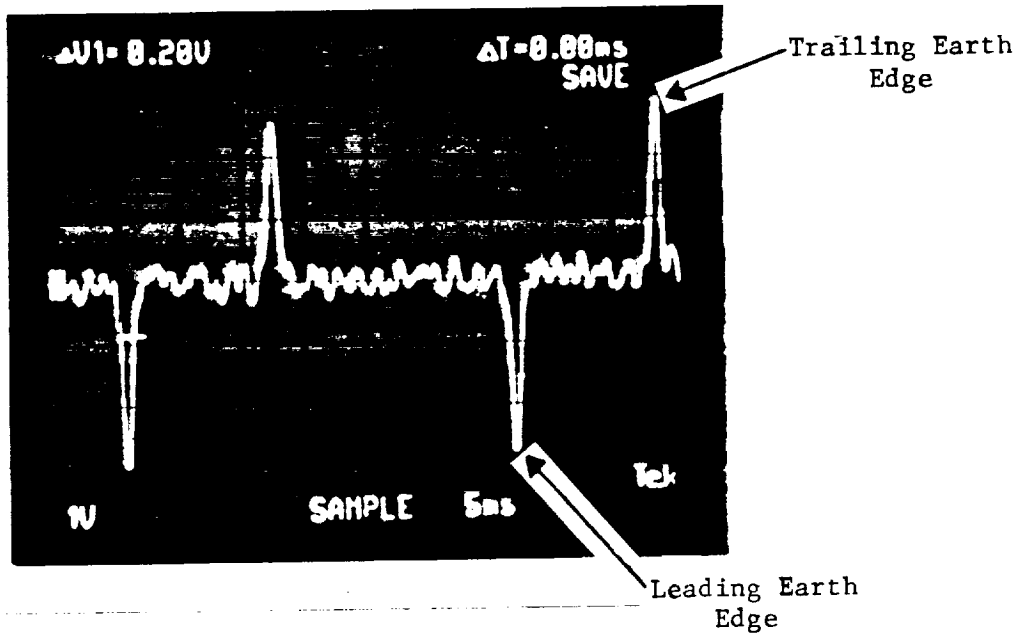

Figure 8-2: Differentiated output waveform from simulated earth

Table 8-1

Detector	Noise		Signal	Signal/Noise
	wheel off	wheel running	p/p max	
Infrared Associates Detector #1	0.85 mV	1.05 mV	460 mV	438.1
Infrared Associates Detector #2	0.95 mV	2.40 mV	530 mV	220.8
Infrared Associates Detector #3	0.95 mV	1.30 mV	475 mV	365.4
Servo Detector #1	1.30 mV	2.50 mV	360 mV	144.0
Servo Detector #2	0.75 mV	0.85 mV	355 mV	417.7
Servo Detector #3	0.80 mV	0.82 mV	280 mV	341.5

9.0 PHASE III STATUS

The SBIR successfully transitioned into Phase III development with a contract to deliver the first flight Reaction Wheel Assembly to the University of Bremen in Germany, which will fly on BREMSAT, a small microgravity experiment to be launched from a Get Away Special cannister on a space shuttle mission. Production on this unit is nearing completion. A contract has also been awarded to deliver a Reaction Wheel Assembly and two SCANWHEELs for the Air Force STEP (Space Test Experiment Platform) mission, with follow on contracts imminent for this series of small satellites. The full term development of the SCANWHEEL hardware is continuing with the Phase III production of spaceflight hardware for the STEP missions. ITHACO has also internally funded a life test of the Reaction Wheel Assembly which is currently accumulating operating time.

The design of a larger version of the SCANWHEEL is underway, under a contract with Space Industries, Inc., for an attitude control system for the Wake Shield Facility, which is a free flying spacecraft delivered to orbit by the Space Shuttle and retrieved on a single mission. This hardware to be delivered on this program includes a 5 ft-lbf-sec SCANWHEEL operating at 2000 rpm and a supplementary 15 ft-lbf-sec reaction wheel operating at 6000 rpm. The enlarged version will use the identical bearing system and IRSA, with dimensional changes in the flywheel and housing to accomodate the higher momentum storage requirements.

Potential spacecraft which have baselined the reaction wheel or SCANWHEEL include APEX, SeaStar, and SeaWiffs with Orbital Sciences Corporation, TOMS with TRW and Fairchild, and IRIDIUM with Motorola. These missions generally fall into the category of a new breed of small, low cost satellites requiring low cost, short lead time, proven attitude control systems. The Modular Attitude Determination and Control System (MADACS) developed by ITHACO utilizing the SCANWHEEL and optional supplementary reaction wheels has been found to satisfy the cost, power consumption, and weight requirements for these types of missions.

10.0 CONCLUSION

The development effort did not encounter any insurmountable obstacles which would preclude the low-cost manufacture of a low-power consumption SCANWHEEL. Simplistic and reliable techniques were employed to result in a rugged, yet efficient, design. Processes are in place to manufacture the reaction wheel in large or small quantities, and with options for various levels of traceability and documentation. An interface description of the final design available for off-the-shelf delivery of the reaction wheel is included as Appendix A.

APPENDIX A

ITHACO REPORT 94050

Report 94050
March 21, 1991

SW2A28V

SCANWHEEL ASSEMBLY

INTERFACE DESCRIPTION

Prepared by:

ITHACO, Inc.
735 W. Clinton St.
P.O. Box 6437
Ithaca, NY 14851-6437

TABLE OF CONTENTS

TABLE OF CONTENTS (Cont'd)

1.0 SCOPE

The component hardware described herein consists of one SCANWHEEL (SW) and an electronics box consisting of one Motor Driver (MD) card and one Signal Conditioner (SC) card.

The SCANWHEEL is a combination momentum wheel and scanning earth sensor capable of providing instantaneous reaction torque to a spacecraft, storing angular momentum, and providing data for attitude determination.

This document contains descriptions of component capabilities, interconnection requirements, and user interfaces.

2.0 REFERENCE DOCUMENTS AND DEFINITIONS

2.1 ITHACO Drawings

D43393	SWA Mechanical Outline Drawing
D43428	SW Electronics Box Mechanical Outline Drawing

2.2 ITHACO Documents

RQPS 64.7 ESD Operating Procedure, SSD Manufacturing

2.3 Definitions and Abbreviations

CCW	Counterclockwise
CW	Clockwise
Horizon Locator	Circuit which detects timing and type of a horizon crossing
ILOS	Infrared Line of Sight
LE	Leading Edge (of Infrared Body)
MD	Motor Driver
Motor Torque	Motor torque is the torque generated in the armature of the RW motor.
N	Newton
Reaction Torque	Reaction torque is the torque applied to the spacecraft mounting surface. This is equal to the RW motor torque minus the drag torque.
SC	Signal Conditioner
SW	SCANWHEEL
SWA	SCANWHEEL Assembly (SCANWHEEL plus Motor Driver and Signal Conditioner
TBC	To Be Confirmed
TBD	To Be Determined

3.0 HARDWARE ENVIRONMENTAL CAPABILITIES

This section outlines the environmental capabilities and requirements of the ITHACO supplied hardware.

3.1 Thermal

All supplied components utilize conduction as the primary mode of heat rejection. Aluminum mounting interfaces are flat within 2 mm/m (.002 inch/inch), have surface finishes better than 62 microinches, and are finished with alondine per MIL-C-5541. Similar interfaces are required on the mating surfaces of the spacecraft in order to sufficiently preserve the conduction scheme.

3.1.1 Temperature Range

All components will tolerate an operating baseplate temperature range of -20 to +50°C and operate within spec.

Non-operating temperature range for all hardware is -50 to +85°C.

3.2 Vibration

All components are compatible with random vibration environment shown in Figure 3-1.

3.2.1 Vibration Dynamics (FOR REFERENCE ONLY)

The standard 6" x 6" ITHACO card frames have demonstrated resonant frequencies greater than 200 Hz. The flywheel in the Reaction Wheel is suspended on a set of flexures which results in three vibration modes. The first mode occurs in the axial direction at 100 Hz, with a Q of 6. The second mode is a rocking resonance of the flywheel at 122 Hz. The third mode is a radial translation mode at 350 Hz and a Q of 10.

3.3 Electromagnetic Compatibility

In general, good Engineering practices, such as ground plane construction and on-board power filtering, are used. In addition, most components contain low frequency analog and digital circuitry which do not generate substantial emissions.

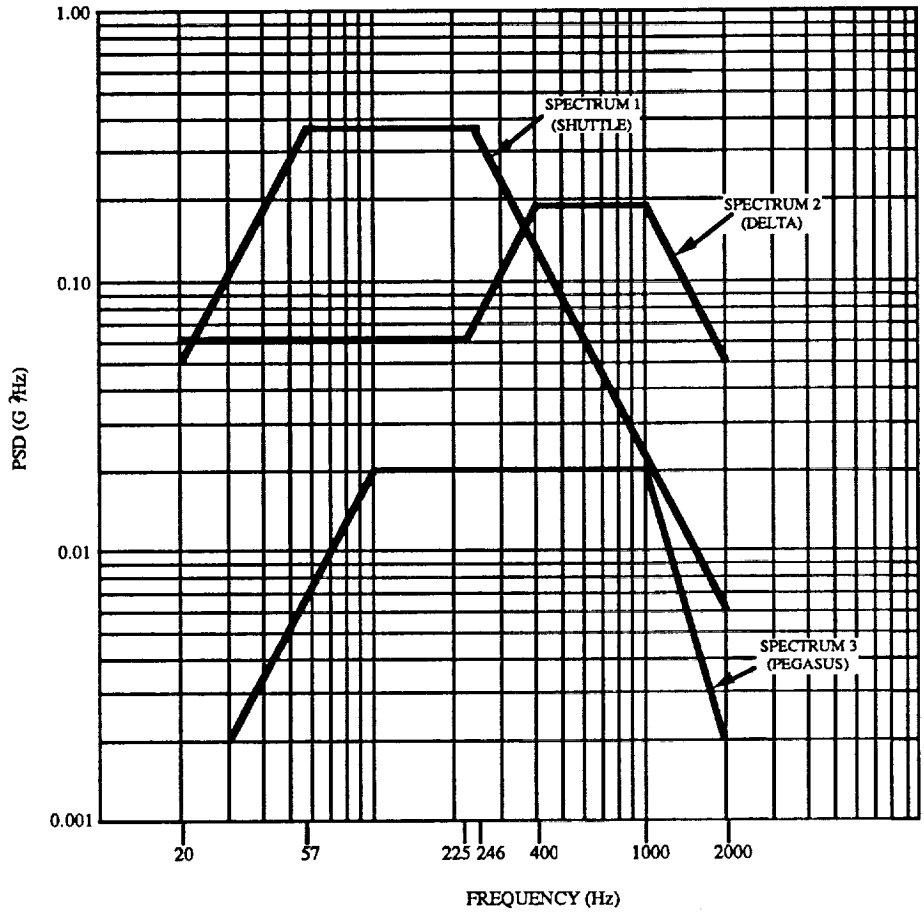

SPECTRUM 1

20 Hz	= .047 G2/Hz
20-57 Hz	= +6 dB/OCTAVE
57-246 Hz	= .36 G2/Hz
246-2000 Hz	= -6 dB/OCTAVE
2000 Hz	= .006 G2/Hz
OVERALL	= 12.4 Grms
DURATION	= 180 SEC/AXIS

SPECTRUM 2

20-225 Hz	= 0.062 G2/Hz
225-400 Hz	= +6 dB/OCTAVE
400-1000 Hz	= 0.193 G2/Hz
1000-2000 Hz	= -6 dB/OCTAVE
TOLERANCE	= ±3 dB
OVERALL	= 15.8 Grms ±10%
DURATION	= 60 SEC ±10%

SPECTRUM 3

20-100 Hz	= +6 dB/OCTAVE
100-1000 Hz	= .02 G2/Hz
1000-2000 Hz	= -12 dB/OCTAVE

FIGURE 3-1
RANDOM VIBRATION SPECTRUM

3.3.1 Regulated Power EMC Requirements

The components require regulated voltages of +5 V ± 5% and ±15 V± 5%. The ITHACO components are designed to tolerate:

Ripple:

+5 V Supply:	50 mV p-p Max,	0-10 MHz
±15 V Supply:	100 mV p-p Max,	0-10 MHz

Transients:

+5 V Supply:	±5 V Max,	10 usec max duration
±15 V Supply:	±15 V Max,	10 usec max duration

Source Impedance:

0.1 to 1 Ω at DC, rising to 50 Ω at 2 MHz.

Emissions of the components onto the regulated power lines are limited by local R-C and L-C decoupling as appropriate.

3.3.2 Power Bus Requirements

The Motor Driver draws power directly from the spacecraft unregulated bus. Requirements are as follows:

Voltage:	28 ± 6 V
Transients:	±28 V, 10 μsec max
Ripple Voltage:	1 V RMS Max, 30 Hz - 400 MHz

3.3.3 External Magnetic Field

The external magnetic field produced by the permanant magnets in the brushless DC motor exhibits a once per revolution alternating flux field which is attributed to the asymmetry of the strength of the individual motor magnets. Figure 3-2 shows nominal measurements of the field strengh amplitude taken in line with the RWA rotation axis. Figure 3-3 shows nominal measurements of the field strength amplitude taken radially from the RWA rotation axis.

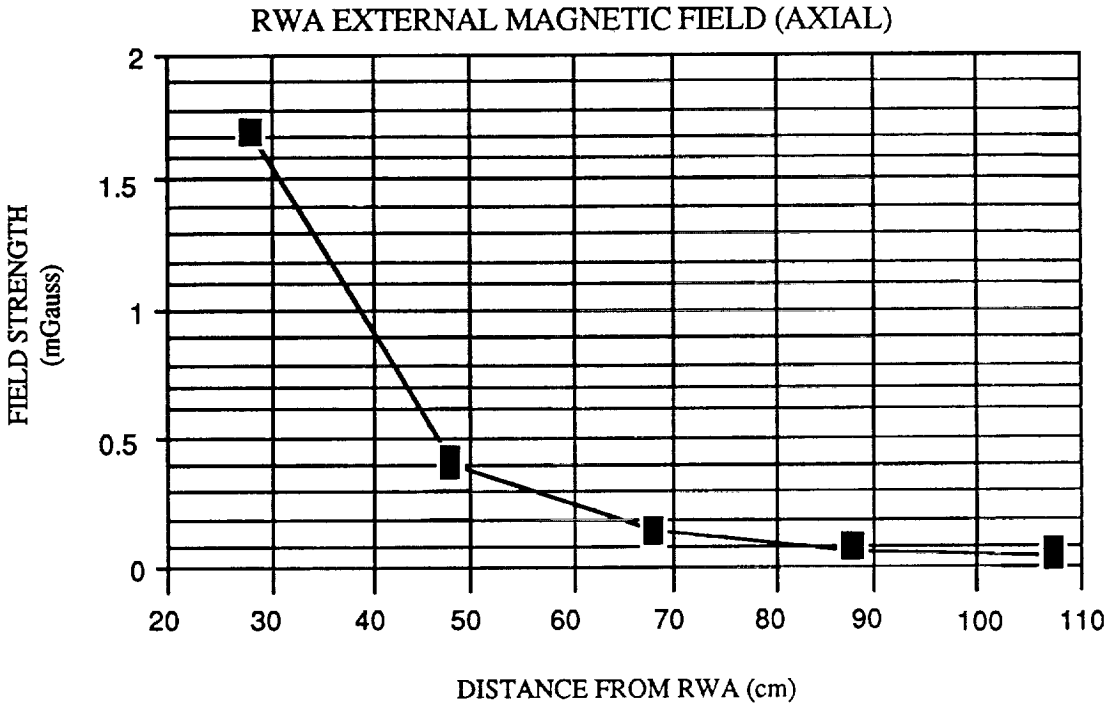

FIGURE 3-2

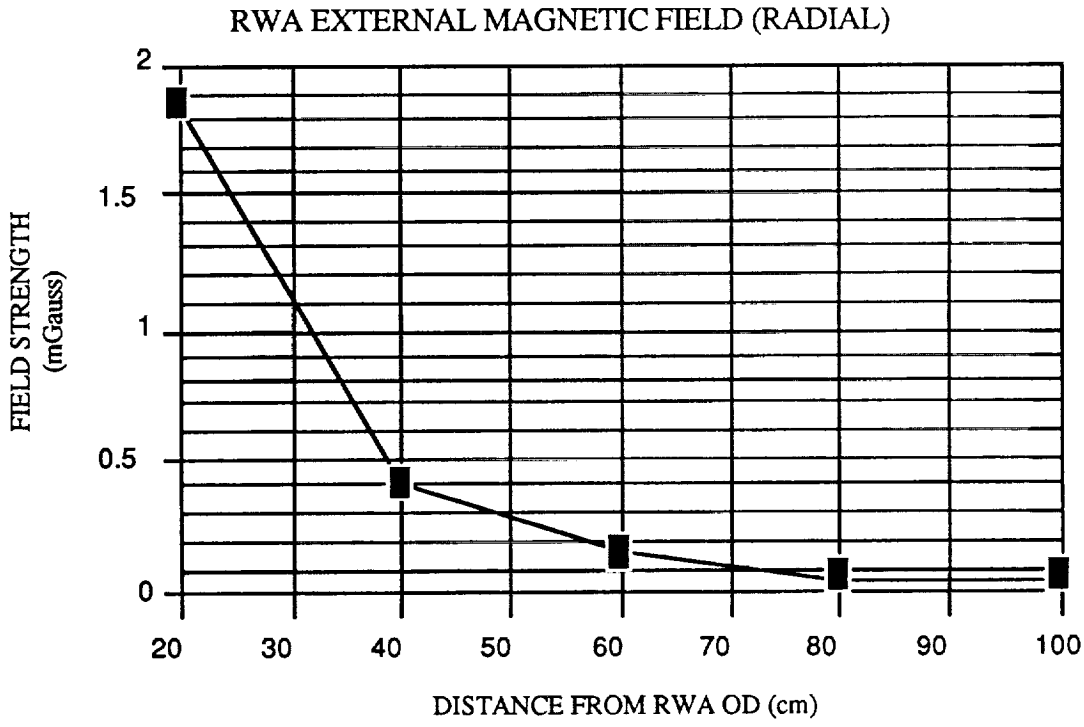

FIGURE 3-3

3.4 Charged Particle Radiation

There are no requirements for radiation tolerance.

3.5 Operating Lifetime

3.5.1 Bearing Lifetime

The bearing lubrication system in the Reaction Wheel is the only life limiting mechanical item in the components. The lubricant quantity is compatible with an expected operating lifetime of 3 years.

3.5.2 Radiation Damage

Electronics lifetime is governed by the charged particle radiation environment and the inherent hardness of the semiconductors. The components will tolerate approximately 10^4 Rad(Si).

3.6 Handling Precautions

The following precautions should be observed when handling the hardware:

1. When unpacked from their shipping cartons, the RWA should be maintained in a Class 100 K Clean area. Any disassembly of the RWA which exposes the bearings should only be performed in a Class 100 Clean area.

2. All hardware is ESD sensitive and should be handled per the guidelines of ITHACO RQPS 64.7.

3. The RWA should be securely attached to a workbench or suitable structure prior to being operated at any speed.

3.7 Hardware Storage Requirements

Optional conditions for long-term storage of the RW and SW are as follows:

1. Spin Axis: Horizontal
2. Ambient Temperature: As low as practical but above -50°C
3. Cleanliness: Unit packaged. Store in Class 100 K clean area.

4.0 SCANWHEEL ASSEMBLY

4.1 SW Requirements

The SWA provides reaction torque to the spacecraft mounting surface and storage of angular momentum in addition to providing earth horizon location information. The SWA consists of three separate units; an SW, an MD, and an SC. Interface cables are required to interconnect the units.

4.1.1 SW Specifications

4.1.1.1 Torque Capability

When operated in a vacuum, the SWA will be capable of providing a minimum reaction torque of 20 mN-m (2.8 oz-in) in the speed range from 0 to 3000 RPM, provided that temperatures and voltages are within specified limits of Section 3.0. Figure 4-1 shows the relationship between nominal drag torque and wheel speed. Maximum breakaway torque is 0.0015 N-m (0.21 oz-in). Maximum stall torque is 0.0005 N-m (0.071 oz-in).

4.1.1.2 Torque Command

Motor Torque is commanded by a bipolar analog voltage.

4.1.1.3 Motor Torque Scale Factor

The scale factor of motor torque vs. command voltage is projected to be 0.005 N-m/V (0.71 oz-in/V). The actual Motor Torque Scale Factor will be measured in test.

4.1.1.4 Motor Torque Ripple

The torque ripple during steady state operation within the specified speed range is projected to be less than 1.0 mN-m (0.14 oz-in) 0-pk at the primary motor commutation frequency of 54 times the wheel rotation rate.

4.1.1.5 Operating Speed Range

The SWA will be capable of operating in the CW or CCW direction to a minimum speed of 3000 RPM while in a vacuum or when operating in air at atmospheric pressure.

4.1.1.6 Momentum Storage Capacity

The SWA will be capable of storing a minimum of 1.5 N-m-s (1.1 ft-lb-sec) of angular momentum at 2000 RPM. Flywheel inertia will be 0.0077 n-m-sec^2 (0.0057 ft-lbf-sec^2) ±5%.

4.1.1.7 Digital Tachometer

A tachometer provides 54 square wave pulses per revolution to indicate wheel speed.

NOMINAL RWA/SWA DRAG TORQUE IN VACUUM

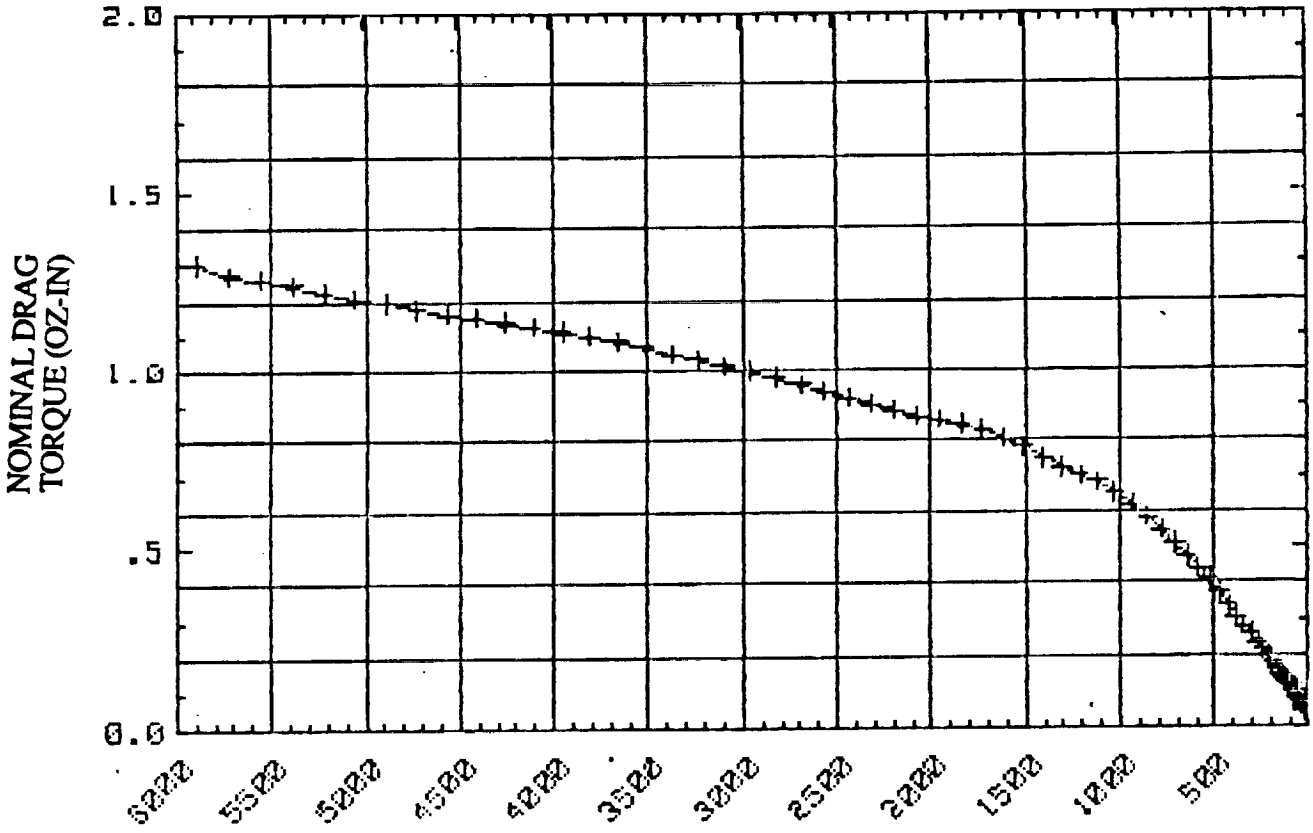

FIGURE 4-1

4.1.1.8 Analog Tachometer

A secondary tachometer provides an analog signal proportional to absolute speed with a scale factor of 1000 RPM/V.

The maximum SW speed as a function of bus voltage is:

$$RPM_{max} = (149\ RPM/V)\ V_{BUS}$$

4.1.1.9 Index Pulse

A separate once per revolution index pulse, the Bottom Dead Center (BDC) Tach signal, supplies a reference signal to mark the relative position of the flywheel and scanning mirror. The index pulse occurs at BDC. BDC is when the Infrared Line of Sight (ILOS) is 180° opposite the center of the 90° blanked region.

4.1.1.10 Minimum Speed Loop

Correct functioning of the SC card requires a minimum SW speed of approximately 200 RPM. The user must implement a control loop to maintain this minimum speed. An optional hardware minimum speed loop can be added to the MD.

4.1.1.11 Recommended Speed Range

In order to maintain optimal attitude determination accuracy, the SW speed should be maintained as close to 2000 RPM as practical. 2000 ± 200 RPM is the recommended operating range.

4.1.2 SW Component Interfaces

4.1.2.1 MD - SW Interface

Figure 4-2 identifies the cabling requirements for the interface between the motor and the MD. Due to the switchmode driver waveforms and the significant influence of wiring resistance on SW efficiency, it is recommended that the cabling be less than 2 m (79 in) in length. Due to the critical nature of this interconnect, it is imperative that the designated shielding be used.

4.1.2.2 SW - SC Interface

Figure 4-3 identifies the interconnection requirements for the SW - SC interface. Due to the small signal amplitudes in this interconnection, this interface cable must be constructed as defined in this document.

4.1.2.3 MD - SC Interface

The signal conditioner requires the digital tach signal generated by the motor associated with the same SW. The user must make this interconnection. This interconnection should be as short as practical. Refer to Table 4-3 for additional detail.

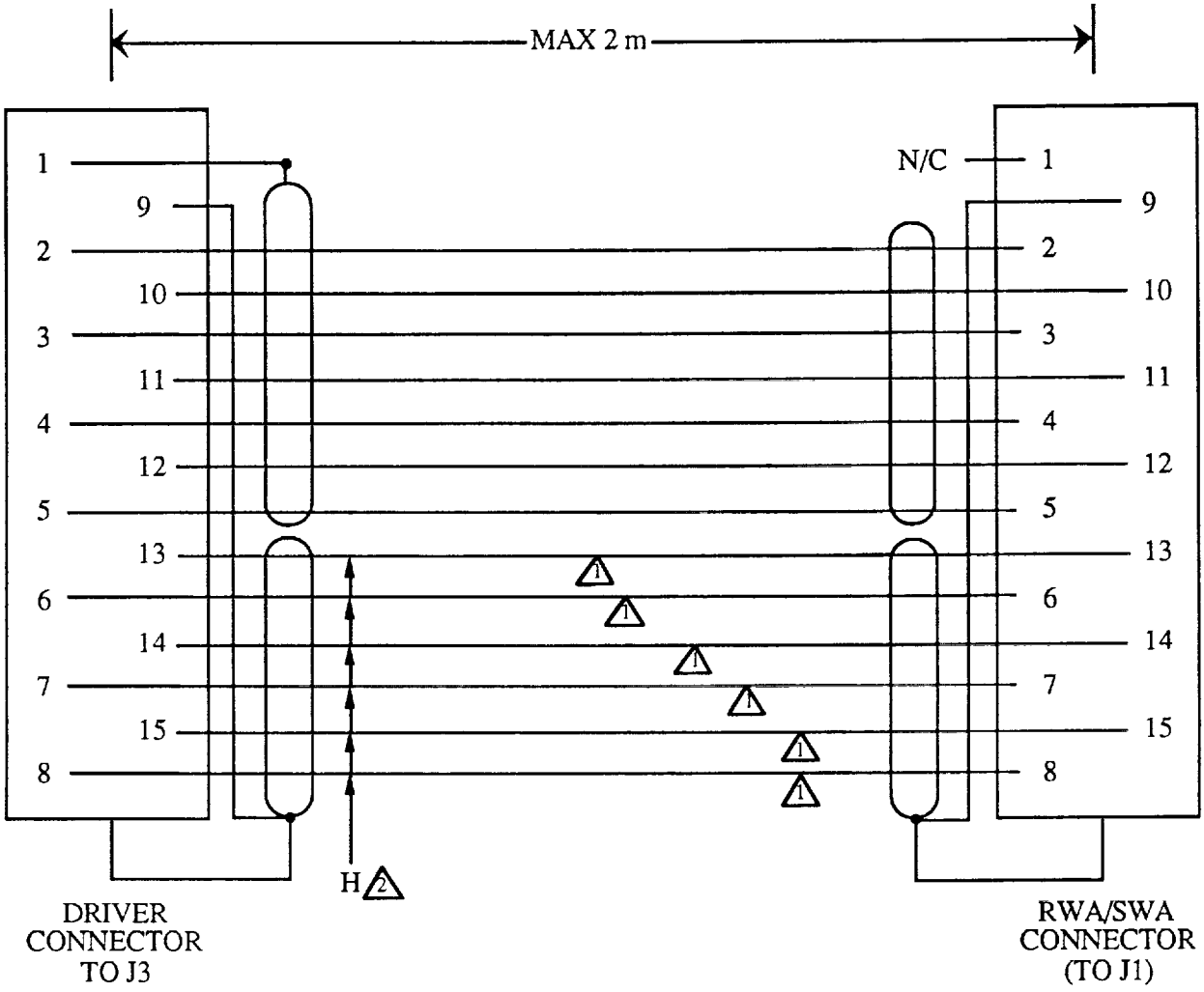

1 Recommended Wire Gauge 20 AWG

2 Twisted Hex

Connectors to be Female Non-Magnetic Subminiature D Shell

FIGURE 4-2
MOTOR DRIVER - SW-J1 INTERFACE CABLE

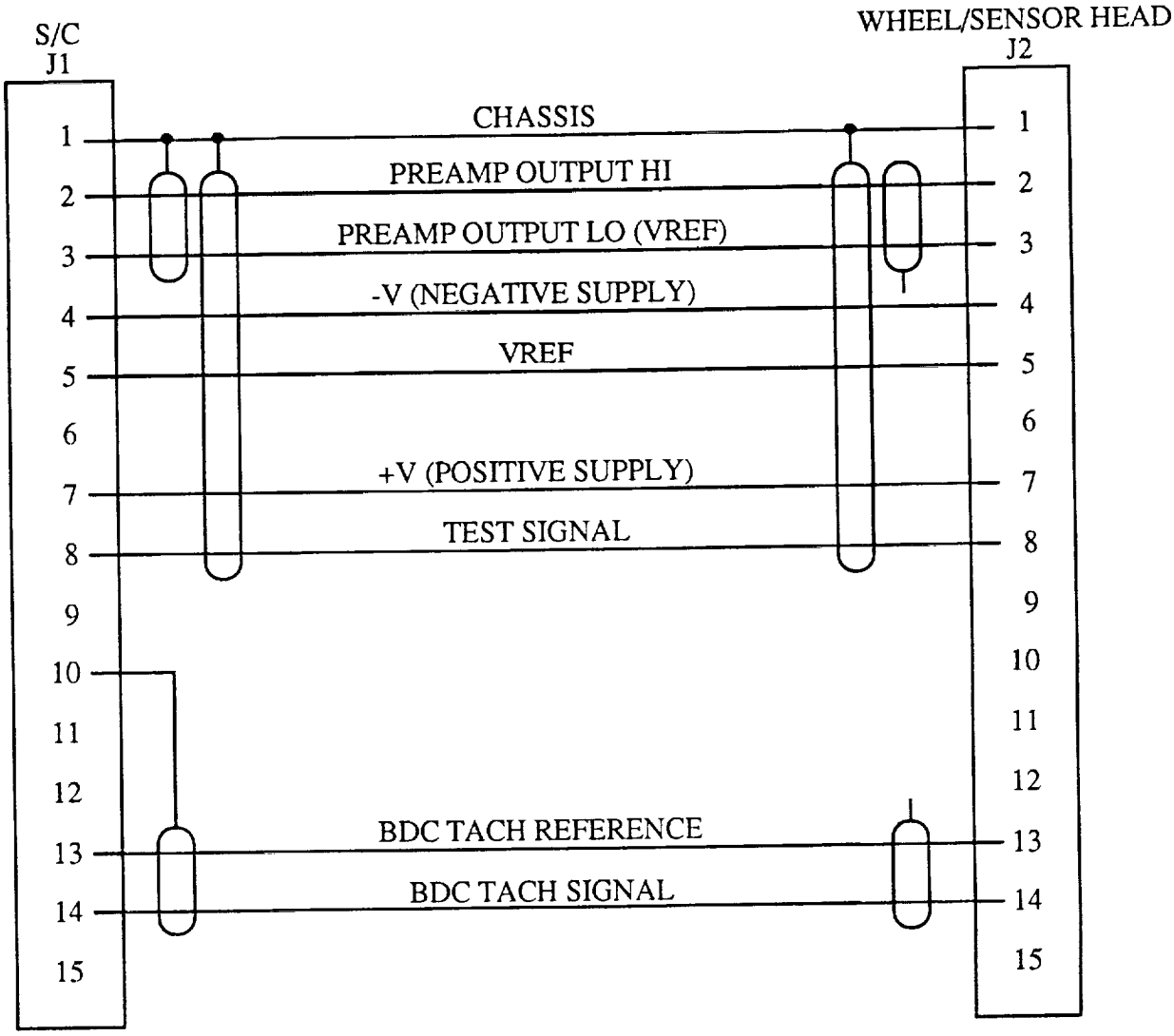

FIGURE 4-3
SW-J2 - SIGNAL CONDITIONER CABLE REQUIREMENTS

4.2 SWA Mechanical

4.2.1 Outline Drawings

The outline for the SW is defined on drawing D43393. The MD and SC are included in the Electronics Assembly Drawing D43428. See Appendix A for outline drawing.

4.2.2 Mounting Requirements

The SW may be mounted from either of the two mounting surfaces indicated on the outline drawing as Datums A and B. Six equally spaced holes on Datum A and four holes on Datum B provide mounting provision for #8 screws or bolts.

4.2.3 Mass Properties

The mass of the SW will be 3.3 Kg (7.2 lbm max). The mass of the MD and SC is projected to be less than 1.14 Kg (2.5 lbm).

4.2.4 Torque Output Vector/Momentum Vector Alignment

The Spin axis, Torque Output Vector, and Momentum Vector axes will be perpendicular to either of the wheel mounting surfaces within ±15 arcminutes.

4.2.5 Direction of Rotation

Relative to the connector side of the RW, a CW torque will result on the flywheel when a positive torque command is applied. This will result in a CCW reaction torque on the spacecraft. If started from zero RPM, the application of CW motor torque will cause the flywheel to rotate in the CW direction, resulting in a logic "1" from the direction telemetry. If the flywheel is rotating in the CCW direction, a logic "0" will result. The analog tach polarity is positive when the flywheel rotates in the CW direction.

4.3 MD Electronic

4.3.1 Functional Description

Refer to Figure 4-4 for a Functional Block Diagram of the MD. The MD interfaces the Brushless DC motor in the reaction wheel to the Power Bus. The MD/RW combination has true DC servo capability and can provide instantaneous torque in either direction. In addition, the wheel can operate in either direction of rotation, and near zero speed without the need for intentional direction switching.

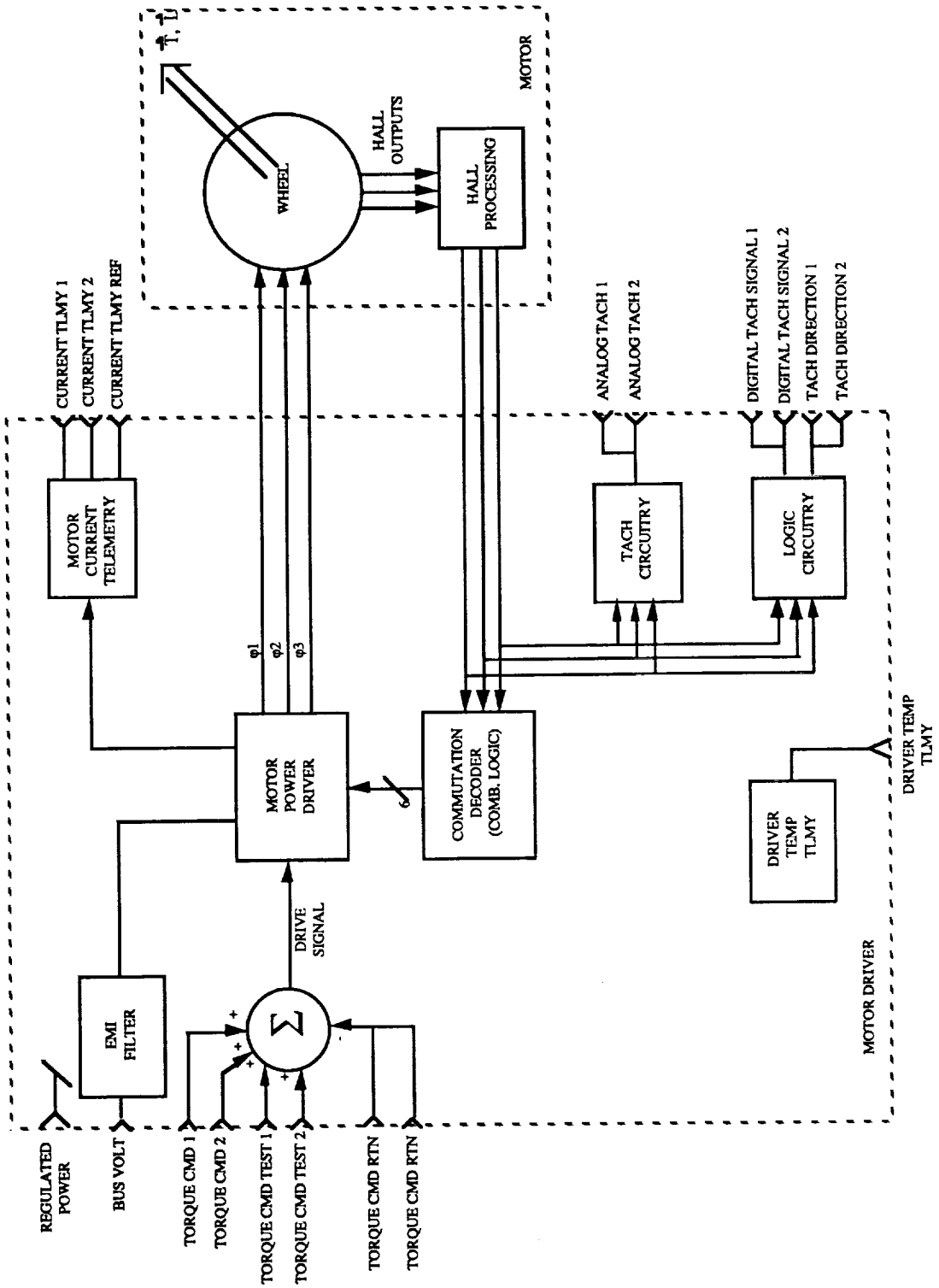

FIGURE 4-4
MOTOR DRIVER - FUNCTIONAL BLOCK DIAGRAM

4.3.2 Pinout Definitions

Each MD contains the following connectors:

Designation	Function	No. of Pins	Connector Type
J2	Test/Telemetry	25	Male Subminiature D Shell
J3	Motor Interface	15	Male Subminiature D Shell
J8	Power Interface	15	Male Subminiature D Shell
J9	Command/Signals	9	Male Subminiature D Shell

Table 4-1 describes the motor driver pinouts.

4.3.3 Power Interface & Grounding

MD power interface is to the J8 connector. Refer to Table 4-1 for detailed information.

MD power requirements are as follows:

Voltage	Type	Max Current	Max Turn on Surge
+15 V	Regulated	15 mA	300 mA
-15 V	Regulated	15 mA	300 mA
+5 V	Regulated	25 mA	300 mA
+28 ± 6 V	Unregulated or regulated	1.5 A	**Input filter always tied to bus**

The returns of the regulated voltages are connected internally to the power bus return.

The MD contains no internal power switching for the ±15 V and +5 V power. This power must be switched by the user.

Power can be applied in any sequence without overstressing the MD. For an orderly power up, the 5 V should be applied last. For an orderly shutdown, remove the 5 V first.

This driver configuration will not return energy to the bus. If the commanded torque requires a motor speed reduction, kinetic energy stored in the motor is dissipated by a ballast transistor in the driver card frame.

The MD can be effectively disconnected from the 28 V power bus with the bus power command on J8-8. This CMOS level input simply disables the drive signals to the MD bridge, so that the driver draws no current from the 28 V bus regardless of torque command or power status. The MD power circuitry remains connected to the 28 V power bus regardless of the state of the bus power command. ITHACO recommends fusing the MD bus power for redundant applications. The motor driver will not operate unless the bus power command is tied to +5 V.

TABLE 4-1: MOTOR DRIVER - PINOUTS

Connector	Pin	Name	Destination	Comments	Input/ Output	Impedance	Min Volt	Max Volt	I/O Type
J8	1	Chassis							
J8	2	Power Bus +	Power Bus +	Note 1	Input	N/A	-1.00	35.00	Power
J8	3	Power Bus Return	Power Bus Return	Note 1	Input	N/A	N/A	N/A	Power
J8	4	Neg 15V Input	Neg 15V Input	Note 1	Input	N/A	-15.75	1.00	Power
J8	5	Power Return	Power Return	Note 1	Input	N/A			
J8	6	Pos 15 V Input	Pos 15 V Input	Note 1	Input	N/A	-1.00	15.75	Power
J8	7	5 V Input	5 V Input	Note 1	Input	N/A	-1.00	5.25	Power
J8	8	Bus Power Command	User Interface	Active High	Input	50 KΩ	0V	5V	CMOS
J8	9	Chassis							
J8	10	Power Bus +	Power Bus +	Note 1	Input	N/A	-1.00	35.00	Power
J8	11	Power Bus Return	Power Bus Return	Note 1	Input	N/A	N/A	N/A	Power
J8	12	Neg 15V Input	Neg 15V Input	Note 1	Input	N/A	-15.75	1.00	Power
J8	13	Power Return	Power Return	Note 1	Input	N/A			
J8	14	Pos 15 V Input	Pos 15 V Input	Note 1	Input	N/A	-1.00	15.75	Power
J8	15	5 V Input	5 V Input	Note 1	Input	N/A			
J9	1	Chassis							
J9	2	Torque Command 2	User Interface	Protected to ±15V, 0.005n-m/V Note 2	Input	50KΩ min	-5.00	5.00	Analog
J9	3	Torque Command 1	User Interface	Protected to ±15V, 0.005n-M/V Note 2	Input	50KΩ	-5.00	5.00	Analog
J9	5	Torque Cmd Reference	User Interface	For input ground isolation, Note 1	Input	50kΩ min	-5.00	5.00	Analog
J9	6	Digital Tach 1	User Interface	54 pulses per revolution	Output	5KΩ max	0.00	5.00	CMOS
J9	7	Analog Tach 1	User Interface	1000 RPM/V	Output	5KΩ	-10.00	10.00	Analog
J9	8	Tach Direction 1	User Interface	1=TBD, 0=TBD	Output	5KΩ max	0.00	5.00	CMOS
J9	9	Signal Reference	User Interface						
J2	1	Chassis							
J2	2	Analog Tach 2	User Interface	1000 RPM/V	Output	5KΩ	-10.0	10.0	CMOS
J2	3	Torque CMD Test 1	Opt User Interface/Test	0.005n-M/V, Note 2	Input	50KΩ	-15 V	15 V	Analog
J2	4	Torque CMD Test 2	Opt User Interface/Test	0.005n-M/V, Note 2	Input	50KΩ	-15.00	15.00	Analog
J2	5	Torque CMD Reference	Opt User Interface/Test	For input isolation, Note 1	Input	50KΩ Min	-15.00	15.00	Analog

Note 1: Connector pins bearing identical names are redundant and are connected together within the card.
Note 2: Torque command voltages are summed by the motor as follows:
Total Torque Command = (J9-2) + (J9-3) + (J2-3) + (J2-4) - (J9-5).
Unused Torque Command inputs must be tied to J9-5 or J2-5.

TABLE 4-1 (CONT'D): MOTOR DRIVER - PINOUTS

Connector	Pin	Name	Destination	Comments	Input/ Output	Impedance	Min Volt	Max Volt	I/O Type
J2	6	Current Telemetry 2	User Interface	0.4 A/V (RW), 0.2 A/V (SW)	Output	5KΩ Max	-15.00	15.00	Analog
J2	7	Current Telemetry 1	User Interface	0.4 A/V (RW), 0.2 A/V (SW)	Output	5KΩ Max	-15.00	15.00	Analog
J2	8	Sig RTN							
J2	9	Sig RTN							
J2	10	Digital Tach 2	User Interface	54 pulses per revolution	Output	5KΩ max	0.00	5.00	CMOS
J2	11	Current TLM Reference	User Interface	For TLMY ground isolation	Output	5KΩ Max	-15.00	15.00	Analog
J2	12	Driver Phase 3 Test	Test Only	Switchmode driver outputs	Output	100KΩ	0.00	35.00	Analog
J2	13	Driver Phase 2 Test	Test Only	Switchmode driver outputs	Output	100KΩ	0.00	35.00	Analog
J2	14	Tach Direction 2	User Interface	1=TBD, 0=TBD	Output	5KΩ max	0.00	5.00	CMOS
J2	15-19	Spare		Open					
J2	20-21	Sig RTN							
J2	22	Spare		Open					
J2	23	Temp TLM	User Interface	Biased Thermistor TLMY	Output	5KΩ Max	0.00	5.00	Analog
J2	24	Temp TLM Return	User Interface	Biased Thermistor TLMY	Output	5KΩ Max	0.00	5.00	Analog
J2	25	Driver Phase 1 Test	Test Only	Switchmode driver outputs	Output	100KΩ	0.00	35.00	Analog
J3	1	Chassis	Motor	NOT USER INTERFACE					
J3	2	Tach 1	Motor	NOT USER INTERFACE	Input	15K	0.00	5.00	CMOS
J3	3	Tach 2	Motor	NOT USER INTERFACE	Input	15 K	0.00	5.00	CMOS
J3	4	Tach 3	Motor	NOT USER INTERFACE	Input	15 K	0.00	5.00	CMOS
J3	5	Sig Rtn	Motor	NOT USER INTERFACE	Output	N/A	0.00	5.00	Analog
J3	6	Motor Winding A	Motor	NOT USER INTERFACE	Output	N/A	-1.00	35.00	Power
J3	7	Motor Winding B	Motor	NOT USER INTERFACE	Output	N/A	-1.00	35.00	Power
J3	8	Motor Winding C	Motor	NOT USER INTERFACE	Output	N/A	-1.00	35.00	Power
J3	9	Chassis	Motor	NOT USER INTERFACE					
J3	10	5 V	Motor Hall Sensors	NOT USER INTERFACE	Output	N/A	4.75	5.25	Power
J3	11	5V	Motor Hall Sensors	NOT USER INTERFACE	Output	N/A	4.75	5.25	Power
J3	12	Sig Rtn	Motor	NOT USER INTERFACE	Output				
J3	13	Motor Winding A	Motor	NOT USER INTERFACE	Output	N/A	-1.00	35.00	Power
J3	14	Motor Winding B	Motor	NOT USER INTERFACE	Output	N/A	-1.00	35.00	Power
J3	15	Motor Winding C	Motor	NOT USER INTERFACE	Output	N/A	-1.00	35.00	Power

4.3.3 Power Interface & Grounding (Cont'd)

MD 28 V bus power can be directly switched by the user if desired. Under these conditions, maximum inrush current is approximately 16.5 A. This inrush estimate excludes the current into a 0.1 μf capacitor connected between the +28 V and 28 V return terminals.

CAUTION:

All signal returns in the MD are tied internally to the power bus return. In order to maintain isolation for the analog inputs and outputs, the Torque Command inputs and the Current Telemetry outputs are implemented using differential amplifiers. Further detail is given in Sections 4.3.4 and 4.3.5.

4.3.4 Torque Control Interface

MD control interface is to the J9 connector. Refer to Table 4-1 for detailed information.

The Wheel Torque Command input is implemented with a multiple input differential amplifier. The differential amplifier allows communication between ground systems with less than 5 V difference. The differential amplifier sums the 4 Torque Command and Torque Test inputs on J9 and J2. All Torque Command inputs must have the same reference. For true differential operation of the input amplifier, unused torque command inputs must be tied to the Torque Command reference pins J9-5 or J2-5.

The user should be aware that the Torque Command does not account for motor bearing drag.

The transfer function between the wheel torque output and torque command input has a single pole at approximately 1000 Hz.

4.3.5 Signal Interface

The MD produces the following output signals on the J9 connector:

Digital Tach
Tach Direction
Analog Tach

Interface details are provided in Table 4-1. All signals are referenced to the power supply returns.

Due to the 4.64 KΩ nominal output impedance of the Digital Telemetries, ITHACO recommends that the user use a line receiver with hysteresis and no internal pullup resistors such as the CD40106 hex Schmitt buffer.

4.3.6 Telemetry Interface

4.3.6.1 Telemetry Connector

MD telemetry interface is to the J2 connector. Refer to Table 4-1 for detailed information.

The MD produces an analog tach telemetry, an MD temperature telemetry, a motor current telemetry, digital tach telemetry and motor direction telemetry. Details of these signals and their scale factors are provided in Table 4-1.

4.3.6.2 Motor Current Telemetry

The motor current telemetry has a differential output amplifier to permit easy communication between ground systems. All other telemetry outputs are referenced to the power bus return. Current telemetry outputs are buffered so that a short circuit on one telemetry will not affect the other telemetry.

4.3.6.3 Driver Temperature Telemetry

Driver temeprature telmeetry is provided by a biased thermistor. Table 4-2 shows the temperature telemetry output voltage as a function of temperature.

4.3.6.4 Motor Driver Analog Tach

The motor driver provides two isolated bipolar analog tach telemetries scaled to 1000 rpm/V. The polarity of the tach voltage indicates tach direction. Maximum DC output voltage is ±10 V. The tach telemetry transfer function has a two-pole filter with a corner frequency of 5 Hz. Ripple voltage at 100 rpm or higher is less than 5 mV. Ripple voltage at any speed will not exceed 15 mV. The analog tach outputs are buffered so that a short circuit on one tach output will not affect the other tach output.

4.3.6.5 Digital Tach Telemetry

The motor driver provides two buffered digital tach telemetries and two buffered motor direction telemetries. The digital tach telemetry produces 54, approximately square, pulses per motor revolution. Both tach and direction outputs are 5 V CMOS compatible signals.

4.4 SC Electronic

4.4.1 Functional Description

Refer to Figure 4-5 for a functional block diagram of the SC. The SC first amplifies and treble boosts the detector flake signal. Sun clipping, DC restoration, filtering and differentiation are then performed. The differentiated signal is thresholded to produce a leading and trailing edge output. Logic circuitry in the signal conditioner generates a high frequency clock signal of 18,432 pulses per revolution synchronized to the MD Tach output, as well as a Reconstructed Earth Pulse and blanking signal.

4.4.2 Pinout Definitions

Each SC card contains the following connectors:

Designation	Function	No. of Pins	Connector Type
J1	HCI Interface	15	Male Subminiature D Shell
J2	Test/Telemetry	25	Male Subminiature D Shell
J8	Power /Command/Signal	25	Male Subminiature D Shell

Refer to Table 4-3 for SC pinout definitions and interface specifications.

TABLE 4-2

Temperature (°C)	Temp TLMY Min (V)	Temp TLMY Nom (V)	Temp TLMY Max (V)
-30	4.48	4.82	5.16
-25	4.43	4.77	5.10
-20	4.37	4.70	5.03
-15	4.30	4.62	4.95
-10	4.21	4.53	4.84
-5	4.10	4.41	4.72
0	3.98	4.28	4.58
5	3.83	4.12	4.41
10	3.67	3.95	4.23
15	3.50	3.76	4.02
20	3.30	3.55	3.80
25	3.10	3.34	3.57
30	2.89	3.11	3.33
35	2.67	2.88	3.08
40	2.46	2.64	2.83
45	2.24	2.41	2.58
50	2.04	2.19	2.34
55	1.84	1.98	2.12
60	1.66	1.78	1.91
65	1.48	1.60	1.71
70	1.33	1.43	1.53
75	1.18	1.27	1.36
80	1.05	1.13	1.21
85	0.93	1.00	1.08
90	0.83	0.89	0.95
95	0.74	0.79	0.85
100	0.65	0.70	0.75

TABLE 4-3: SIGNAL CONDITIONER PIN ASSIGNMENTS

Pin #	Signal Name	Input/ Output	Function	Imped-ance	Comments	Voltage Range
J1-1	Chassis Ground		Chassis Ground		Connected to chassis	
J1-2	Preamp Output HI	Output	Signal from sensor head preamp	100 Ω	Op-amp output	0-4 mV
J1-3	Preamp Output LO	Output	Reference voltage of preamp output	100 Ω		0 V
J1-4	-V	Input	Negative power supply line to preamp	N/A	-15 V at <2 mA	-15 V ± 5%
J1-5	VREF	Input	Signal reference voltage	N/A	Analog signal ground	0 V
J1-6	VREF	Input	Signal reference voltage	N/A	Analog signal ground	0 V
J1-7	+V	Input	Positive power supply line to preamp	N/A	+15 V at <2 mA	+15 V ± 5%
J1-8	Simulated Earth Test Input	Input	Test signal to preamp	0 Ω	Inject signal at J2-14	0-400 mV
J1-9	Chassis Ground		Chassis ground		Connected to chassis	
J1-10	BDC Tach Chassis Ground		Shield for magnetic position sensor wires		Connected to chassis	
J1-11	Not Used					
J1-12	Not Used					
J1-13	BDC Tach Reference	Input	Reference line for magnetic position sensor signal			0 V
J1-14	BDC Tach Signal	Input	Signal line for magnetic position sensor signal			0-5 V
J1-15	To J2-15 (Spare)		Connection between indicated connector pins		Normally not used	

TABLE 4-3 (CONT'D): SIGNAL CONDITIONER PIN ASSIGNMENTS

Pin #	Signal Name	Input/ Output	Function	Imped-ance	Comments	Voltage Range
J2-1	Chassis Ground		Chassis ground		Connected to chassis	
J2-2	Bessel Output	Output	Test point at Bessel filter output	10 K	Op-amp output	-1 to +1 V
J2-3	Differentiator Output	Output	Test point at output of differentiator circuit	10 K	Op-amp output	-3 to +3 V
J2-4	LE	Output	Test point at output of LE (leading edge) circuit		Op-amp output Polarity: active high	-14 to +14 V
J2-5	TE	Output	Test point at output of TE (trailing edge) circuit		Op-amp output Polarity: active high	-14 to +14 V
J2-6	VREF	Input	Signal reference voltage		Analog signal ground	
J2-7	Not Used					
J2-8	Not Used					
J2-9	Not Used					
J2-10	Not Used					
J2-11	Not Used					
J2-12	Not Used					
J2-13	BDC Reference Pulse	Output	Test point for Bottom Dead Center reference pulse	100 K	Op-amp output (squared-up magnetic position sensor signal) Polarity: active low	-14 to +14 V
J2-14	Simulated Earth Test Input	Input	Test point for insertion of a simulated earth signal		Typical Earth test signal approximately 400 mV	0-400 mV
J2-15	To J1-15 (Spare)		Connection between indicated connector pins		Normally not used	
J2-16	Amplifier Output	Output	Test point for the first stage of the signal conditioner	10 K	Op-amp output	-14 to +14 V
J2-17	DC Restorer First Stage	Output	Test point for the first stage of the DC restorer circuit	10 K	Op-amp output	-14 to +14 V
J2-18	DC Restorer Second Stage	Output	Test point for the second stage of the DC restorer circuit	10 K	Op-amp output	-14 to +14 V

TABLE 4-3 (CONT'D): SIGNAL CONDITIONER PIN ASSIGNMENTS

Pin #	Signal Name	Input/ Output	Function	Imped-ance	Comments	Voltage Range
J2-19	Not Used					
J2-20	Not Used					
J2-21	Not Used					
J2-22	Not Used					
J2-23	Not Used					
J2-24	Not Used					
J2-25	BDC Tach Signal	Output	Test point for processed BDC signal	10 K	CMOS output BDC Reference Pulse translated to CMOS levels and inverted	0-15 V
J9-1	Chassis Ground		Chassis Ground			
J9-2	Not Used					
J9-3	TE Threshold Enable/Disable	Input	Disables TE Threshold slaving	317 K	FET input -15 V will disable	-15 to +15 V
J9-4	LE Threshold Enable/Disable	Input	Disables LE Threshold slaving	317 K	FET input -15 V will disable	-15 to +15 V
J9-5	VREF		Signal reference voltage		Analog signal ground	
J9-6	Neg 15 V Input	Input	Input point for the negative (-15 V) supply		Requires 50 mA at -15 V Connected to J9-7	-15 V ± 5%
J9-7	Neg 15 V Input	Input	Input point for the negative (-15 V) supply		Requires 50 mA at -15 V Connected to J9-6	-15 V ± 5%
J9-8	+V	Output	Access to +15 V supply which can be tied to uncommitted transistor collectors		+15 V	+15 V ± 5%
J9-9	TE Collector	Output	Open collector output for TE signal	N/A	Tie J9-10 to J9-11 for open-collector output Polarity: active high	Open Collector sinks 1 mA at 1 V
J9-10	TE Emitter	Output	Emitter output of TE signal	500 Ω	Tie J9-9 to J9-8 for emitter follower output Polarity: active low	

TABLE 4-3 (CONT'D): SIGNAL CONDITIONER PIN ASSIGNMENTS

Pin #	Signal Name	Input/ Output	Function	Imped-ance	Comments	Voltage Range
J9-11	VREF		Access to signal reference intended to be used with open collector/emitter transistors			
J9-12	LE Collector	Output	Open collector output for LE signal	N/A	Tie J9-13 to J9-11 for open-collector output Polarity: active high	Open Collector sinks 1 mA at 1 V
J9-13	LE Emitter	Output	Emitter output of LE signal	500 Ω	Tie J9-12 to J9-8 for emitter follower output Polarity: active low	
J9-14	Blank Output	Output	Blanking signal	10 K	CMOS output low during the blanked section of rotation	0-15 V
J9-15	54 PPT Tach Signal	Input	Input point for tachometer signal from motor driver card	10 K	Signal from motor driver is approximately 5 V peak square wave	0-5 V
J9-16	Delayed BDC Reference Pulse	Output	BDC pulse delayed to match actual Earth pulse delay	14.7 K	Active low CMOS output Approximately 620 µs delay Falling edge indicates BDC time PW = 500 µs	0-15 V
J9-17	18432 PPT	Output	Test point for the phase locked tach signal	14.7 K	CMOS output	0-15 V
J9-18	VREF		Signal reference voltage		Analog signal ground	
J9-19	Pos 15 V Input	Input	Input point for the positive (+15 V) supply		Requires 50 mA at +15 V	+15 V ± 5%
J9-20	Pos 15 V Input	Input	Input point for the positive (+15 V) supply		Requires 50 mA at +15 V	+15 V ± 5%
J9-21	VLRI	Input	Common point (low side) of the CMOS logic supply		Logic return	
J9-22	VL	Input	High side of the CMOS supply		Requires 10 mA at +15 V	+15 V ± 5%
J9-23	VL	Input	High side of the CMOS supply		Requires 10 mA at +15 V	+15 V ± 5%
J9-24	Reconst Earth Pulse (Emitter)	Output	Available emitter for the reconstructed Earth pulse signal	500 Ω	Tie J9-25 to J9-8 for emitter follower output Polarity: active high	
J9-25	Reconst Earth Pulse (Collector)	Output	Open collector for the reconstructed Earth pulse signal	N/A	Tie J9-24 to J9-11 for open-collector output Polarity: active low	Open Collector sinks 1 mA at 1 V

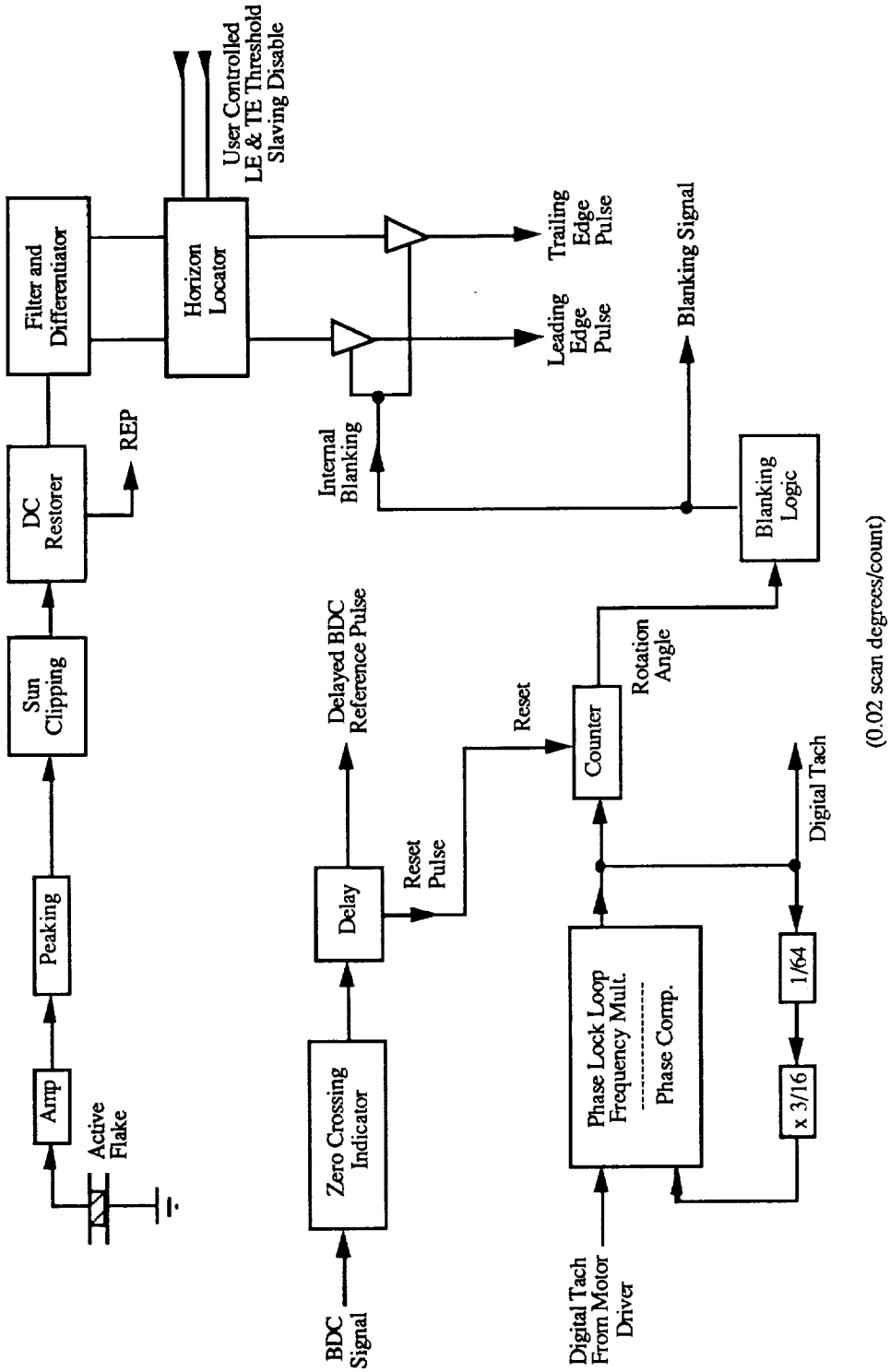

FIGURE 4-5
SIGNAL CONDITIONER - FUNCTIONAL BLOCK DIAGRAM

4.4.3 Power Interface

The SC requires +15 V ± 5% at 50 mA and -15 V ± 5% at 50 mA for logic and analog circuitry. The logic and analog circuitry have independent supply and return inputs, which the user must configure as defined in Table 4-3. The regulated power return is common to the signal and logic returns.

4.4.4 Signal Interfaces/Signal Timing

4.4.4.1 Signal Timing Diagram

The following paragraphs describe a typical SWA application in which the center of the Earth typically occurs at BDC. Figure 4-6 shows the timing relationships between SC outputs, infrared input and user inputs for a nominal condition with only the Earth in the SW Infrared Line of Sight (ILOS). The horizontal axis of Figure 4-6 is shown in scan degrees as the actual timing of the signals depends on exact wheel speed.

The digital tach of 18,432 pulses per SW revolution is derived from the MD tach via a phase locked loop. It can be used for high accuracy instantaneous SW position resolution.

The BDC signal indicates when the ILOS is pointing directly at nadir. The BDC signal is electronically delayed to match filter delays in the LE and TE circuitry. This eliminates the need for the user to compensate for these delays.

The centers of the LE and TE pulses define the exact time of the Earth leading and trailing edges (plus the filter delays), respectively. The user must determine the center of these pulses and compare the LE and TE times to the leading edge of the BDC signal.

The Reconstructed Earth Pulse is a digital logic compatible version of the Infrared Earth signal which has been derived from the horizon locator circuitry in the SC. This signal is useful for Earth Presence detection, Wide Angle operation, etc.

The blanking pulse in Figure 4-6 indicates that the sensor mounting bracket is in the ILOS. LE and TE signals are inhibited when the blanking pulse is low. The user must make provisions for blanking signals for spacecraft structure components which are in the ILOS but not in the blanking region.

Use of LE and TE Threshold Slaving disable inputs are described in Section 4.4.5.

4.4.4.2 Uncommitted Transistor Logic Interfaces

LE, TE, Restored Earth Pulse signals have uncommitted output transistors to allow flexibility in interfacing. These transistors can be used as open-collector or emitter follower outputs.

For use as an open collector output, the user ties the emitter of the output transistor to logic ground. The user must supply an external pullup resistor. The open collector configuration allows interface to several logic families operating at either 5 or 15 V.

For use as an emitter follower, the user ties collector of the output transistor to the appropriate supply voltage (5 or 15 V). For interface to CMOS logic families, an external pulldown resistor may be required.

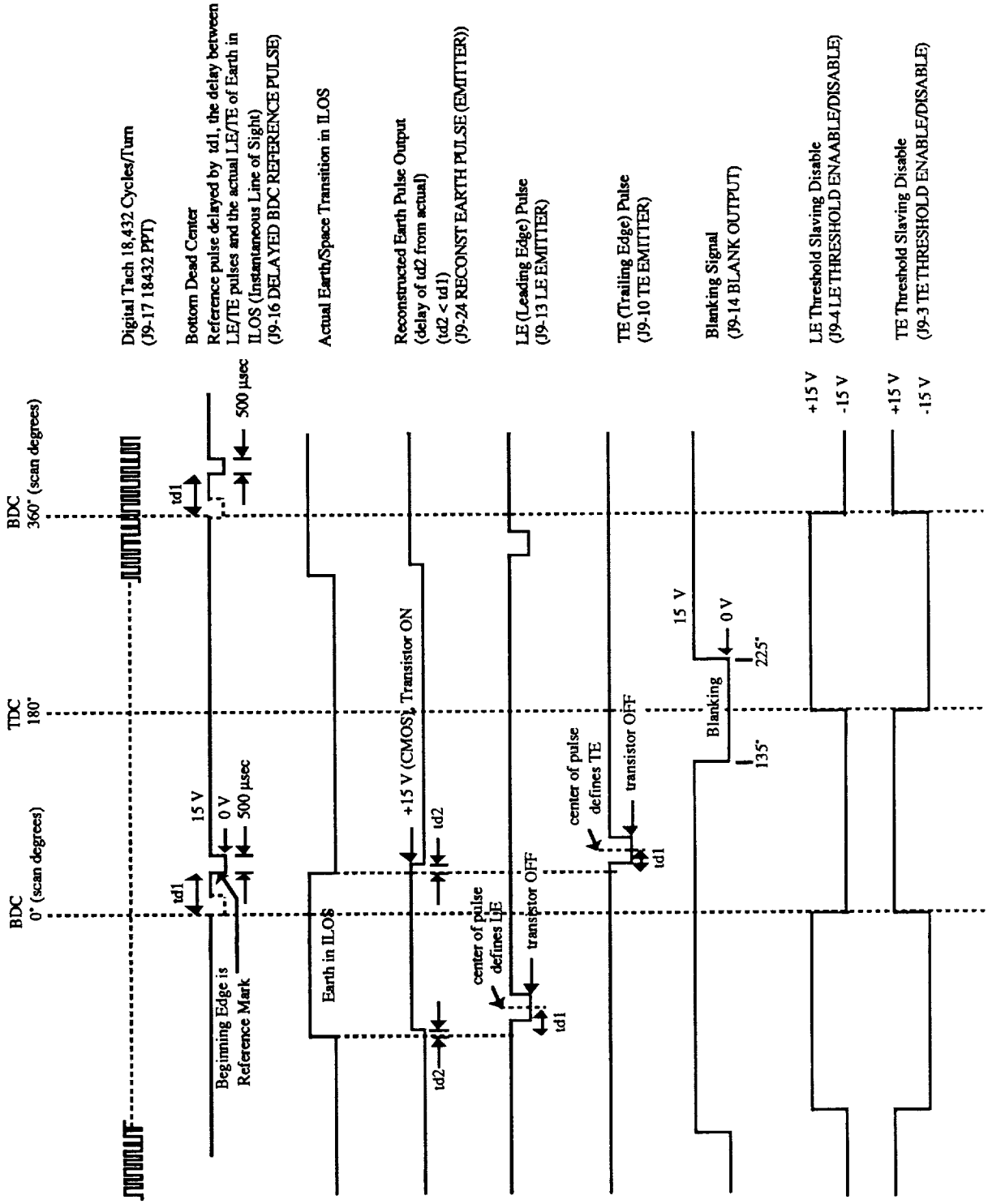

FIGURE 4-6
TYPICAL SC TIMING DIAGRAM

4.4.5 Control Interface

The user must generate the LE and TE threshold slaving disable control signals. For typical conditions, with only the Earth in the ILOS, these signals are set or reset at Top Dead Center (TDC) and BDC as shown in Figure 4-6.

Figure 4-7 shows the use of LE and TE threshold slaving disable commands required with the sun (and/or moon) in the field of view. If the sun is between TDC and BDC, the LE threshold disable signal should remain high until the ILOS passes the sun. If the sun is in between BDC and TDC, the TE threshold disable command must be asserted high immediately following any leading edge detected after BDC and before TDC.

4.4.6 Telemetry Interface

The SC supplies several intermediate stage test and telemetry signals. All logic signals are 15 V CMOS compatible. Table 4-3 defines the details of these outputs.

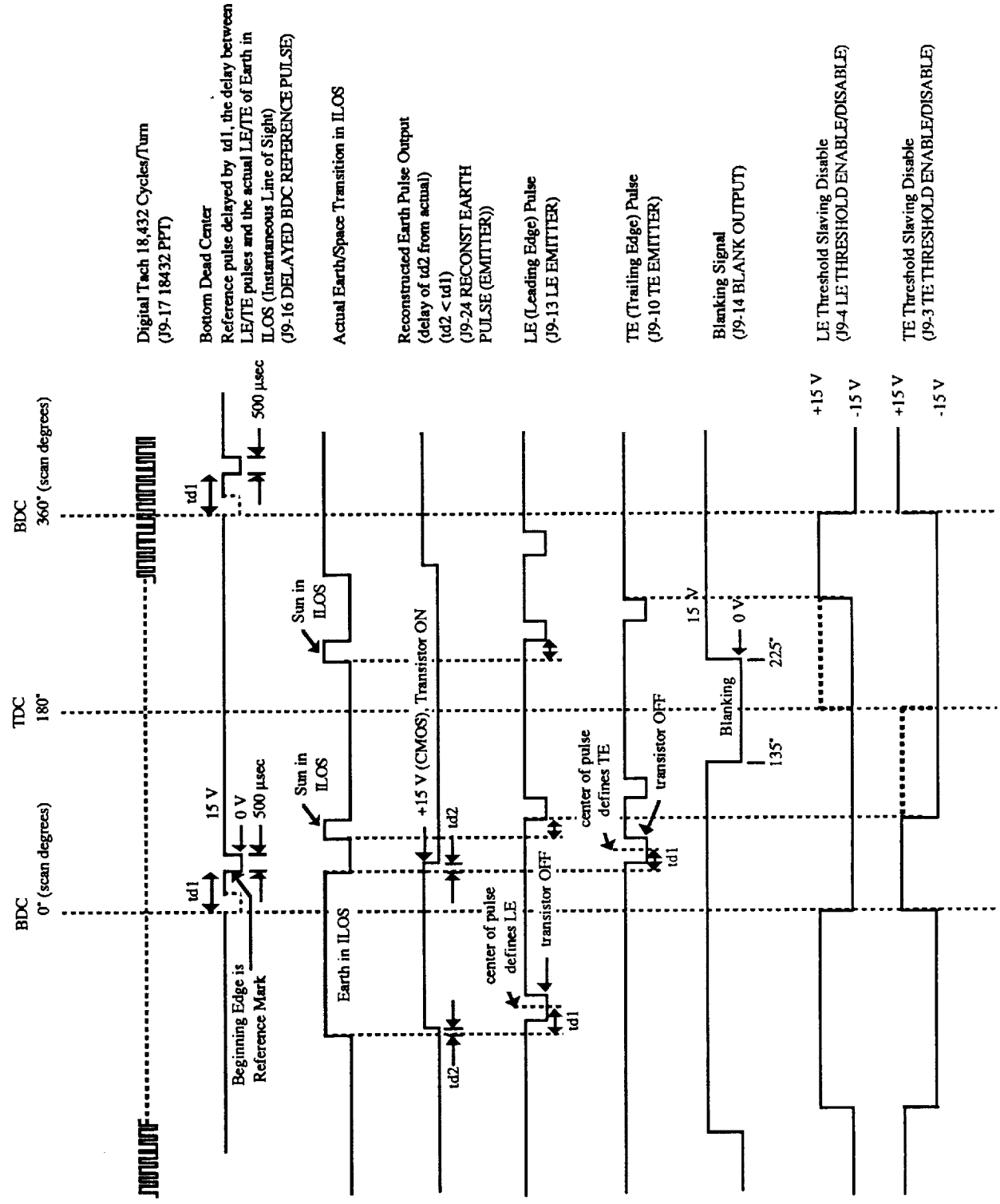

FIGURE 4-7
SIGNAL CONDITIONER TIMING DIAGRAM WITH SUN IN FOV

4.4.8 Error Budget

Errors are in Scan Degrees. This analysis assumes a geometrical gain of 2. All numbers are rough estimates.

Error Source	3-σ Error in Scan Degrees
Noise (White up to RPM/120 Hz)	2.0 per scan (3000 RPM)
Rotor Position reset (1 V/SD, 20 mV noise)	0.02 per scan
EOL & Temperature (40 ppm/°C, 50 C, 0.00025 s)	0.01
Flutter & Wow (negligible with wheel inertia)	0
Alignment (our fixtures only, absolute) (matched pairs) (spacecraft stability, unknown)	0.08 0.02 (TBD)
Speed Error (over entire range, 300-3000 RPM) (Calibration to be provided) (Applicable speed range unknown to ITHACO)	0.1 (uncorrected) 0.01
Radiance Error (base upon Landsat 4, 5 flight data) (orbital parameters and mounting geometry unknown to ITHACO)	0.6 (winter polar regions)
Estimated Performance with Restricted IR Passband	0.2 (winter polar regions) 0.08 lower latitudes
Sun/Moon Interference Data (>15° away from Earth Horizon)	0.02
Oblateness Error (unknown orbital parameters) (remove in computer)	0.6° max. 0.01
Results	
Total Worst Case, No Processing, Single Sensor	3.43 (scan degrees)
Total Worst Case, Pointing Error (approx.)	1.7 attitude degrees
RSS, 1 second average, 3000 RPM, oblateness modelling and calibration curves applied	0.36 (scan degrees) 0.18 attitude degrees
RSS, 1 second average, 3000 RPM, dual SW, with modelling and calibration	0.25 (scan degrees) 0.12 attitude degrees
RSS, 10 second average, 3000 RPM, dual SW, modelling, etc., excepting winter poles	0.09 (scan degrees) 0.04 attitude degrees

To arrive at the 10 second average, the random noise numbers are divided by SQR(1000). Lower latitude radiance error is divided by SQR(2) since radiance error tends to be random and affect one SW at a time. Oblateness errors are assumed to be 1/6 as large for a two-SW system. Sun/moon is halved since they are assumed to affect only one SW at a time. Calibration, EOL and alignment are included in the RSS values. It is assumed that all available data is averaged.

4.5 Power Profile

4.5.1 Power Consumption

The power consumption for the SW and MD at 2000 RPM and minimum 20 mN-m (2.8 oz-in) commanded motor torque will be less than 10 W (8 W typical) at 23°C.

The power consumption for the SW and MD at 2000 RPM steady state operation will be less than 4 W (2.1 W typical) at 23°C.

The power consumption for each SC is projected to be less than 1.5 W.

4.5.2 Power Dissipation

Measured SW dissipations are:

Speed	Reaction Torque	Driver Dissipation	Wheel Dissipation	SC Dissipation
2000 RPM	0	1.0 W	1.2 W	1.2 W
2000 RPM	Max (increase speed)	5.0 W	2.0 W	1.2 W
2000 RPM	Max (decrease speed)	10.0 W	2.0 W	1.2 W

Refer to Figure 4-8 for a curve of the motor/motor driver power consumption as a function of speed. This curve is only valid up to 3000 RPM for the SW.

4.6 Infrared Optical Interface

4.6.1 Field of View

The scan beam width (field of view) nominally subtends a 1.5° (0 ± .75°) arc.

4.6.2 Scan Cone Angle

The rotating infrared scan cone has a semi-vertex angle of 45 ± 1°.

4.6.3 Optical Passband

The optical passband nominally covers the 14.2 - 15.7 μm range.

4.6.4 Required Clearances

The required clearances to avoid interfering with the optical scan path are shown on the outline drawing D43327 (see Appendix A).

TYPICAL RWA/DRIVER STEADY STATE POWER CONSUMPTION IN VACUUM

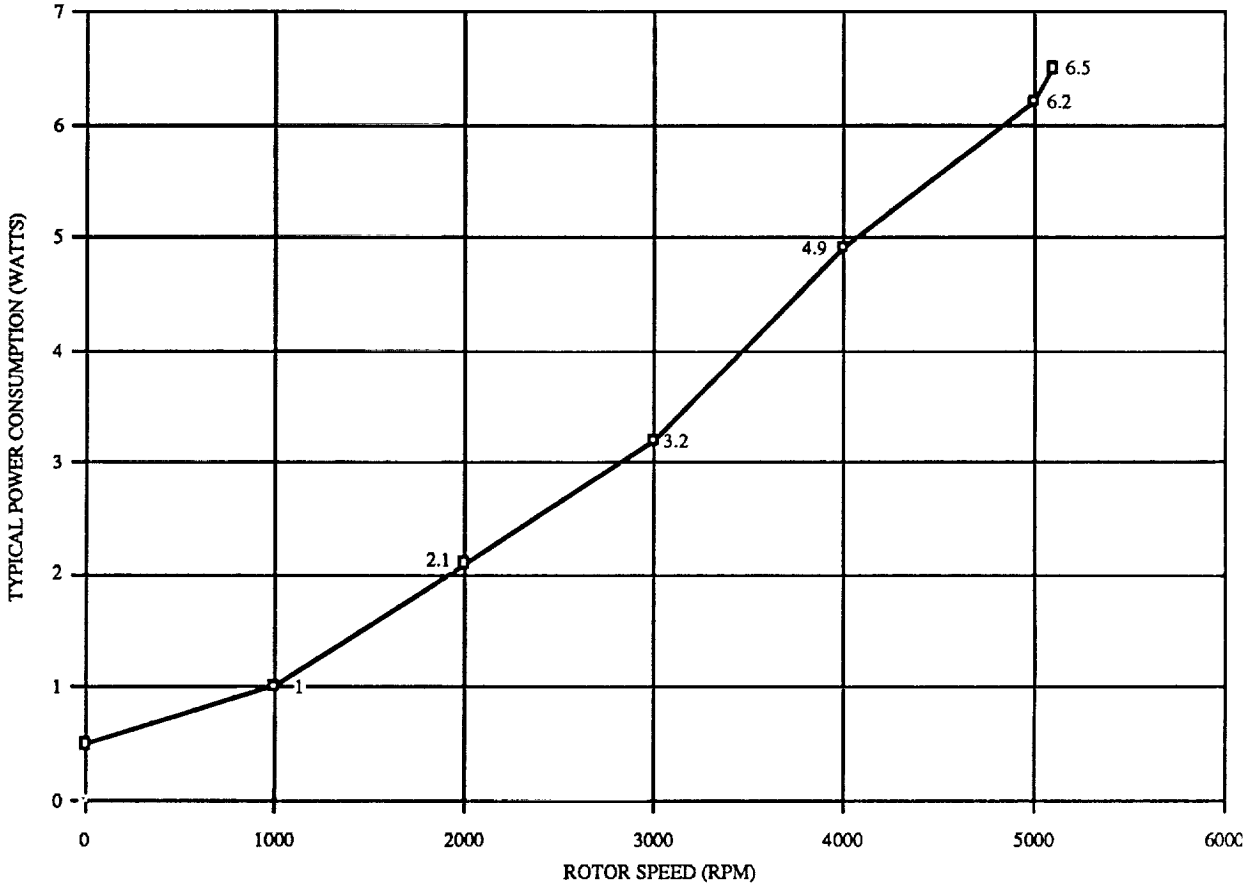

FIGURE 4-8

4.6.5 Blanking

The signal from the scanning sensor is electronically blanked for a minimum sector of 90° as defined on outline drawing D43327 (see Appendix A).

4.6.6 Optical Alignment

The SW optical alignment is defined with respect to 2 mirrors mounted to the HCI. An alignment procedure and data will be provided with the End Item Data Package.

APPENDIX A

OUTLINE DRAWINGS

FOLDOUT FRAME

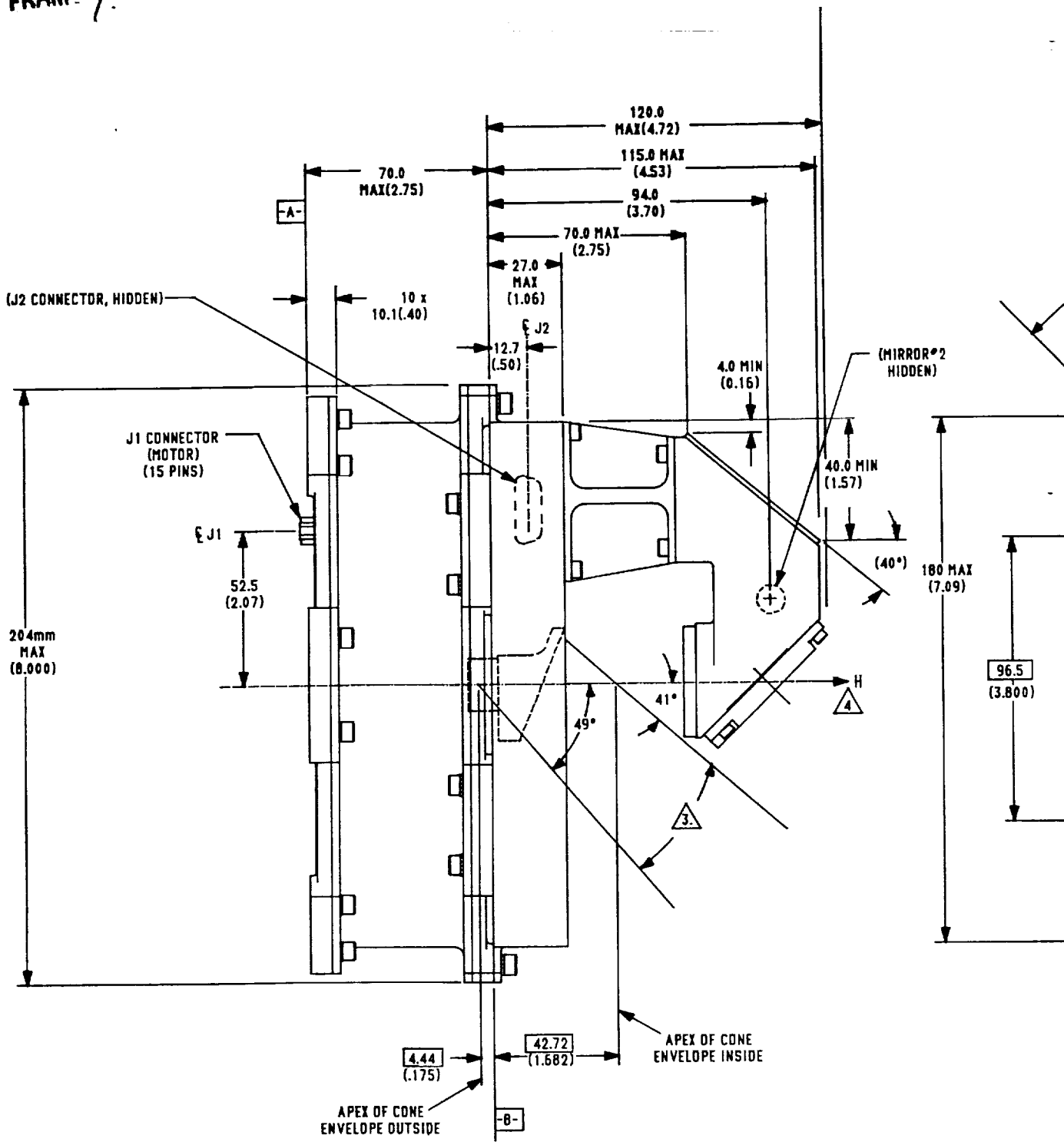

FOLDOUT FRAME 2

REVISIONS		D 43393 SHT 1 OF 1	
SYM	DESCRIPTION	DATE	APPROVAL
A	REVISED PER 8751 WJT 10-24-90	9-24-90	

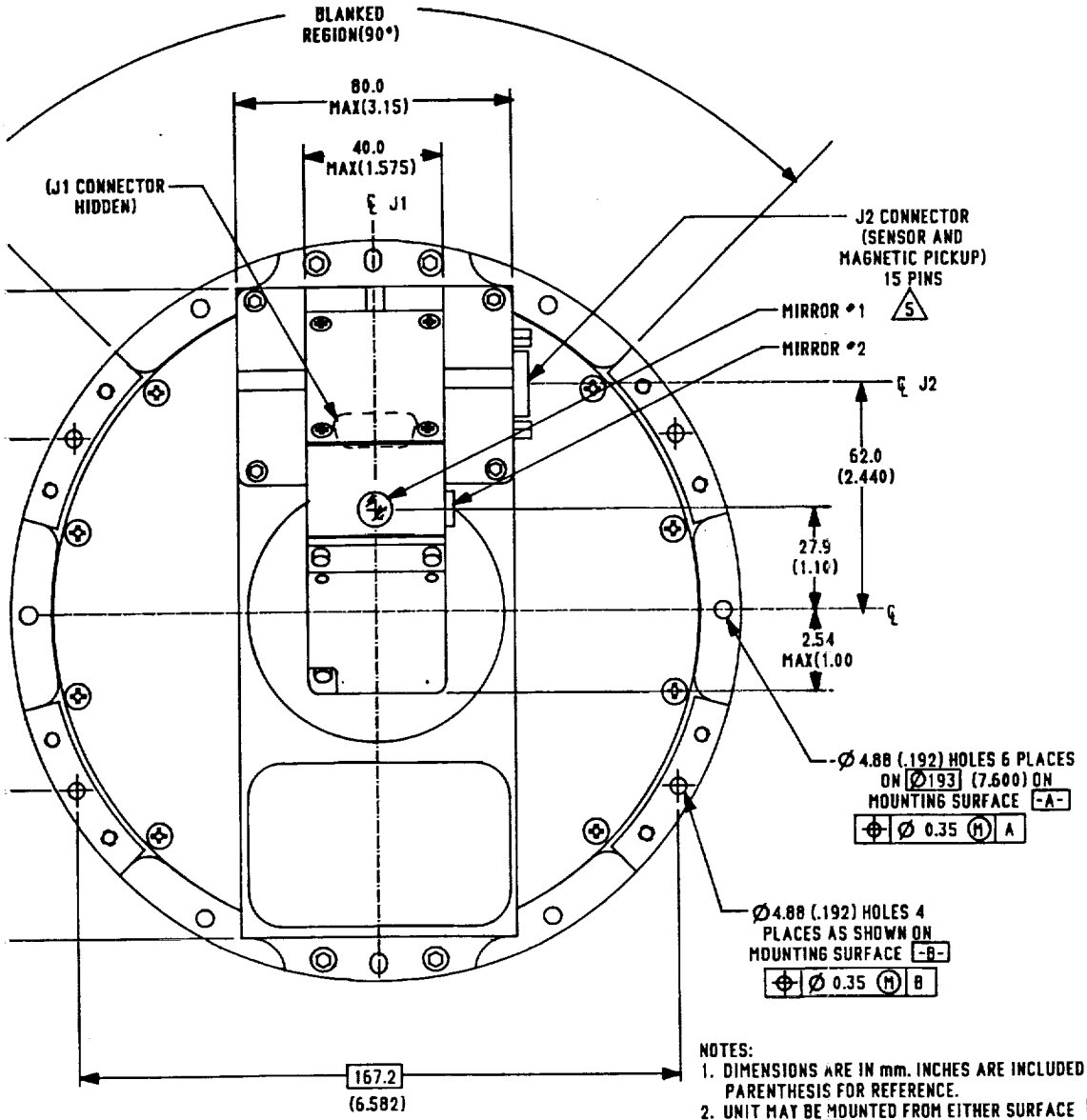

NOTES:
1. DIMENSIONS ARE IN mm. INCHES ARE INCLUDED IN PARENTHESIS FOR REFERENCE.
2. UNIT MAY BE MOUNTED FROM EITHER SURFACE -A- OR SURFACE -B- .
3. UNOBSTRUCTED FIELD OF VIEW REQUIRED FOR ROTATING SCAN CONE. CONE ANGLES IDENTIFIED DEFINE INSIDE AND OUTSIDE LIMITS OF SCAN CONE ENVELOPE.
4. SCAN CONE ROTATION AXIS IS COINCIDENT WITH ANGULAR MOMENTUM VECTOR.
5. CONNECTORS ARE 15 PIN MALE SUBMINIATURE D (MECHANICAL INTERFACE COMPATIBLE WITH M24308/3-2 AND MIL-C-24308/3
6. TOLERANCE: XX.X = ±2 mm XXX = ±0.2 mm
7. WEIGHT: 3.3 KG (7.2 LBS) MAX.

C.2

WHERE USED			UNLESS OTHERWISE SPECIFIED DIMENSIONS ARE IN INCHES	OUTLINE SCANWHEEL	ITHACO INC. ITHACA, NEW YORK
DRAWING	IDENTIFICATION NO.	MODEL/PROG	LINEAR: ANGULAR:		
		STEP	XX ± .02 XXX ± .010 ± 0.5°		
			APPROVALS	FMP: JOB NO.	
			CHK WJT 9-26-90 MFG TLC 9-27-90	DRAWN BY: W.THURSTON DATE: 9-26-90	CODE IDENT. NO. 20502
			DFTG WJT 9-26-90 R&QA TMM 9-27-90	DO NOT SCALE PRINT. REPRODUCTIONS OF THIS DRAWING MAY NOT BE TO SCALE.	D 43393
			ENG BB 9-26-90 KB 9-27-90	DRAWING SCALE: 1/1	SHT 1 OF 1
			ISSUE DATE 9-27-90		

FOLDOUT FRAME

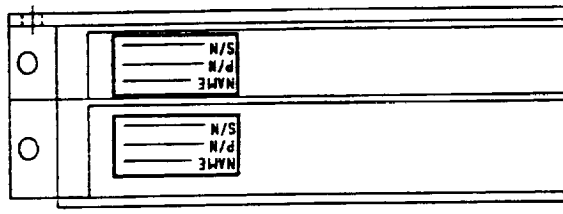

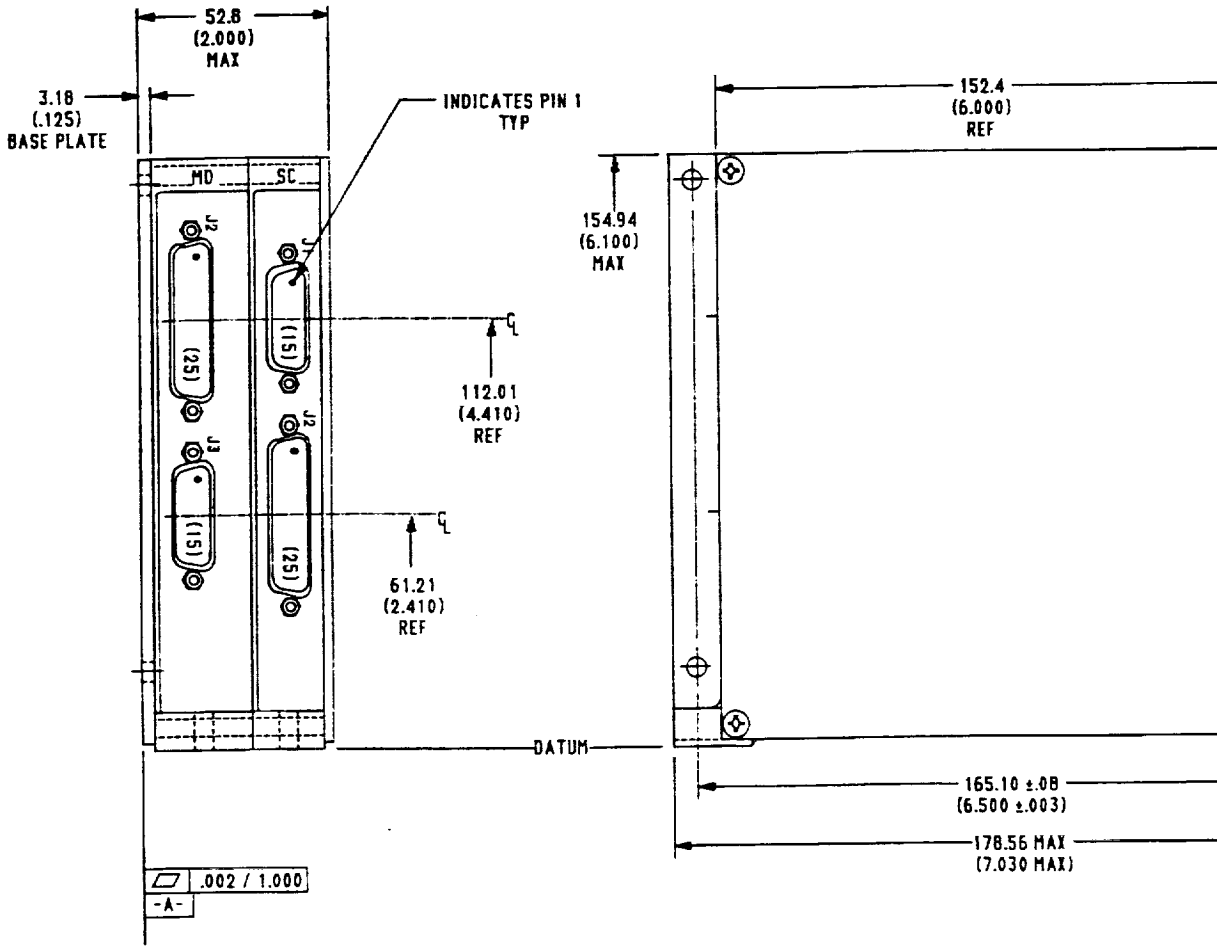

SYM	DESCRIPTION	DATE	APPROVAL
A	RELEASE FOR PRODUCTION	3-27-91	

2.

FOLDOUT FRAME

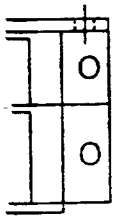

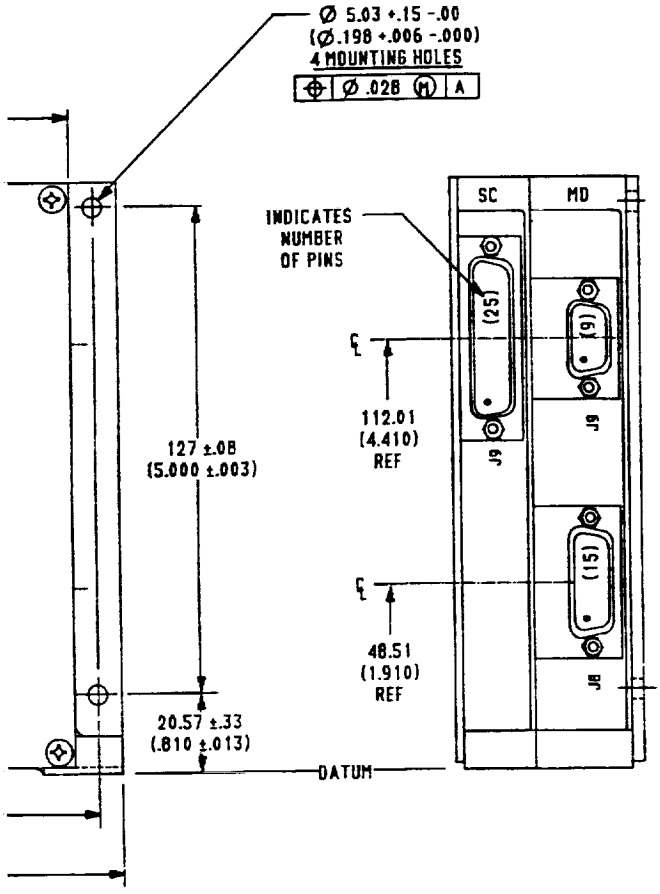

NOTES
1. DIMENSIONS ARE IN MM, INCHES ARE IN PARENTHESIS ( ).
2. WEIGHT: 1.14 kg (2.5 LBS) MAX.
3. CONNECTORS: ARE MALE SUBMINIATURE D (MECHANICAL INTERFACE COMPATIBLE WITH M24308/3-2.
4. MOUNTING SURFACE ROUGHNESS 16 √ (62 √).

TOLERANCES
X.X = ± 1 mm (.04)
X.XX = ±0.2 mm (.008)

INTERPRET DIMENSIONS AND TOLERANCES PER ANSI Y 14.5M - 1982

MAR 27 1991

WHERE USED			UNLESS OTHERWISE SPECIFIED DIMENSIONS ARE IN INCHES	SCANWHEEL ELECTRONIC ASSEMBLY OUTLINE	ITHACO INC. ITHACA, NEW YORK
DRAWING	IDENTIFICATION NO.	MODEL/PROG	LINEAR: .XX ± .02 .XXX ± .010 ANGULAR: ± 0.5°		
			APPROVALS	PMF: JOB NO.	
			CHK (KY) 3-27-91 MFG (RJ) 3-25-91	DRAWN BY: [signature] DATE: 3/22/91	CODE IDENT. NO. 99503
			DFTG (KY) 3-27-91 REGA Tom 3-27-91	DO NOT SCALE PRINT. REPRODUCTIONS OF THIS DRAWING MAY NOT BE TO SCALE.	D 43428
			ENG (RS) 3-27-91 AE 3-25-91		
			ISSUE DATE 3-27-91	DRAWING SCALE: 1/1	SHT 1 OF 1